Number 39 Year 2022

Journal of New Theory

ISSN: 2149-1402

Editor-in-Chief
Naim Çağman

www.dergipark.org.tr/en/pub/jnt

CONTENTS

About

Journal of New Theory (abbreviated as J. New Theory or JNT) is a mathematical journal focusing on new mathematical theories or a mathematical theory's applications to science.

J. New Theory is an international open access journal.

Language: JNT accepts contributions in English only.

JNT was founded on 18 November 2014, and its first issue was published on 27 January 2015.

Editor-in-Chief: Naim Çağman

E-mail: journalofnewtheory@gmail.com

APC: JNT incurs no article processing charges.

Review Process: Blind Peer Review

Policy of Screening for Plagiarism: JNT accepts submissions for pre-review only if their reference-excluded similarity rate is a **maximum of 30%**.

Publication Ethics: The governance structure of Journal New Theory and its acceptance procedures are transparent and designed to ensure the highest quality of published material. JNT adheres to the international standards developed by the Committee on Publication Ethics (COPE).

Aim & Scope

Journal of New Theory aims to share new ideas in pure or applied mathematics with the world of science.

Journal of New Theory publishes original research articles and reviews from all science branches that use mathematics theories.

Journal of New Theory is concerned with the studies in the areas of AMS2020, but not limited to:

· Fuzzy Sets

· Soft Sets

· Neutrosophic Sets

· Decision-Making

· Algebra

· Number Theory

· Analysis

· Theory of Functions

· Geometry
· Applied Mathematics
· Topology
· Fundamental of Mathematics
· Mathematical Logic
· Mathematical Physics
· Mathematical Statistics

Journal Boards

Bijan Davvaz
Department of Mathematics, Yazd University, Yazd, Iran
davvaz@yazd.ac.ir
Pabitra Kumar Maji
Department of Mathematics, Bidhan Chandra College, Asansol 713301, Burdwan (W), West Bengal, India.
pabitra_maji@yahoo.com
Harish Garg
School of Mathematics, Thapar Institute of Engineering & Technology, Deemed University, Patiala-147004, Punjab, India
harish.garg@thapar.edu
Jianming Zhan
Department of Mathematics, Hubei University for Nationalities, Hubei Province, 445000, P. R. China
zhanjianming@hotmail.com
Surapati Pramanik
Department of Mathematics, Nandalal Ghosh B.T. College, Narayanpur, Dist- North 24 Parganas, West Bengal 743126, India
sura_pati@yaho.co.in
Muhammad Irfan Ali
Department of Mathematics, COMSATS Institute of Information Technology Attock, Attock 43600, Pakistan
mirfanali13@yahoo.com
Said Broumi
Department of Mathematics, Hassan II Mohammedia-Casablanca University, Kasablanka 20000, Morocco
broumisaid78@gmail.com
Mumtaz Ali
The University of Southern Queensland, Darling Heights QLD 4350, Australia
Mumtaz.Ali@usq.edu.au
Oktay Muhtaroğlu
Department of Mathematics, Gaziosmanpaşa University, 60250 Tokat, Turkey
oktay.muhtaroglu@gop.edu.tr
Ahmed A. Ramadan
Mathematics Department, Faculty of Science, Beni-Suef University, Beni-Suef, Egypt
aramadan58@gmail.com

Journal of New Theory
ISSN: 2149-1402

39 (2022) 1-7
Journal of New Theory
https://dergipark.org.tr/en/pub/jnt
Open Access

I-Connectedness

Selahattin Kılınç[1]

Article Info
Received: 16 Apr 2022
Accepted: 30 Jun 2022
Published: 30 Jun 2022
doi:10.53570/jnt.1104540
Research Article

Abstract — In this paper, we introduce a weak form of connectedness with respect to an ideal. We also investigate its relation to connectedness. We examine the I-connectedness property on the new topology introduced by the ideal. In addition, it is revealed under what conditions I-connectedness and connectedness coincide and one differs from another.

Keywords — *Connectedness, I-connectedness, ideal topological space*

Mathematics Subject Classification (2020) — 54A05, 54D05

1. Introduction

Vaidyanathaswamy [1] and Kuratowski [2] introduced the concept of an ideal in a topological space and also introduced a new topology using this concept of an ideal. Later, more detailed investigations were carried out on the ideal and the new topology it determines. An ideal I on a non-empty set X is a collection of subsets of X, which is closed under taking subsets and finite union operations. If (X,τ) is a topological space and I is an ideal on X, then (X,τ,I) is called an ideal topological space. If (X,τ) is a topological space and $A \subseteq X$, then the closure and the interior of A are denoted by $\bar{A}$ and $\overset{\circ}{A}$, respectively. $V(x)$ will denote the open neighborhood system at x, ($V(x) = \{V \in \tau : x \in V\}$), Given a topological space (X,τ) and a subset A of X, the subspace topology on A is defined by $\tau_{|A} = \{A \cap U : U \in \tau\}$.

Previously, some types of connectedness and their details in ideal topological spaces were studied by Ekici and Noiri [3], Sathiyasundari and Renukadevi [4], Modak and Noiri [5], Kılınç [6] and Tyagi, Bhardwaj and Singh [7], respectively. In this study, we have studied a different type of connectedness from earlier existing connectedness of ideal topological spaces. Then, using this new type of connectedness, new component and new locally-connectedness definitions were introduced. It has been shown that some of the basic properties of connectedness are also preserved according to this new type of connectedness.

This article is organized as follows. In the next section some basic notions and properties of ideal and ideal topological space are reviewed. In Section 3, we introduce the concept of I-connectedness. Moreover, we introduce the concept of I-component, locally I-connectedness, and totally I- disconnectedness. We show that not connected space is not I-connected and it has been shown that I-connectedness is preserved under bijective continuous functions. Then, we study some basic properties of them.

[1]selahattinkilinc@hotmail.com (Corresponding Author)
[1]Department of Mathematics, Faculty of Arts and Sciences, Çukurova University, Adana, Turkiye

2. Preliminaries

Definition 2.1. [2] Let (X,τ) be a topological space, and I be an ideal on X. The set $A^*(I,\tau) = \{x \in X : A \cap U \notin I \text{ for every } U \in V(x)\}$ is called the local function of A with respect to τ and I. We will write simply A^* for $A^*(I,\tau)$.

Definition 2.2. [8] Let (X,τ) be a topological space, and I be an ideal on X. It well known, the operator $Cl^*(.)$ from $\mathcal{P}(X)$ to $\mathcal{P}(X)$ defined by $Cl^*(A) = A \cup A^*(I)$ for every subset A of X, is a Kuratowski closure operator. Thus, $\{U \subseteq X : Cl^*(X-U) = X-U\}$ is a topology on X. The topology is denoted by $\tau^*(I)$.

When there is no chance for confusion $\tau^*(I)$ is denoted by τ^*. The topology τ^* has as a base $\beta(\tau,I) = \{W - B : W \in \tau \text{ and } B \in I\}$. [8]. It is easy to show that $\tau \subset \tau^*$. Also note that, if $I = \{\emptyset\}$ then $\tau = \tau^*$ and if $I = \mathcal{P}(X)$ then $A^*(\mathcal{P}(X),\tau) = \emptyset$ which implies $\tau^* = \mathcal{P}(X)$. We will call each element of τ^* as a $*$-open set.

Definition 2.3. [9] Let (X,τ,I) be an ideal topological space. For every $A \subset X$, if

$$\forall x \in A, \exists U \in V(x) | U \cap A \in I \Rightarrow A \in I$$

Then the topology τ is compatible with the ideal and denoted by $\tau \sim I$.

Lemma 2.4. [10] Let (X,τ) and (Y,φ) be two topological spaces. If $f : X \to Y$ is a function and I is an ideal on X, then the set $f(I) = \{f(A) : A \in I\}$ is an ideal on Y. Furthermore, If $f : X \to Y$ is a one to one function and J is an ideal on Y, then the set $f^{-1}(J) = \left\{f^{-1}(B) : B \in J\right\}$ is an ideal on X.

3. Main Results

Definition 3.1. Let (X,τ,I) be an ideal topological space. If there exist open sets U and V with $U \neq \emptyset, V \neq \emptyset$, and $U \cap V \in I$, such that $X = U \cup V$, then X is called a not I-connected (I-disconnected) space. If the open sets U and V can not be found to meet the above conditions, the space X is called I-connected..

Theorem 3.2. Every not connected space is a not I-connected.

Proof. Let (X,τ) be a disconnected space. There exist nonempty disjoint open sets U, V in X such that $X = U \cup V$. Since $U \cap V = \emptyset \in I$, then X is not an I-connected space. □

We can see from the following example that the inverse of the above theorem is not always true.

Example 3.3. Let $X = \{a,b,c\}$, $\tau = \{\emptyset, X, \{a\}, \{a,b\}, \{a,c\}\}$, $I = \{\emptyset, \{a\}\}$, $U = \{a,b\}$, and $V = \{a,c\}$. Since $X = U \cup V$ and $U \cap V = \{a\} \in I$, then X is not I-connected. Moreover, since $\emptyset$ and X are the only subsets of X being open and closed sets, then X is a connected space.

Theorem 3.4. [9] Let (X,τ) be a topological space and I be a ideal on X. If $\tau \sim I$, then $\beta(\tau,I)$ is a topology on X.

Theorem 3.5. Let the ideal topological space (X,τ,I) be an I-connected space. If $\tau \sim I$, then the topological space (X,τ^*) is connected.

Proof. Let $\tau \sim I$. Suppose that, (X,τ^*) is not connected. Since (X,τ^*) is not connected, then there are disjoint $*-$open sets $M \neq \emptyset, N \neq \emptyset$ such that $X = M \cup N$. Moreover, since $\tau \sim I$, then $U, V \in \tau$ and $A, B \in I$ such that $M = U - A$ and $N = V - B$. Here,

$$\begin{aligned} M \cap N =& (U - A) \cap (V - B) \\ =& (U \cap A^c) \cap (V \cap B^c) \\ =& (U \cap V) \cap (A^c \cap B^c) \\ =& (U \cap V) \cap (A \cup B)^c \\ =& (U \cap V) - (A \cup B) \end{aligned}$$

$U \cap V \in \tau$ and $A \cup B \in I$. Thus, M and N are disjoint $*$-open sets, $(U \cap V) - (A \cup B) = \emptyset$. That is $(U \cap V) \subset (A \cup B)$. Hence, since I is an ideal on X, $U \cap V \in I$. Consequently, $X = M \cup N$ and $M \subseteq U$, $N \subseteq V$, so it becomes $X = U \cup V$. This shows that X is not I-connected, a contradiction. $\square$

Example 3.6. Let (X, τ) be a space and $A \subseteq X$. We know that $I(A) = \{B \subseteq X : B \subseteq A\}$ is an ideal on X [8]. Let's choose $X = \mathbb{R}$, $\tau = \{\emptyset, X\}$, and for $p \in X$, $I(X - \{p\}) = \{A \subseteq X : p \notin A\}$ specifically. We know $\tau \sim I$. This ideal generates a topology $\tau^* = \{A \subseteq X : p \in A\} \cup \{\emptyset\}$ known as a particular point topology [8]. The space X is I-connected because the only open set of X that is different from the empty set is X, if $U = V = X$ is selected, then $U \cap V = X \notin I$. Moreover, we know particular point topology is connected.

Theorem 3.7. If (X, τ^*) is a connected space and $\tau \cap I = \{\emptyset\}$, then the ideal topological space (X, τ, I) is I-connected.

Proof. Suppose that (X, τ, I) is not I-connected. Then, there are non-empty open subsets U, V with $U \cap V \in I$ such that $X = U \cup V$. Since $\tau \cap I = \{\emptyset\}$ and $U \cap V \in I$, then $U \cap V = \emptyset$. Proceeding from this, the contradiction arises that the space (X, τ^*) is not connected because $U, V \in \tau \subseteq \tau^*$, so our assumption is wrong, that is, the ideal topological space (X, τ, I) is I-connected. $\square$

Theorem 3.8. Let $f : (X, \tau, I) \to (Y, \varphi, f(I))$ be a bijective and continuous function. If X is an $I-$connected space, then Y is a $f(I)-$connected space.

Proof. Let X be an I-connected space. Suppose that Y is not $f(I)-$connected. Then, there are non-empty open subsets U, V with $U \cap V \in f(I)$ such that $Y = U \cup V$. Since the function f is bijective, then $f^{-1}(U)$ and $f^{-1}(V)$ are non-empty open subsets of X. Then, $X = f^{-1}(U \cup V) = f^{-1}(U) \cup f^{-1}(V)$. Simultaneously, since $f^{-1}(U) \cap f^{-1}(V) = f^{-1}(U \cap V)$, $U \cap V \in f(I)$ and f is bijective, it becomes $f^{-1}(U \cap V) \in f^{-1}(f(I)) = I$. Hence X is not I-connected. This is a contradicition. Consequently, Y is a $f(I)$-connected space. $\square$

Recall, let (X, τ, I) be an ideal topological space and A be a nonempty subset of X. Then, $I_{|A} = \{B \cap A : B \in I\}$ is an ideal on A, and $\left(A, \tau_{|A}, I_{|A}\right)$ is an ideal topological space.

Definition 3.9. Let (X, τ, I) be an ideal topological space and A be a subset of X. If subspace $\left(A, \tau_{|A}, I_{|A}\right)$ is $I_{|A}$-connected, the set A is called an $I_{|A}$-connected set in the ideal topological space (X, τ, I).

Definition 3.10. An I-component A of an ideal topological space (X, τ, I) is a maximal $I-$connected subset of X; that is A is $I-$connected and A is not a proper subset of any $I-$connected subset of X.

Theorem 3.11. Let the space X be equal to the union of non-empty and open subsets of U and V with $U \cap V \in I$. If the set $A \subset X$ is an $I_{|A}-$connected subset in the ideal topological space (X, τ, I), then $A \subset U$ or $A \subset V$.

Proof. Because of the hypothesis, there exist non-empty open subsets U and V of X such that, $X = U \cup V$ and $U \cap V \in I$. Let $A \subset X$ be an $I_{|A}-$connected space. Moreover, let $A \cap U \neq \emptyset$ and $A \cap V \neq \emptyset$. Since U and V are open subsets, then $A \cap U \in \tau_{|A}$ and $A \cap V \in \tau_{|A}$. Besides, since $U \cap V \in I$, then $(A \cap U) \cap (A \cap V) \in I_{|A}$. Since $A \subset X$ and $X = U \cup V$, then $A = A \cap (U \cup V) = (A \cap U) \cup (A \cap V)$ and so A is not $I_{|A}$ connected, a contradiction. Thus either$A \cap U = \emptyset$ or $A \cap V \neq \emptyset$. If $A \cap U = \emptyset$, then $A \subset V$. If $A \cap V = \emptyset$, then $A \subset U$. $\square$

Theorem 3.12. If $\{A_j : j \in J\}$ is a non-empty family of $I_{|A}-$connected sets with $\tau_{|\mathrm{A}} \cap I_{|\mathrm{A}} = \{\emptyset\}$, then $\underset{j}{\cup} A_j$ is $I_{|A}-$connected.

Proof. Let $B = \underset{j}{\cup} A_j$. Suppose that B is not $I_{|A}-$connected. Then, there are non-emty subsets $U, V \in \tau_{|\mathrm{A}}$ with $U \cap V \in I_{|A}$ such that $B = U \cup V$. From Theorem 3.11, we know that, for every j, either $A_j \subset U$ or $A_j \subset V$. Assume that for j, $A_j \subset U$ and for k, $A_k \subset V$. Then, $A_j \cap A_k \subseteq U \cap V$.

By the definition of I, $A_i \cap A_j \in I_{|A}$, which contradicts the fact that $\cap A_j \notin I$. Here, for every j, either $A_j \subset U$ or $A_j \subset V$. Assume that for every j, $A_j \subset U$, then $B = \cup A_j = U$. Thus, $V \subset U$. Since $\tau_{|A} \cap I_{|A} = \{\emptyset\}$, then $V \cap U = V \in I_{|A}$. Hence $V = \emptyset$, which contradicts the fact that $V \neq \emptyset$. If $A_j \subset V$ is chosen, a similar contradiction is obtained. □

Theorem 3.13. Let A be an $I_{|A}-$connected subset of (X, τ, I). If there is a set B such that $A \subset B \subset \overline{A}$, then B is $I_{|B}-$connected.

PROOF. Suppose that B is not $I_{|\mathrm{B}}-$connected. Then, there are non-empty subsets $U, V \in \tau_{|\mathrm{B}}$ with $U \cap V \in I_{|B}$ such that $B = U \cup V$. Since A is an $I_{|A}-$connected subset of B, from Theorem 3.11 we know that either $A \subset U$ or $A \subset V$. It also happens that $A \cap U \in \tau_{|A}$, $A \cap V \in \tau_{|\mathrm{A}}$, $(A \cap U) \cap (A \cap V) = A \cap (U \cap V) \in I_{|A}$, and $A = A \cap (U \cup V) = (A \cap U) \cup (A \cap V)$. Now let's consider three different cases of $A \cap U$ and $A \cap V$.

Case 1. If $A \cap U \neq \emptyset$ and $A \cap V \neq \emptyset$, then A is not $I_{|A}-$connected, it contradicts the fact that A is a $I_{|A}$ connected.

Case 2. In the case of $A \cap U = \emptyset$ and $A \cap V \neq \emptyset$. By the definition of $\overline{A}$, for any $x \in A$, $A \cap W \neq \emptyset$ for every neighborhood W of the point x. Since every point of B is an element of $\overline{A}$, the intersection of A with the neighborhood of any of these points will be different from the empty set. Therefore, if $A \cap U = \emptyset$, then $U = \emptyset$ must be. This is a contradiction. A similar contradiction is obtained if $A \cap U \neq \emptyset$ and $A \cap V = \emptyset$.

Case 3. If $A \cap U = \emptyset$ and $A \cap V = \emptyset$, then A is an empty set. This is a contradiction.

Consequently, our assumption is not true, and the set B is $I_{|B}-$connected. □

Corollary 3.14. Let (X, τ, I) be an ideal topological space. If A is an $I_{|A}$-connected subset of X, then $\bar{A}$ is an $I_{|\bar{A}}$-connected subset of X.

PROOF. Let A be an $I_{|A}$-connected subset of X. From Theorem 3.13, we know every set B such that $A \subset B \subset \bar{A}$ is an $I_{|B}$-connected. Moreover, since $A \subset B$, then $\bar{A} \subset \bar{B}$ and $A \subset B \subset \bar{A} \subset \bar{B}$. Therefore, from Theorem 3.13 since $B \subset \bar{A} \subset \bar{B}$ and B is an $I_{|B}$-connected, then $\bar{A}$ is an $I_{|\bar{A}}$ -connected. □

Theorem 3.15. Let (X, τ, I) be an ideal topological space. If A is an $I_{|A}-$connected subset of X, then $cl^*(A)$ is $I_{cl^*(A)}-$connected.

PROOF. Since $A \subseteq cl^*(A) \subseteq \overline{A}$ in an ideal topological space (X, τ, I), then the proof is obvious from Theorem 3.13. □

Theorem 3.16. Let (X, τ, I) be an ideal topological space and $A \subset X$. If A is an $I_{|A}-$connected and dense subset of X, then X is an I-connected space.

PROOF. Let (X, τ, I) be an ideal topological space, A be an $I_{|A}$-connected, and a dense subset of X. Suppose that X is not I-connected. Then, there exist $U, V \in \tau$ such that $U \neq \emptyset, V \neq \emptyset, U \cap V \in I$, and $X = U \cup V$. Moreover, since A is a dense subset of X, then $\bar{A} = X$. Thus, $W \cap A \neq \emptyset$, for all $W \in \tau$. Besides, since $\tau_{|A} := \{G \cap A : G \in \tau\}$, then $A \cap U \in \tau_{|A}, A \cap V \in \tau_{|A}, A \cap U \neq \emptyset$, and $A \cap V \neq \emptyset$. Furthermore, from $I_{|A} := \{H \cap A : H \in I\}$, since $U \cap V \in I$, then $(A \cap U) \cap (A \cap V) \in I_{|A}$. Additionally, since $A \subset X$ and $X = U \cup V$, then $A \subset U \cup V$ and so $A = A \cap (U \cup V) = (A \cap U) \cup (A \cap V)$. Consequently, since there exist $A \cap U \in \tau_{|A}, A \cap V \in \tau_{|A}$ such that $A \cap U \neq \emptyset, A \cap V \neq \emptyset, A \cap (U \cap V) \in I_{|A}$ and $A = (A \cap U) \cup (A \cap V)$, then A is not $I_{|A}$-connected. Hence, this is a contradiction. Therefore, X is an I-connected space. □

The following theorem will show us the necessary and sufficient conditions for a subspace $A \subset X$ to be $I_{|A}$-connected.

Theorem 3.17. Let A be a subset of an ideal topological space (X, τ, I). Then, A is $I_{|A}-$connected if and only if for every $U, V \in \tau$, $A \subset U \cup V$, $A \cap U \neq \emptyset$, and $A \cap V \neq \emptyset$ such that $A \cap U \cap V \notin I$.

Proof. $\Rightarrow$: Let A be $I_{|A}$-connected, for $U, V \in \tau, A \subset U \cup V, A \cap U \neq \emptyset$ and $A \cap V \neq \emptyset$. Suppose that $A \cap U \cap V \in I$. Therefore, there exist $A \cap U \in \tau_{|A}, A \cap V \in \tau_{|A}$ such that $A \cap U \neq \emptyset, A \cap V \neq \emptyset, A \cap (U \cap V) \in I_{|A}$ and $A = (A \cap U) \cup (A \cap V)$, then A is not $I_{|A}$-connected. Thus, this is a contradiction. Hence, $A \cap U \cap V \notin I$.
$\Leftarrow$: Let for every $U, V \in \tau, A \subset U \cup V, A \cap U \neq \emptyset$, and $A \cap V \neq \emptyset$ such that $A \cap U \cap V \notin I$. Therefore, there exist $A \cap U \in \tau_{|A}, A \cap V \in \tau_{|A}$ such that $A \cap U \neq \emptyset, A \cap V \neq \emptyset, A = A \cap (U \cup V) = (A \cap U) \cup (A \cap V)$, and $(A \cap U) \cup (A \cap V) \notin I$. Then, A is $I_{|A}$-connected. □

Example 3.18. Let $X = \{a, b, c, d\}$, $\tau = \{\emptyset, X, \{a\}, \{a, b\}\}$, and $A = \{a, b, c\}$. If $I = \{\emptyset, \{c\}\}$, then A is an $I_{|A}-$connected subset of X. If $I = \{\emptyset, \{a\}\}$, then A is not an $I_{|A}-$connected subset of X.

Theorem 3.19. Let (X, τ_1, I) and (Y, τ_2, J) be ideal topological spaces, f be a homeomorphism from X to a dense subset of Y with $J = f(I)$, that is, Y be a compactification of X. If (X, τ, I) is $I-$connected, then (Y, φ, J) is $J-$connected.

Proof. Let (Y, τ_2, J) be a compactification of (X, τ_1, I). Then, there is a homeomorphism $f : X \to A$ such that $\overline{A} = Y$. Since f is bijective and ideal topological space (X, τ, I) is $I-$connected, then from Theorem 3.8 an ideal topological space (Y, τ_2, J) is $J-$connected. □

Corollary 3.20. There is only one I-component of an I-connected space, and that is the space itself.

Corollary 3.21. Let A be an I-component of (X, τ, I). Then, A is a component of (X, τ).

Theorem 3.22. If A is an I-component of (X, τ, I) and $\tau \sim I$, then A is a component of (X, τ^*).

Proof. Let A be a maximal $I_{|A}-$connected subspace of (X, τ). In other words, the space (A, τ_A) is maximal $I_{|A}-$connected subspace of (X, τ). Since $\tau \sim I$, then from Theorem 3.5, A is a maximal $I_{|A}-$connected subspace of (X, τ^*). □

Theorem 3.23. Every I-component of the ideal topological space (X, τ, I) is closed.

Proof. Let A be an I-component of the ideal topological space (X, τ, I). Since A is $I_{|A}-$connected, then from Corollary 3.14, $\overline{A}$ is $I_{|\overline{A}}-$connected. Since A is a maximal $I_{|A}-$connected subset of X, then $\overline{A} \subseteq A$. Moreover, $A \subseteq \overline{A}$. Thus, $A = \overline{A}$. □

Definition 3.24. Let (X, τ, I) be an ideal topological space. For each pair of distinct points $x, y \in X$, if there is a pair of open neighborhoods U and V of x and y such that $U \cap V \in I$ and $X = U \cup V$, then X is called totally I-disconnected.

Corollary 3.25. Every totally disconnected space is totally I-disconnected.

Theorem 3.26. If an ideal topological space (X, τ, I) is totally I-disconnected the I-components in X are the one-point sets.

Proof. Let (X, τ, I) be a totally I-disconnected space and C be an I-component of this space. Suppose that I-component C contains more than one point. Here, let $x \neq y \in C$. Since the ideal topological space (X, τ, I) is totally I-disconnected, then there exist $U, V \in \tau$ such that $x \in U, y \in V$, $U \cap V = \emptyset$, $X = U \cup V$, and $U \cap V \in I$. Since C is I-component of this space, $C \subset U \cup V$, $C \cap U \neq \emptyset$, $C \cap V \neq \emptyset$ and $C \cap (U \cap V) \subseteq U \cap V \in I$. Then, from Theorem 3.17. C is not $I_{|c}-$connected. Thus, C cannot be an I-component, then our assumption is wrong. Hence, C is the one-point set.

□

Definition 3.27. Let (X, τ, I) be an ideal topological space. For all $V \in \tau$ such that $x \in V$, if there exist an I-connected open subset U such that $x \in U$ and $U \subset V$, then (X, τ, I) is called locally I-connected at x.
An ideal topological space (X, τ, I) is called locally I-connected if it is locally connected at x for every $x \in X$.

Theorem 3.28. Every I-component of a locally I-connected space is an open set.

PROOF. Let C be an I-component of a locally I-connected space (X, τ, I) and x be an arbitrary point of C. Since (X, τ, I) is locally I-connected and X is an open neighborhood of x, x belongs to an I-connected open set U of X. Therefore, since C is an I-component, then C is maximal I- connected subset of X, and so $x \in U \subset C$. Hence, C is a neighborhood of each of its points and so C is an open set. □

Theorem 3.29. If an ideal topological space (X, τ, I) is a locally I-connected, then the I-components of every open subspace of (X, τ, I) are open in X.

PROOF. Let (X, τ, I) be locally I-connected. Let Y be an open set in X and C be an I-component of Y. Then by the definition of locally I-connectednes for every $x \in C$, there exists an I-connected open set U in Y containing x. Since C is an I-component, then $U \subset C$. Thus, C contains a neighborhood of each of its points in Y and so C is open in Y. Since Y is open in X, thus C is open in X. □

Corollary 3.30. Every I-component of a locally I-connected space is both closed and open.

Theorem 3.31. Let $f : (X, \tau, I) \to (Y, \varphi, f(I))$ be a homeomorphism. If (X, τ, I) is locally I-connected, then $(Y, \varphi, f(I))$ is locally $f(I)-$connected.

PROOF. Let $f : (X, \tau, I) \to (Y, \varphi, f(I))$ be a homeomorphism. Let y be a point of $f(X) = Y$ and V be any open neighborhood of y in Y. Also, there exists $x \in X$ such that $y = f(x)$. As f is continuous, then $f^{-1}(V)$ is an open neighborhood of x. Since (X, τ, I) is locally I-connected, then there exist I-connected open $U \in \tau$ such that $x \in U \subset f^{-1}(V)$. Thus,

$$y = f(x) \in f(U) \subset f\left(f^{-1}(V)\right) = V$$

Since f is an open map, then $f(U)$ is an open subset of Y. From Theorem 3.8, $f(U)$ is $f(I)$-connected. Consequently, Y is locally $f(I)$-connected. □

4. Conclusion

In this paper, we defined the concept of I-connectedness in ideal topological spaces. Then, we examined the relationship between connectedness and I-connectedness. We shown that every not connected space is not I-connected and the opposite is not true. We shown that some basic properties of connectedness are valid in I-connectedness. Next, we put forward the definitions of I-component, totally I-disconnectedness, and locally I-connectedness. We revealed some of their basic properties.

The relations of I-connectedness defined here in with other types of connectedness previously defined in ideal topological spaces, can be investigated. In addition, the relationship between I-connectedness and $*$-Hyperconnectedness in ideal topological spaces [11] can also be examined. Furthermore, [12] have defined I-extremally disconnected spaces and have revealed the connection of this connectedness concerning some weak continuity varieties. A similar study can also be conducted on the I-connectedness defined here in.

Author Contributions

The author read and approved the last version of the paper.

Conflicts of Interest

The author declares no conflict of interest.

References

[1] R. Vaidyanathaswamy, *The Localisation Theory in Set Topology*, Proceedings of the Indian Academy of Sciences 20 (1945) 51-61.

[2] K. Kuratowski, *Topology*, Volume I, Academic Press, New York, 1966.

[3] E. Ekici, T. Noiri, *Connectedness in Ideal Topological Spaces*, Novi Sad Journal of Mathematics 38 (2) (2008) 65–70.

[4] N. Sathiyasundari, V. Renukadevi, *Note on $*$-Connected Ideal Spaces*, Novi Sad Journal of Mathematics 42 (1) (2012) 15–20.

[5] S. Modak, T. Noiri, *Connectedness of Ideal Topological Spaces*, Filomat 29 (4) (2015) 661–665.

[6] S. Kilinc, *More on $*_*$-Connectedness*, Matematichki Bilten 43 (2) (2019) 53-60.

[7] B. K. Tyagi, M. Bhardwaj, S. Singh, *Cl*-Connectedness and Cl-Cl*-Connectedness in Ideal Topological Spaces*, Matematichki Bilten 42 (2) (2018) 91–100.

[8] D. Jankovic, T. R. Hamlett, *New Topologies from Old via Ideals*, The American Mathematical Monthly 97(4) (1990) 295–310.

[9] O. Njåstad, *Remarks on Topologies Defined by Local Properties*, Avhandlinger Norske Videnskaps-Akademi Oslo, Universitetsforlaget, 1966.

[10] R. L. Newcomb, *Topologies Which are Compact Modulo an Ideal*, PhD Dissertation, University of California (1967) Santa Barbara, USA.

[11] E. Ekici, T. Noiri, *$*$-Hyperconnected Ideal Topological Spaces*, Analele Stiintifice ale Universitatii Al I Cuza din lasi-Matematica, Tomul 58 (1) (2012) 121–129.

[12] A. Keskin, Ş. Yüksel, T. Noiri, *On I-Extremally Disconnected Spaces*, Communications Faculty of Sciences University of Ankara Series A1 Mathematics and Statistics 56 (1) (2007) 33–40.

Journal of
New Theory
ISSN: 2149-1402

39 (2022) 8-18
Journal of New Theory
https://dergipark.org.tr/en/pub/jnt
Open Access

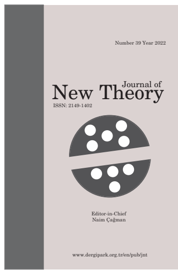

Smarandache-Based Ruled Surfaces with the Darboux Vector According to Frenet Frame in E^3

Süleyman Şenyurt[1], **Davut Canlı**[2], **Elif Çan**[3]

Article Info
Received: 20 Apr 2022
Accepted: 27 Jun 2022
Published: 30 Jun 2022
doi:10.53570/jnt.1106331
Research Article

Abstract — The paper introduces a new kind of special ruled surface. The base of each ruled surface is taken to be one of the Smarandache curves of a given curve according to Frenet frame, and the generator (ruling) is chosen to be the corresponding unit Darboux vector. The characteristics of these newly defined ruled surfaces are investigated by means of first and second fundamental forms and their corresponding curvatures. An example is provided by considering both the helix curve and the Viviani's curve.

Keywords — *Ruled surfaces, Smarandache curve, fundamental forms, curvatures, developable and minimal surfaces*

Mathematics Subject Classification (2020) — 53A04, 53A05

1. Introduction

A surface is defined as an image of a function with two real valued variables (domain) by a mapping to two or three dimensional space. The surfaces are characterized by means of their curvatures and accordingly they are used in many areas such as engineering, architectural designs, computer graphics, automobile industry, etc. Researches on surface curvature went through various stages starting from Ancient Greece, and gained momentum with the calculations developed by Newton and Leibniz in the 17th century after the studies of Descartes, Kepler, Fermat and Huygens. The curvature theory for curves and surfaces is an important subject of differential geometry. The theory was first introduced by Gauss in 19th century and it was named by his name as the Gaussian curvature. It is related to the dimensions of the surface. The developability of a surface can be determined by its Gaussian curvature. A surface with zero Gaussian curvature at every point is known as a developable surface. Another kind of curvature for a surface is named as mean curvature. Since a mean curvature corresponds to a ratio, it is independent of the size of the surfaces. Surfaces with a mean curvature of zero at every point are known as minimal surfaces. In the theory of surfaces, there is a special kind that is known as ruled surfaces. A ruled surface is constructed by infinitely many straight lines moving along a given curve. Among other types, the ruled surfaces are mostly referred in computer based geometric designs to deal with real world problems on modeling the real objects. For this reason, introducing new ruled surfaces may lead new potentials to the related fields. Providing their characteristics by means of curvatures may also enable easy adaptations for interested researchers.

The basic theory related to ruled surfaces can be found in many differential geometry textbooks such as [1–4]. However, the generalization of those was first studied by Juza in the 1960s [5]. The ruled surfaces with rulings of Frenet vectors are already covered in textbooks. Apart from Frenet frame,

[1]senyurtsuleyman52@gmail.com (Corresponding Author); [2]davutcanli@odu.edu.tr; [3]eliff.cann@hotmail.com
[1,2,3]Department of Mathematics, Faculty of Arts and Sciences, Ordu University, Ordu, Turkiye

Şentürk and Yüce (2015) examined the characterizations of ruled surfaces with Darboux frame in [6]. Tunçer (2015) in [7] and Masal and Azak (2019) in [8], separately, studied some characteristics of the ruled surfaces according to Bishop frame (introduced by Bishop, (1975) in [9]), whereas Ouarab et al. (2018) provided the main properties of ruled surfaces according to alternative frame in [10]. Moreover, some characteristics of the ruled surface with Frenet frame of a non-cylindrical one were investigated in 2020 by Ouarab and Chahdi in [11].
Recently, Ouarab, (2021a) put forth a method to generate new ruled surfaces by taking the advantage of the idea of Smarandache geometry introduced in [12, 13]. By assigning the base curve as one of the Smarandache curves and taking the generator as the another vector element of Frenet frame, she introduced these ruled surfaces as Smarandache ruled surfaces according to Frenet frame in [14]. The same method of generating such ruled surfaces is applied to the Darboux frame by Ouarab, (2021b) in [15] and according to the alternative frame by Ouarab, (2021c) in [16].
Motivated by these studies and acknowledging the great potential use of ruled surfaces, it is of interest for us to define and introduce new kinds of ruled surfaces incorporated with the Darboux vector and Smarandache curves. The geometric properties of these have been examined by means of fundamental forms and the corresponding curvatures.

2. Preliminaries

In this section, we recall some basic notions of which we refer through out the paper. Let $\alpha : I \to E^3$ be a regular unit speed curve. We define the quantities of the Frenet apparatus and Frenet formulae as in the following way:

$$T = \alpha', \;\; N = \frac{\alpha''}{\|\alpha''\|}, \;\; B = T \wedge N, \;\; \kappa = \left\|\alpha''\right\|, \;\; \tau = \left\langle N', B \right\rangle$$
$$T' = \kappa N, \;\; N' = -\kappa T + \tau B, \;\; B' = -\tau N$$

The Darboux vector W of Frenet frame is defined as $W = \tau T + \kappa B$. Corresponding to this, the unit Darboux vector is

$$C = \sin\omega\, T + \cos\omega B$$
$$\cos\omega = \frac{\kappa}{\sqrt{\kappa^2+\tau^2}}, \quad \sin\omega = \frac{\tau}{\sqrt{\kappa^2+\tau^2}}, \quad \omega' = \left(\frac{\tau}{\kappa}\right)'\left(1+\frac{\tau^2}{\kappa^2}\right) \tag{1}$$

where $\omega = \angle(B, W)$. Moreover, a unit vector with a linear combination of Frenet vectors can be defined as

$$\gamma = \frac{fT + gN + hB}{\sqrt{f^2+g^2+h^2}} \tag{2}$$

where $f, \; g, \; h : \Re \to \Re$ are some arbitrary functions. For $\forall s \in I \subset \Re$, the image of the vector γ is a special differentiable curve. If, specifically, each function $f, \; g$ and h is considered to be a constant valued function and the vector γ is taken to be the position vector, then the generated curves are known to be the special Smarandache curves [12]. These curves were outlined in many studies by using different frames and considering different spaces, as well [4, 13, 17–23].
On the other hand, a surface is said to be ruled if it is formed with a straight line $r(s)$ sharing the same parameter of the given curve α. The parametric form of a ruled surface is as following:

$$X(s, v) = \alpha(s) + vr(s) \tag{3}$$

The unit normal vector field of a ruled surface $X(s, v)$ is computed as

$$\mathrm{N}_X = \frac{X_s \wedge X_v}{\|X_s \wedge X_v\|} \tag{4}$$

and are the curvatures as:

$$K = -\frac{f^2}{EG - F^2} \quad \text{and} \quad H = \frac{eG - 2fF}{2\left(EG - F^2\right)} \tag{5}$$

where the corresponding coefficients are defined by

$$\begin{aligned} E &= \langle X_s, X_s \rangle, \quad F = \langle X_s, X_v \rangle, \quad \text{and} \quad G = \langle X_v, X_v \rangle \\ e &= \langle X_{ss}, N_X \rangle, \quad f = \langle X_{sv}, N_X \rangle, \quad \text{and} \quad g = \langle X_{vv}, N_X \rangle \end{aligned} \tag{6}$$

3. Smarandache ruled surfaces by Darboux vector according to Frenet frame in $\mathbf{E}^3$

In this section, we define and examine some special ruled surfaces where the base curve is considered to be one of the Smarandache curves of $\alpha = \alpha(s)$ which we define them by referring the equation (2) as:

if $h = 0$ and $f = g = 1$ $\Rightarrow$ the vector $\gamma = \dfrac{T+N}{\sqrt{2}}$ draws the TN-Smarandache curve that is $\gamma_1 = \dfrac{T+N}{\sqrt{2}}$

if $g = 0$ and $f = h = 1$ $\Rightarrow$ the vector $\gamma = \dfrac{T+B}{\sqrt{2}}$ draws the TB-Smarandache curve that is $\gamma_2 = \dfrac{T+B}{\sqrt{2}}$

if $f = 0$ and $g = h = 1$ $\Rightarrow$ the vector $\gamma = \dfrac{N+B}{\sqrt{2}}$ draws the NB-Smarandache curve that is $\gamma_3 = \dfrac{N+B}{\sqrt{2}}$

if $f = g = h = 1$ $\Rightarrow$ the vector $\gamma = \dfrac{T+N+B}{\sqrt{3}}$ draws the TNB-Smarandache curve that is $\gamma_4 = \dfrac{T+N+B}{\sqrt{3}}$

and the generator for each ruled surface is taken to be the unit Darboux vector C given by the relation (1).

Definition 3.1. The ruled surface generated by unit Darboux vector C along the TN- Smarandache curve γ_1 is given as

$$\Phi(s,v) = \frac{1}{\sqrt{2}}(T+N) + vC$$

The first and second partial derivatives of the surface Φ are given in respective order as follows:

$$\begin{cases} \Phi_s = \dfrac{1}{\sqrt{2}}\left(\left(-\kappa + \sqrt{2}v\omega'\cos\omega\right)T + \kappa N + \left(\tau - \sqrt{2}v\omega'\sin\omega\right)B\right) \\ \Phi_{ss} = \dfrac{1}{\sqrt{2}}\left\{\begin{array}{l} \left(\left(-\kappa + \sqrt{2}v\omega'\cos\omega\right)' - \kappa^2\right)T + \left(\left(\tau - \sqrt{2}v\omega'\sin\omega\right)' + \kappa\tau\right)B \\ + \left(-\left(\kappa^2+\tau^2\right) + v\omega'\sqrt{2\kappa^2+2\tau^2}\right)N \end{array}\right\} \\ \Phi_{sv} = \omega'\left(\cos\omega T - \sin\omega B\right), \quad \Phi_v = \sin\omega T + \cos\omega B, \quad \Phi_{vv} = 0 \end{cases}$$

By considering (4), we first compute

$$\Phi_s \wedge \Phi_v = \frac{1}{\sqrt{2}}\left(\kappa\cos\omega T + \left(\sqrt{\kappa^2+\tau^2} - \sqrt{2}v\omega'\right)N - \kappa\sin\omega B\right)$$

$$\|\Phi_s \wedge \Phi_v\| = \frac{1}{\sqrt{2}}\sqrt{2\kappa^2 + \tau^2 - v\omega'\sqrt{2\kappa^2+2\tau^2} + 2(v\omega')^2}$$

to provide the unit normal vector as

$$N_\Phi = \frac{\kappa\cos\omega T + \left(\sqrt{\kappa^2+\tau^2} - \sqrt{2}v\omega'\right)N - \kappa\sin\omega B}{\sqrt{2\kappa^2+\tau^2 - v\omega'\sqrt{2\kappa^2+2\tau^2} + 2(v\omega')^2}}$$

From (6), the coefficients of the first and second fundamental forms are

$$E_\Phi = \frac{1}{2}\left(2\kappa^2 + \tau^2 - 2\sqrt{2}v\omega'\sqrt{\kappa^2+\tau^2} + 2\big(v\omega'\big)^2\right), \quad F_\Phi = 0, \quad G_\Phi = 1$$

$$e_\Phi = \frac{-\kappa\left(\sqrt{\kappa^2+\tau^2}\right)' - \kappa\left(\kappa^2+\tau^2\right)^{\frac{3}{2}} + \sqrt{2}v\kappa\left(\omega'' + 2\omega'\left(\kappa^2+\tau^2\right)\right) - 2v^2\omega'^2\kappa\sqrt{\kappa^2+\tau^2}}{\sqrt{2}\sqrt{2\kappa^2+\tau^2 - v\omega'\sqrt{2\kappa^2+2\tau^2} + 2(v\omega')^2}}$$

$$f_\Phi = \frac{\omega'\kappa}{\sqrt{2\kappa^2+\tau^2 - v\omega'\sqrt{2\kappa^2+2\tau^2} + 2(v\omega')^2}}, \quad g_\Phi = 0$$

Thus, by using (5) we compute the mean and Gaussian curvatures as following:

$$K_\Phi = -2\left(\frac{\omega'\kappa}{2\kappa^2+\tau^2 - v\omega' 2\sqrt{2}\sqrt{\kappa^2+\tau^2} + 2(v\omega')^2}\right)^2$$

$$H_\Phi = \frac{-\kappa\left(\sqrt{\kappa^2+\tau^2}\right)' - \kappa\left(\kappa^2+\tau^2\right)^{\frac{3}{2}} + \sqrt{2}v\kappa\left(\omega'' + 2\omega'\left(\kappa^2+\tau^2\right)\right) - 2v^2\omega'^2\kappa\sqrt{\kappa^2+\tau^2}}{\sqrt{2}\left(2\kappa^2+\tau^2 - v\omega' 2\sqrt{2}\sqrt{\kappa^2+\tau^2} + 2(v\omega')^2\right)^{\frac{3}{2}}}$$

Corollary 3.2. If the curve $\alpha = \alpha(s)$ is planar or general helix, then the surface Φ is developable.

PROOF. From (1), $\omega' = \left(\frac{\tau}{\kappa}\right)'\left(1 + \frac{\tau^2}{\kappa^2}\right)$. If α is either planar or general helix, then $\omega' = 0$ which corresponds to that $K_\Phi = 0$. □

Definition 3.3. Another ruled surface generated by unit Darboux vector C along the TB- Smarandache curve γ_2 is given as

$$\Psi(s,v) = \frac{1}{\sqrt{2}}(T+B) + vC$$

The first and second partial derivatives of $\Psi(s,v)$ are given in respective order as follows:

$$\begin{cases} \Psi_s = v\omega'\cos\omega T + \dfrac{\kappa-\tau}{\sqrt{2}}N - v\omega'\sin\omega B \\ \Psi_{ss} = \left(\left(v\omega'\cos\omega\right)' - \dfrac{\kappa^2-\kappa\tau}{\sqrt{2}}\right)T + \left(v\omega'\sqrt{\kappa^2+\tau^2} + \dfrac{\kappa'-\tau'}{\sqrt{2}}\right)N \\ \quad + \left(\left(-v\omega'\sin\omega\right)' + \dfrac{\kappa\tau-\tau^2}{\sqrt{2}}\right)B \\ \Psi_{sv} = \omega'\cos\omega T - \omega'\sin\omega B, \quad \Psi_v = \sin\omega T + \cos\omega B, \quad \Psi_{vv} = 0 \end{cases}$$

By considering (4), we first compute

$$\Psi_s \wedge \Psi_v = \frac{(\kappa-\tau)\cos\omega}{\sqrt{2}}T - v\omega' N - \frac{(\kappa-\tau)\sin\omega}{\sqrt{2}}B$$

$$\|\Psi_s \wedge \Psi_v\| = \frac{1}{\sqrt{2}}\sqrt{(\kappa-\tau)^2 + 2(v\omega')^2}$$

to get the unit normal vector denoted by N_Φ as

$$N_\Psi = \frac{(\kappa-\tau)\cos\omega T - \sqrt{2}v\omega' N - (\kappa-\tau)\sin\omega B}{\sqrt{(\kappa-\tau)^2 + 2(v\omega')^2}}$$

Next, by using (6), the coefficients of the first and second fundamental forms are

$$E_\Psi = \frac{1}{2}\left((\kappa-\tau)^2 + 2\left(v\omega'\right)^2\right), \quad F_\Psi = 0, \quad G_\Psi = 1$$

$$e_\Psi = \frac{\sqrt{2}(v\omega')'(\kappa-\tau) - \sqrt{\kappa^2+\tau^2}\left(2(v\omega')^2 + (\kappa-\tau)^2\right) - \sqrt{2}v\omega'(\kappa'-\tau')}{\sqrt{2}\sqrt{(\kappa-\tau)^2 + 2(v\omega')^2}}$$

$$f_\Psi = \frac{\omega'(\kappa-\tau)}{\sqrt{(\kappa-\tau)^2 + 2(v\omega')^2}}, \quad g_\Psi = 0.$$

Thus, from (5) the mean and Gaussian curvatures can be written as in the following way:

$$K_\Psi = -2\left(\frac{\omega'(\kappa-\tau)}{(\kappa-\tau)^2 + 2v^2\omega'^2}\right)^2, \qquad \kappa-\tau \neq 0,$$

$$H_\Psi = \frac{\sqrt{2}(\kappa-\tau)(v\omega')' - \sqrt{\kappa^2+\tau^2}\left(2(v\omega')^2 + (\kappa-\tau)^2\right) - \sqrt{2}v\omega'(\kappa'-\tau')}{\sqrt{2}\left((\kappa-\tau)^2 + 2(v\omega')^2\right)^{\frac{3}{2}}}$$

Corollary 3.4. If the curve $\alpha = \alpha(s)$ is planar or general helix, then the surface Ψ is developable.

Proof. The proof is as same as of the proof of Corollary 3.2 □

Definition 3.5. The ruled surface generated by unit Darboux vector C along the NB- Smarandache curve γ_3 is given as

$$\Omega(s,v) = \frac{1}{\sqrt{2}}(N+B) + vC$$

The first and second partial derivatives of $\Psi(s,v)$ are given in respective order as follows:

$$\begin{cases} \Omega_s = \left(-\frac{\kappa}{\sqrt{2}} + v\omega'\cos\omega\right)T - \frac{\tau}{\sqrt{2}}N + \left(\frac{\tau}{\sqrt{2}} - v\omega'\sin\omega\right)B \\ \Omega_{ss} = \frac{1}{\sqrt{2}}\left(\begin{array}{l}\left(\kappa\tau - \kappa' + \sqrt{2}\left(v\omega'\cos\omega\right)'\right)T + \left(\sqrt{2}v\omega'\sqrt{\kappa^2+\tau^2} - \tau' - \kappa^2 - \tau^2\right)N \\ + \left(\tau' - \tau^2 - \sqrt{2}\left(v\omega'\sin\omega\right)'\right)B\end{array}\right) \\ \Omega_{sv} = \omega'\cos\omega T - \omega'\sin\omega B, \quad \Omega_v = \sin\omega T + \cos\omega B, \quad \Omega_{vv} = 0 \end{cases}$$

By considering (4), we first compute

$$\Omega_s \wedge \Omega_v = \frac{1}{\sqrt{2}}\left(-\tau\cos\omega T + \left(\sqrt{\kappa^2+\tau^2} - \sqrt{2}v\omega'\right)N + \tau\sin\omega B\right)$$

$$\|\Omega_s \wedge \Omega_v\| = \frac{1}{\sqrt{2}}\sqrt{\kappa^2 + 2\tau^2 - v\omega'\sqrt{2\kappa^2+2\tau^2} + 2(v\omega')^2}$$

to get the unit normal vector denoted by N_Φ as

$$N_\Omega = \frac{-\tau\cos\omega T + \left(\sqrt{\kappa^2+\tau^2} - \sqrt{2}v\omega'\right)N + \tau\sin\omega B}{\sqrt{\kappa^2 + 2\tau^2 - v\omega'\sqrt{2\kappa^2+2\tau^2} + 2(v\omega')^2}}$$

Next, by using (6), the coefficients of the first and second fundamental forms are

$$E_\Omega = \frac{\kappa^2+2\tau^2}{2} + \left(v\omega'\right)^2 - \sqrt{2\kappa^2+2\tau^2}v\omega', \quad F_\Omega = 0, \quad G_\Omega = 1$$

$$e_\Omega = \frac{\begin{array}{l}\tau\left(\sqrt{\kappa^2+\tau^2}-\sqrt{2}v\omega'\right)' - \tau^2\sqrt{\kappa^2+\tau^2} \\ \quad + \left(\sqrt{\kappa^2+\tau^2}-\sqrt{2}v\omega'\right)\left(v\omega'\sqrt{2}\sqrt{\kappa^2+\tau^2}-\tau'-\kappa^2-\tau^2\right)\end{array}}{\sqrt{2}\sqrt{\kappa^2+2\tau^2-v\omega'\sqrt{2\kappa^2+2\tau^2}+2(v\omega')^2}}$$

$$f_\Omega = -\frac{\omega'\tau}{\sqrt{\kappa^2+2\tau^2-v\omega'\sqrt{2\kappa^2+2\tau^2}+2(v\omega')^2}}$$

Thus, from (5) the mean and Gaussian curvatures can be written as in the following way:

$$K_\Omega = -2\left(\frac{\omega'\tau}{\kappa^2+2\tau^2+2(v\omega')^2 - v\omega' 2\sqrt{2\kappa^2+2\tau^2}}\right)^2$$

$$H_\Omega = \frac{\begin{array}{l}\tau\left(\sqrt{\kappa^2+\tau^2}-\sqrt{2}v\omega'\right)' - \tau^2\sqrt{\kappa^2+\tau^2} \\ \quad + \left(\sqrt{\kappa^2+\tau^2}-\sqrt{2}v\omega'\right)\left(v\omega'\sqrt{2}\sqrt{\kappa^2+\tau^2}-\tau'-\kappa^2-\tau^2\right)\end{array}}{\sqrt{2}\left(\kappa^2+2\tau^2+2(v\omega')^2-\sqrt{2\kappa^2+2\tau^2}v\omega'\right)^{\frac{3}{2}}}$$

Corollary 3.6. If the curve $\alpha = \alpha(s)$ is planar or general helix, then the surface Ω is developable.

Proof. The proof is the same as of the previous proofs. □

Definition 3.7. The ruled surface generated by unit Darboux vector C along the TNB- Smarandache curve γ_4 is given as:

$$\xi(s,v) = \frac{1}{\sqrt{3}}(T+N+B) + vC$$

The first and second partial derivatives of $\Psi(s,v)$ are given in respective order as follows:

$$\begin{cases} \xi_s = \left(-\frac{\kappa}{\sqrt{3}} + v\omega'\cos\omega\right)T + \frac{\kappa-\tau}{\sqrt{3}}N + \left(\frac{\tau}{\sqrt{3}} - v\omega'\sin\omega\right)B \\ \xi_{ss} = \begin{array}{l}\left(\left(-\frac{\kappa}{\sqrt{3}} + v\omega'\cos\omega\right)' - \frac{\kappa^2-\kappa\tau}{\sqrt{3}}\right)T + \left(-\frac{\kappa^2+\tau^2-\kappa'+\tau'}{\sqrt{3}} + v\omega'\sqrt{\kappa^2+\tau^2}\right)N \\ + \left(\left(\frac{\tau}{\sqrt{3}} - v\omega'\sin\omega\right)' + \frac{\kappa\tau-\tau^2}{\sqrt{3}}\right)B\end{array} \\ \xi_{sv} = \omega'\cos\omega T - \omega'\sin\omega B, \quad \xi_v = \sin\omega T + \cos\omega B, \quad \xi_{vv} = 0 \end{cases}$$

By considering (4), we first compute

$$\xi_s \wedge \xi_v = \frac{1}{\sqrt{3}}\left((\kappa-\tau)\cos\omega T + \left(\sqrt{\kappa^2+\tau^2} - \sqrt{3}v\omega'\right)N - (\kappa-\tau)\sin\omega B\right)$$

$$\|\xi_s \wedge \xi_v\| = \frac{1}{\sqrt{3}}\sqrt{(\kappa-\tau)^2 + \left(\sqrt{\kappa^2+\tau^2} - \sqrt{3}v\omega'\right)^2}$$

to get the unit normal vector denoted by N_Φ as

$$N_\xi = \frac{(\kappa-\tau)\cos\omega T + \left(\sqrt{\kappa^2+\tau^2} - \sqrt{3}v\omega'\right)N - (\kappa-\tau)\sin\omega B}{\sqrt{(\kappa-\tau)^2 + \left(\sqrt{\kappa^2+\tau^2} - \sqrt{3}v\omega'\right)^2}}$$

Next, by using (6), the coefficients of the first and second fundamental forms are

$$E_\xi = \frac{1}{3}\left((\kappa-\tau)^2 + \left(\sqrt{\kappa^2+\tau^2} - \sqrt{3}v\omega'\right)^2\right), \quad F_\xi = 0, \quad G_\xi = 1$$

$$e_\xi = \frac{\begin{array}{c}\left(\kappa' - \tau' - \kappa^2 - \tau^2 + v\omega'\sqrt{3}\sqrt{\kappa^2+\tau^2}\right)\left(\kappa^2+\tau^2 - v\omega'\sqrt{3}\sqrt{\kappa^2+\tau^2}\right) \\ +(\kappa-\tau)\left(\sqrt{3}v\omega' - \sqrt{\kappa^2+\tau^2}\right)' - (\kappa-\tau)^2\sqrt{\kappa^2+\tau^2}\end{array}}{\sqrt{3}\sqrt{(\kappa-\tau)^2 + \left(\sqrt{\kappa^2+\tau^2} - \sqrt{3}v\omega'\right)^2}}$$

$$f_\xi = \frac{\omega'(\kappa-\tau)}{\sqrt{(\kappa-\tau)^2 + \left(\kappa^2+\tau^2 - \sqrt{3}v\omega'\right)^2}}, \quad g_\xi = 0$$

Thus, from (5) the mean and Gaussian curvatures can be written as in the following way:

$$K_\xi = -3\left(\frac{\omega'(\kappa-\tau)}{(\kappa-\tau)^2 + \left(\sqrt{\kappa^2+\tau^2} - \sqrt{3}v\omega'\right)^2}\right)^2$$

$$H_\xi = \frac{\begin{array}{c}\left((\kappa-\tau)' - \left(\kappa^2+\tau^2\right) + v\omega'\sqrt{3\kappa^2+3\tau^2}\right)\left(\kappa^2+\tau^2 - v\omega'\sqrt{3\kappa^2+3\tau^2}\right) \\ +(\kappa-\tau)\left(\sqrt{3}v\omega' - \sqrt{\kappa^2+\tau^2}\right)' - (\kappa-\tau)^2\sqrt{\kappa^2+\tau^2}\end{array}}{2\left(\sqrt{3}\right)^{-1}\left((\kappa-\tau)^2 + \left(\sqrt{\kappa^2+\tau^2} - \sqrt{3}v\omega'\right)^2\right)^{\frac{3}{2}}}$$

Corollary 3.8. If the curve $\alpha = \alpha(s)$ is planar or general helix, then the surface ξ is developable.

PROOF. The proof is the same as of the previous proofs. □

Example 3.9. Let us consider the well known Viviani's curve parameterized as

$$\gamma(t) = \left(a(1+cost), asint, 2asin\frac{1}{2}t\right), \quad t \in [-2\pi, 2\pi], \qquad [2]$$

For $a = 0.5$ and by changing the parameter as $t = 2s$, we easily represent the given Viviani's curve as in the following way

$$\alpha(s) = \left(\cos^2(s), \sin(s)\cos(s), \sin(s)\right) \quad s \in [-\pi, \pi]$$

Then, the Frenet apparatus of $\alpha = \alpha(s)$ are given as

$$T(s) = \frac{2}{\sqrt{2\cos(2s)+6}}\left(-\sin(2s), \cos(2s), \cos(s)\right)$$

$$N(s) = \frac{-1}{\sqrt{2\cos(2s)+6}\sqrt{6\cos(2s)+26}}\begin{pmatrix}\cos(4s) + 12\cos(2s) + 3 \\ \sin(4s) + 12\sin(2s) \\ 4\sin(s)\end{pmatrix}$$

$$B(s) = \frac{1}{\sqrt{6\cos(2s)+26}}\left(\sin(3s) + 3\sin(s), -\cos(3s) - 3\cos(s), 4\right)$$

$$\kappa = \frac{2\sqrt{3cos(2s)+13}}{(3+cos(2s))^{\frac{3}{2}}} \quad \text{and} \quad \tau = \frac{12cos(s)}{3cos(2s)+13}$$

and the unit Darboux vector is found by

$$C(s)=\begin{pmatrix}\dfrac{2\sqrt{2}\sin(s)^3\left(6\cos(s)^2+5\right)}{\sqrt{18\cos(2s)^4+207\cos(2s)^3+999\cos(2s)^2+2493\cos(2s)+2683}}\\ \dfrac{4\sqrt{2}\cos(s)\left(3\cos(s)^4-2\cos(s)^2-3\right)}{\sqrt{18\cos(2s)^4+207\cos(2s)^3+999\cos(2s)^2+2493\cos(2s)+2683}}\\ \dfrac{\sqrt{2}\left(3\cos(2s)^2+18\cos(2s)+35\right)}{\sqrt{18\cos(2s)^4+207\cos(2s)^3+999\cos(2s)^2+2493\cos(2s)+2683}}\end{pmatrix}$$

The figures of each ruled surface for $-0.5 \leq v \leq 0.5$ and $-\pi \leq s \leq \pi$ is presented in the following:

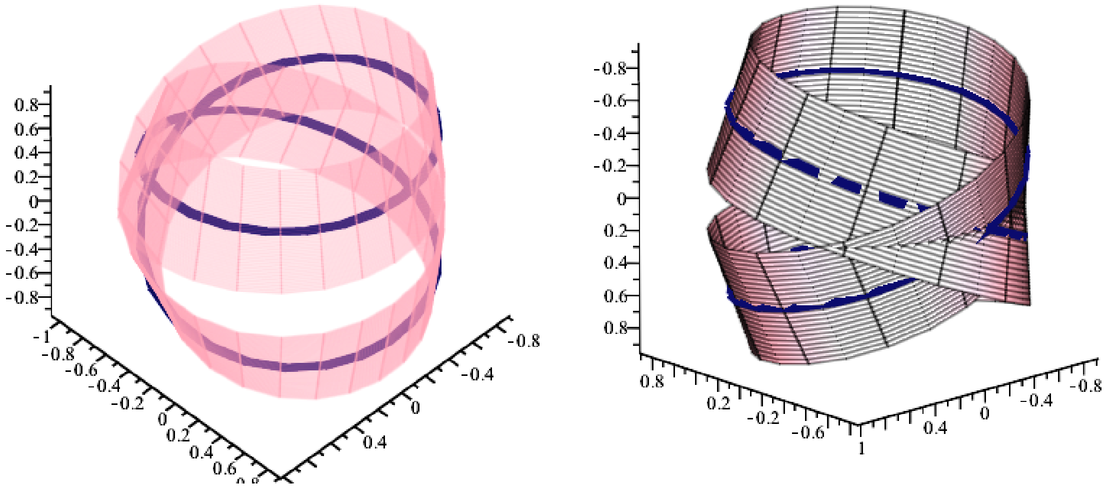

(a) Transparent (default view) **(b)** Solid (oriented)

Fig. 1. The ruled surface $\Phi(s, v)$ from different orientations

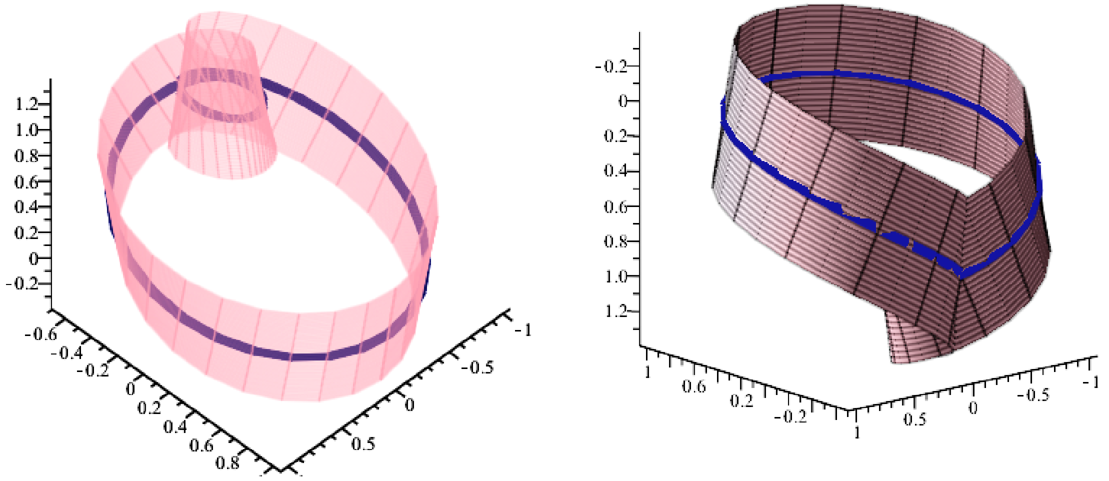

(a) Transparent (default view) **(b)** Solid (oriented)

Fig. 2. The ruled surface $\Psi(s, v)$ from different orientations

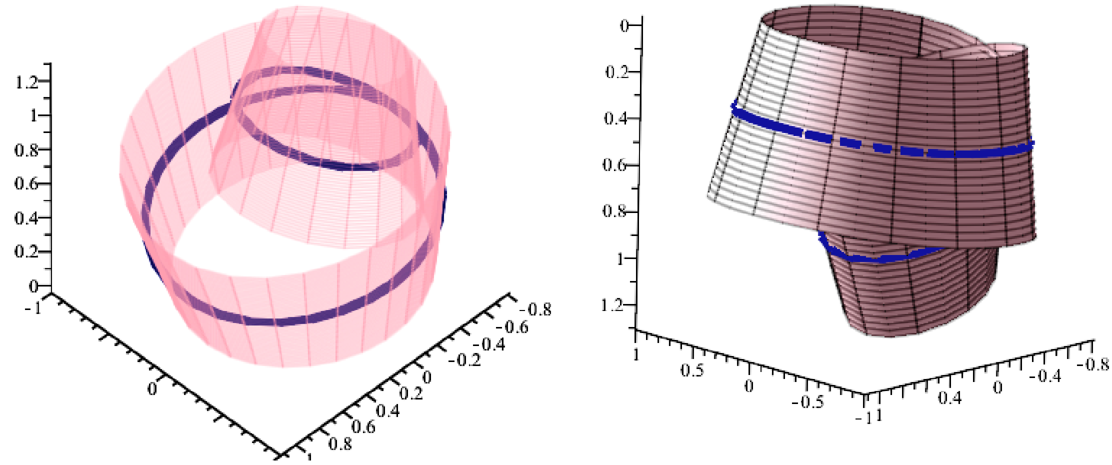

(a) Transparent (default view) **(b)** Solid (oriented)

Fig. 3. The ruled surface $\Omega(s, v)$ from different orientations

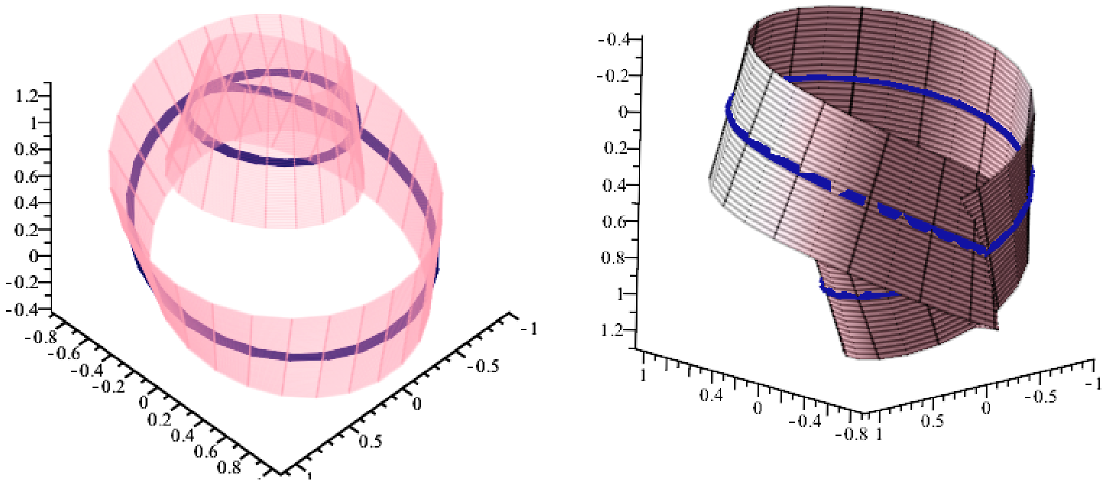

(a) Transparent (default view) **(b)** Solid (oriented)

Fig. 4. The ruled surface $\xi(s, v)$ from different orientations

Example 3.10. To generate a developable surface, we consider this time the regular unit speed circular helix parameterized as $\beta = \dfrac{1}{\sqrt{2}}\Big(\cos(s), \sin(s), s\Big)$.
The Frenet apparatus and the corresponding unit Darboux vector are given in following:

$$T(s) = \frac{1}{\sqrt{2}}\left(-\sin(s), \cos(s), 1\right) \quad \text{and} \quad N(s) = \left(-\cos(s), -\sin(s), 0\right)$$
$$B(s) = \frac{1}{\sqrt{2}}\left(\sin(s), -\cos(s), 1\right), \quad \kappa(s) = \tau(s) = \frac{1}{\sqrt{2}}, \quad \text{and} \quad C(s) = (0, 0, 1)$$

The figure (5) given below is the image of Φ, Ω, and ξ which simply corresponds to cylinder as a developable ruled surface for $-0.5 \leq v \leq 0.5$ and $-\pi \leq s \leq \pi$. However, the image of Ψ is simply a line the space, because the TB- Smarandache curve corresponds to a single point.

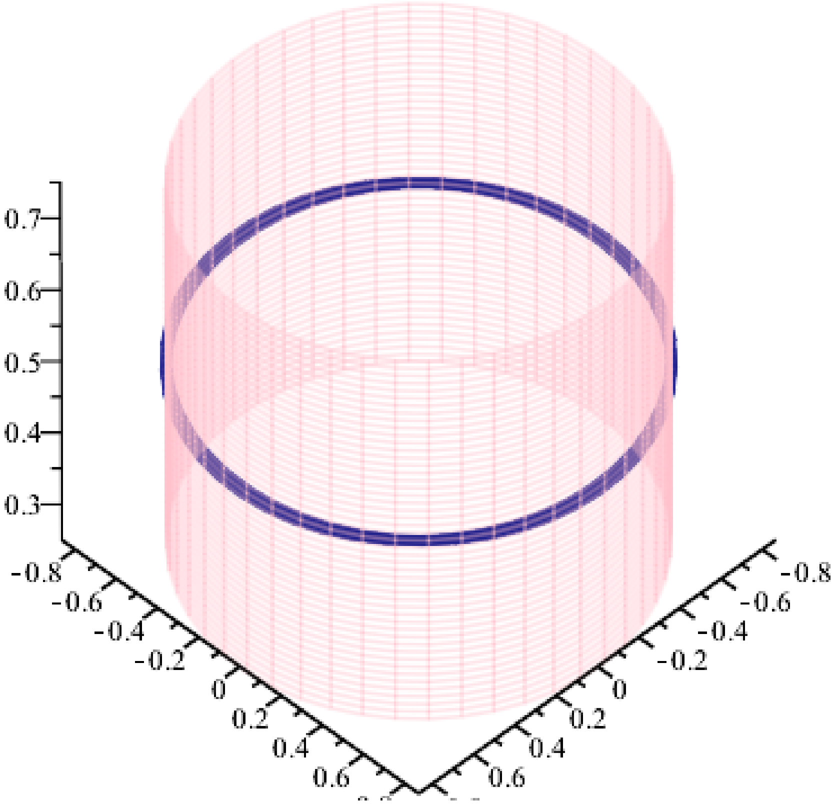

Fig. 5. The image as a developable ruled surface of each Φ, Ω, and ξ is same

4. Conclusion

Overall, in the paper, four new ruled surfaces based on Smarandache curves and ruled by unit Darboux vector have been introduced. The characteristics of each surface have been drawn. It is seen that the characteristics of surfaces are effected if the initial curve α is chosen to be a special curve general or circular helix.

Author Contributions

All authors contributed equally to this work. They all read and approved the last version of the paper.

Conflicts of Interest

The authors declare no conflict of interest.

References

[1] P. do-Carmo, Differential Geometry of Curves and Surfaces, Prentice Hall, Englewood Cliff, 1976.

[2] A. Gray E. Abbena, S. Salamon, Modern Differential Geometry of Curves and Surfaces with Mathematica, Chapman and Hall/CRC, New York, 2017.

[3] H. H. Hacısalihoğlu, Differential Geometry II, Ankara University Press, Ankara, 2000.

[4] D. J. Struik, Lectures on classical differential geometry, Addison-Wesley Publishing Company, 1961.

[5] M. Juza, *Ligne De Striction Sur Unegeneralisation a Plusieururs Dimensions D'une Surface Regle*, Czechoslovak Mathematical Journal 12 (1962) 243–250.

[6] G. Y. Şentürk, S. Yuce, *Characteristic Properties of Ruled Surface with Darboux Frame in E^3*, Kuwait Journal of Science 42 (2) (2015) 14–33.

[7] Y. Tunçer, *Ruled Surfaces with the Bishop Frame in Euclidean 3 Space*, General Mathematics Notes 26 (2015) 74–83.

[8] M. Masal, A. Z. Azak, *Ruled Surfaces according to Bishop Frame in the Euclidean 3-Space*, Proceedings of the National Academy of Sciences, India Section A: Physical Sciences 89 (2019) 415–424.

[9] R. L. Bishop *There is More Than One Way to Frame a Curve*, The American Mathematical Monthly 82 (1975) 246–251.

[10] S. Ouarab, A. O. Chahdi, M. Izid, *Ruled Surfaces with Alternative Moving Frame in Euclidean 3-Space*, International Journal of Mathematical Sciences and Engineering Applications 12 (2018) 43–58.

[11] S. Ouarab, A. O. Chahdi, *Some Characteristic Properties of Ruled Surface with Frenet Frame of an Arbitrary Non-Cylindrical Ruled Surface in Euclidean 3-Space*, International Journal of Applied Physics and Mathematics 10 (1) (2020) 16–24.

[12] M. Turgut, S. Yılmaz, *Smarandache Curves in Minkowski Spacetime*, International Journal of Mathematical Combinatorics 3 (2008) 51–55.

[13] A. T. Ali, *Special Smarandache Curves in the Euclidean Space*, International Journal of Mathematical Combinatorics 2 (2010) 30–36.

[14] S. Ouarab, *Smarandache Ruled Surfaces according to Frenet-Serret Frame of a Regular Curve in E^3*, Abstract and Applied Analysis Hindawi 2021 Article ID: 5526536.

[15] S. Ouarab, *Smarandache Ruled Surfaces according to Darboux Frame in E^3*, Journal of Mathematics 2021 Article ID: 9912624.

[16] S. Ouarab, *NC-Smarandache Ruled Surface and NW-Smarandache Ruled Surface according to Alternative Moving Frame in E^3*, Journal of Mathematics 2021 Article ID: 9951434.

[17] Ö. Bektaş, S. Yüce, *Special Smarandache Curves According to Darboux Frame in E^3*, Romanian Journal of Mathematics and Computer Science 3 (2013) 48–59.

[18] A. Berk, *A Structural Basis for Surface Discretization of Free Form Structures: Integration of Geometry, Materials and Fabrication*, PhD Dissertation, Michigan University (2012) Ann Arbor, USA.

[19] M. Çetin, H. Kocayiğit, *On the Quaternionic Smarandache Curves in Euclidean 3-Space*, International Journal of Contemporary Mathematical Sciences 8 (3) (2013) 139–150.

[20] H. Pottmann, A. Asperl, M. Hofer, A. Killian, Architectural Geometry, Bentley Institute Press, Exton, 2007.

[21] S. Şenyurt, S. Sivas, *An Application of Smarandache Curve*, Ordu University Journal of Science and Tecnology 3 (1) (2013) 46–60.

[22] J. Stillwell, Mathematics and Its History, Undergraduate Texts in Mathematics, Springer, New York, 2010.

[23] K. Taşköprü, M. Tosun, *Smarandache Curves on S^2*, Boletim da Sociedade Paranaense de Matematica 32 (1) (2014) 51–59.

Journal of
New Theory
ISSN: 2149-1402

39 (2022) 19-41
Journal of New Theory
https://dergipark.org.tr/en/pub/jnt
Open Access

A New Family of Odd Nakagami Exponential (NE-G) Distributions

Mathee Pongkitiwitoon[1], Ibrahim Abdullahi[2], Obalowu Job[3]

Article Info
Received: 07 May 202
Accepted: 27 Jun 2022
Published: 30 Jun 2022
doi:10.53570/jnt.1112959
Research Article

Abstract — In this study, a new family of odd nakagami exponential (NE-G) distributions is introduced and investigated as a new generator of continuous distributions. Quantile, hazard rate function, moments, incomplete moments, order statistics, and entropies are only a few of the statistical features that are investigated. A unique model is presented and thoroughly examined. To estimate model parameters based on describing real-life data sets, the maximum likelihood method is applied. The bias and mean square error of maximum likelihood estimators are investigated using a comprehensive simulation exercise. Finally, the new family adaptability is demonstrated via application to real-world data sets.

Keywords — *Nakagami exponential, order statistics, moment, quantile functions*

Mathematics Subject Classification (2020) — 62E99, 62F99

1. Introduction

There is a great need for expanded variants of classical distributions in many applied disciplines, such as lifetime analysis, finance, and insurance. As a result, various efforts have been made to define new families of probability distributions that expand well-known distributions and allow a high level of flexibility in modelling data in practise.. Many researchers have suggested a variety of methods for producing new families of distributions [1]. The beta-generalized family of distributions was created by Kumaraswamy [2], the Exponentiated-G by [3], the Gamma-G (type I) by [4], the Gamma-G (type II) by [5], the Generalised Gamma-G by [6], the Log-Gamma-G by [7], Additive Weibull-G by [8], Beta Marshall-Olkin-G by [9], Logistic-G family by [4], the Generalized Odd Gamma-G by [10],odd-Gamma-G (type III) by [11], new Weibull-G by [12], the Marshall-Olkin Odd Burr III-G by [13] and Exponentiated Generalized Power Function Distribution by [14] among others.
[15] has developed and investigated a class of the Nakagami-G family of distributions. The goal of this study is to introduce the odd Nakagami Exponential-G (NE-G) family of distributions. This family of distributions is an extension of the Nakagami-G family proposed by [15]. We investigate some of the new distribution's statistical properties in depth, use the MLE method to estimate the parameters of the proposed distribution, and finally fit real-life data sets to the new distribution and some of the existing families of distributions to compare the NE-G family's performance.
The cumulative distribution function (cdf) and probability density function (pdf) of Nakagami Ex-

[1]matpon@kku.ac.th ; [2]ibworld82@yahoo.com (Corresponding Author); [3]obalowu@unilorin.edu.ng
[1]Department of Statistics, Faculty of Science, Khon Kaen University, Thailand
[2]Department of Mathematics and Statistics, Faculty of Science, Yobe State University, Damaturu, Nigeria
[3]Department Statistics, Faculty of Physical Sciences, University of Ilorin, Kwara, Nigeria

ponential distribution (see [15]) is given by

$$F(x) = \gamma_* \left(\lambda, \frac{\lambda}{\beta} \left(\frac{1 - e^{-\alpha x}}{e^{-\alpha x}} \right)^2 \right) \tag{1}$$

$$f(x) = \frac{2\lambda^\lambda \alpha e^{-\alpha x} \left(1 - e^{-\alpha x}\right)^{2\lambda - 1}}{\Gamma(\lambda)\beta^\lambda \left(e^{-\alpha x}\right)^{2\lambda+1}} e^{-\frac{\lambda}{\beta}\left(\frac{1-e^{-\alpha x}}{e^{-\alpha x}}\right)^2} \tag{2}$$

The following is how the paper might look: In Section 2, a construction of the NE-G family of distributions is introduced. A special model is provided, along with plots of pdfs, cdfs, survival functions, and harzad rate functions to demonstrate the models' flexibility. Our applied study will be centred on the uniform distribution as a baseline. The parameter estimation and main statistical properties of the NE-G are presented. In Section 3, a Monte Carlo simulation study is presented. The proposed model is fitted based on two real data sets in Section 4 and compared to other well-known models.

2. Constructions of the NE-G Distributions

Equation 2 can be used to calculate the cumulative distribution of a random variable.

$$P\left(X \le x\right) = F(x) = \int_0^{\frac{G(x)}{1-G(x)}} \frac{2\lambda^\lambda \alpha e^{-\alpha x} \left(1 - e^{-\alpha t}\right)^{2\lambda-1}}{\Gamma(\lambda)\beta^\lambda \left(e^{-\alpha t}\right)^{2\lambda+1}} e^{-\frac{\lambda}{\beta}\left(\frac{1-e^{-\alpha t}}{e^{-\alpha t}}\right)^2} \partial t \tag{3}$$

Therefore,

$$F(x) = \frac{1}{\Gamma(\lambda)} \gamma \left[\lambda, \frac{\lambda}{\beta} \left(\frac{1 - e^{-\alpha\left(\frac{G(x)}{1-G(x)}\right)}}{e^{-\alpha\left(\frac{G(x)}{1-G(x)}\right)}} \right)^2 \right] \tag{4}$$

Equation 4 the pdf of Nakagami Exponential G family becomes

$$f(x) = \frac{2\lambda^\lambda \alpha g(x) \left[1 - e^{-\alpha \frac{G(x)}{1-G(x)}}\right]^{2\lambda-1}}{\Gamma(\lambda)\beta^\lambda \left[1 - G(x)\right]^2 e^{-2\lambda\alpha\left(\frac{G(x)}{1-G(x)}\right)}} e^{-\frac{\lambda}{\beta}\left(\frac{1-e^{-\alpha\left(\frac{G(x)}{1-G(x)}\right)}}{e^{-\alpha\left(\frac{G(x)}{1-G(x)}\right)}}\right)^2} \tag{5}$$

The survival and hazard rate functions of the NE-G family are, respectively, given by:

$$R(x) = 1 - \frac{1}{\Gamma(\lambda)} \gamma \left[\lambda, \frac{\lambda}{\beta} \left(\frac{1 - e^{-\alpha\left(\frac{G(x)}{1-G(x)}\right)}}{e^{-\alpha\left(\frac{G(x)}{1-G(x)}\right)}} \right)^2 \right] \tag{6}$$

and

$$hr(x) = \frac{\frac{2\lambda^\lambda \alpha g(x)\left[1-e^{-\alpha\frac{G(x)}{1-G(x)}}\right]^{2\lambda-1}}{\Gamma(\lambda)\beta^\lambda[1-G(x)]^2 e^{-2\lambda\alpha\left(\frac{G(x)}{1-G(x)}\right)}} e^{-\frac{\lambda}{\beta}\left(\frac{1-e^{-\alpha\left(\frac{G(x)}{1-G(x)}\right)}}{e^{-\alpha\left(\frac{G(x)}{1-G(x)}\right)}}\right)^2}}{1 - \frac{1}{\Gamma(\lambda)}\gamma\left[\lambda, \frac{\lambda}{\beta}\left(\frac{1-e^{-\alpha\left(\frac{G(x)}{1-G(x)}\right)}}{e^{-\alpha\left(\frac{G(x)}{1-G(x)}\right)}}\right)^2\right]} \tag{7}$$

Figures (1), (2), (3), and (4) show that the shapes of the pdf and cdf are flexible for certain parameter values. Plots of the hazard rate and survival functions of the NE-U distribution for some parameter values are shown.

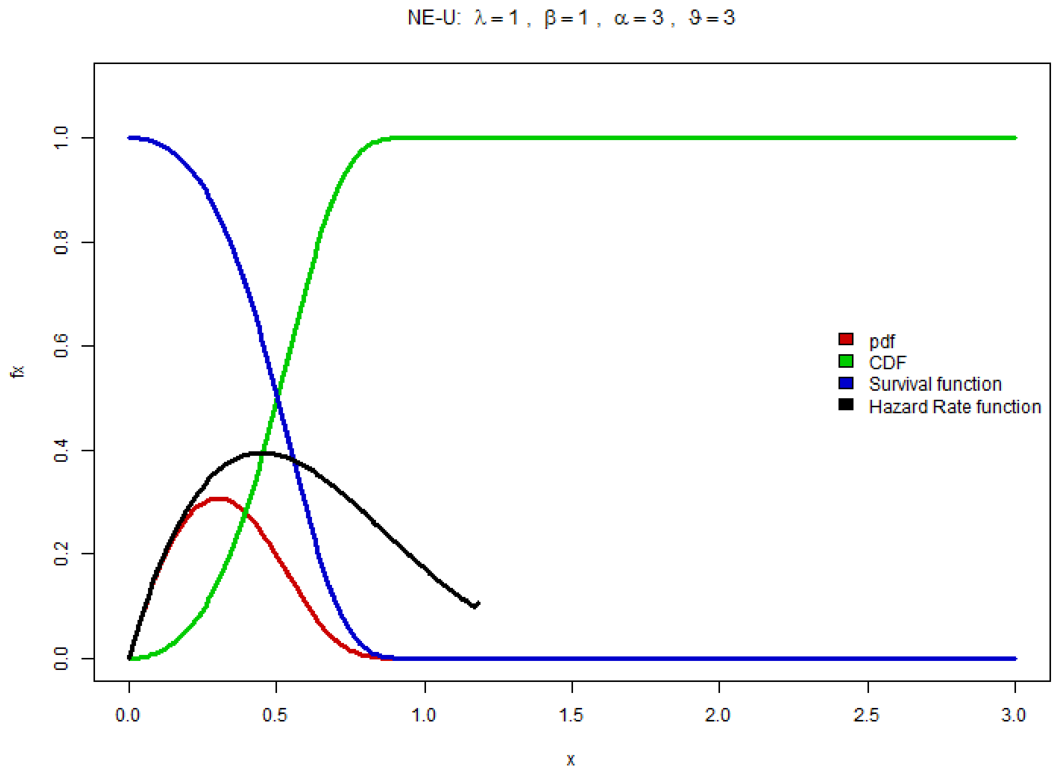

Fig. 1. NE-U function for $\lambda = 1, \beta = 1, \alpha = 3,$ and $\vartheta = 3$

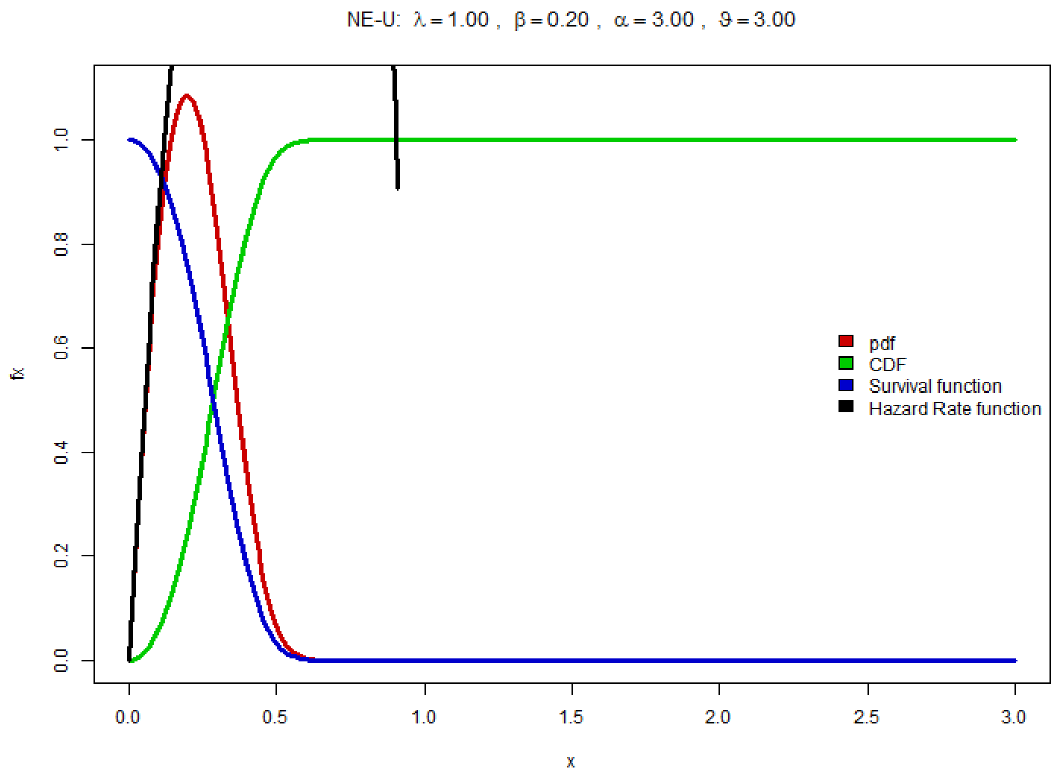

Fig. 2. NE-U function for $\lambda = 1, \beta = 0.2, \alpha = 3,$ and $\vartheta = 3$

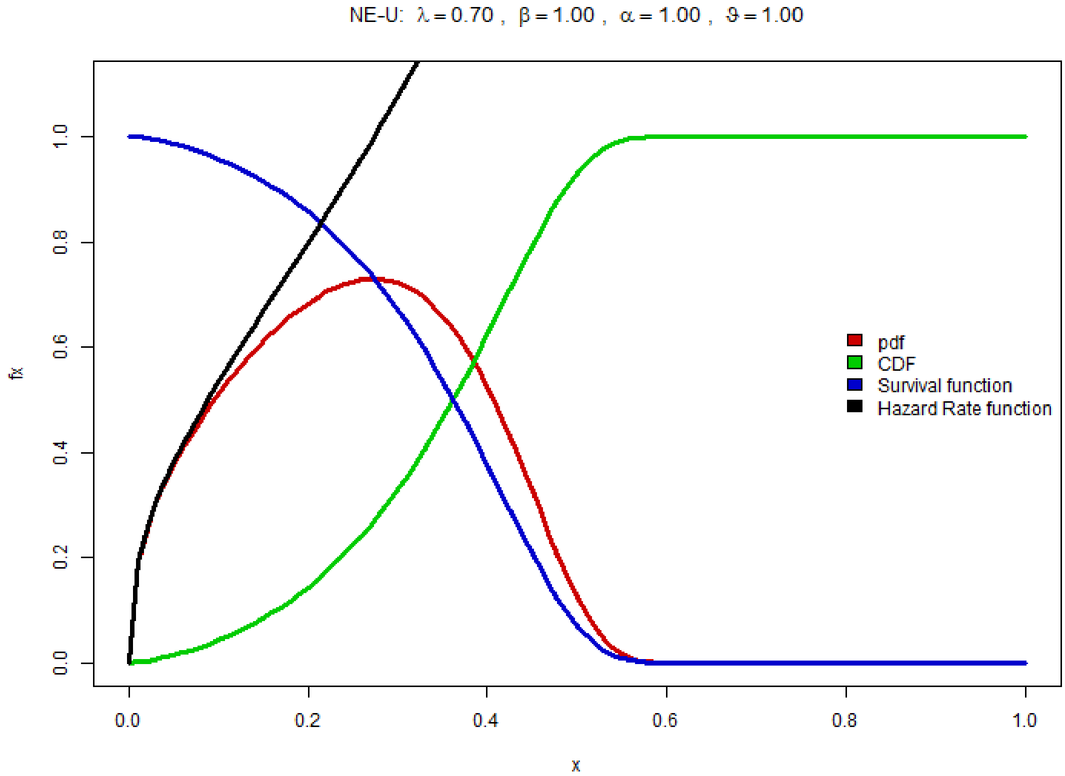

Fig. 3. NE-U function for $\lambda = 0.7, \beta = 1, \alpha = 1,$ and $\vartheta = 1$

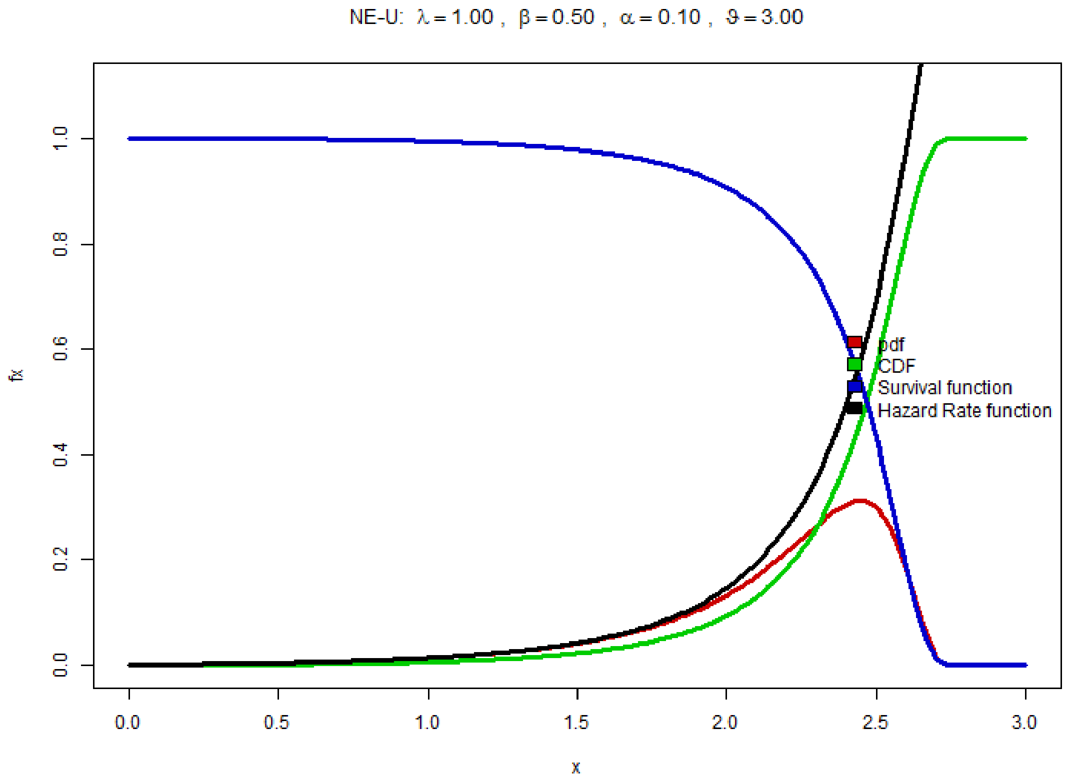

Fig. 4. NE-U function for $\lambda = 1, \beta = 0.5, \alpha = 1,$ and $\vartheta = 3$

2.1. Limiting Behaviour

The cdf defined in Equation 4 must satisfy the Limiting behaviour whether the Nakagami Exponential-G family of distributions is a valid family of distribution function. The behaviour of the NE-U distributions at $x \to 0$ and as $x \to 1$. In this case, what was considered is: when $\lim_{x\to 0} G(x) = 0$ since $\gamma(\lambda, 0) = \int_0^0 t^{\lambda-1}\mathrm{e}^{-t}\partial t = 0$

$$\lim_{G(x)\to 0} F(x) = \frac{1}{\Gamma(\lambda)}\gamma\left[\lambda, \frac{\lambda}{\beta}\left(\frac{1-e^{-\alpha\left(\frac{G(x)}{1-G(x)}\right)}}{e^{-\alpha\left(\frac{G(x)}{1-G(x)}\right)}}\right)^2\right] = 0 \tag{8}$$

when $\lim_{x\to\infty} G(x) = 1$

$$\lim_{G(x)\to \infty} F(x) = \frac{1}{\Gamma(\lambda)}\gamma\left[\lambda, \frac{\lambda}{\beta}\left(\frac{1-e^{-\alpha\left(\frac{G(x)}{1-G(x)}\right)}}{e^{-\alpha\left(\frac{G(x)}{1-G(x)}\right)}}\right)^2\right] = 1 \tag{9}$$

2.2. Investigation of the Proposed NE-G Family of Distribution

The pdf defined in Equation 5 must satisfy the integral to show whether the Nakagami Exponential-G family of distributions is a valid family of probability density function.

$$\int_{-\infty}^{\infty} f(x)\partial x = 1 \tag{10}$$

$$\int_0^\infty \frac{2\lambda^\lambda \alpha g(x)\left[1-e^{-\alpha\frac{G(x)}{1-G(x)}}\right]^{2\lambda-1}}{\Gamma(\lambda)\beta^\lambda\left[1-G(x)\right]^2 e^{-2\lambda\alpha\left(\frac{G(x)}{1-G(x)}\right)}} e^{-\frac{\lambda}{\beta}\left(\frac{1-e^{-\alpha\left(\frac{G(x)}{1-G(x)}\right)}}{e^{-\alpha\left(\frac{G(x)}{1-G(x)}\right)}}\right)^2} \partial x \tag{11}$$

let

$$u = \frac{\lambda}{\beta}\left(\frac{1-e^{-\alpha\left(\frac{G(x)}{1-G(x)}\right)}}{e^{-\alpha\left(\frac{G(x)}{1-G(x)}\right)}}\right)^2 \Rightarrow \left(\frac{u\beta}{\lambda}\right)^{\frac{1}{2}} = \left(\frac{1-e^{-\alpha\left(\frac{G(x)}{1-G(x)}\right)}}{e^{-\alpha\left(\frac{G(x)}{1-G(x)}\right)}}\right)$$

$$\partial x = \frac{\beta\left[1-G(x)\right]^2 e^{-2\alpha\left(\frac{G(x)}{\bar{G}(x)}\right)}}{2\lambda\alpha g(x)\left(1-e^{-\alpha\left(\frac{G(x)}{\bar{G}(x)}\right)}\right)}\partial u \tag{12}$$

substituting 12 into 11 yields

$$\frac{\lambda^{\lambda-1}}{\Gamma(\lambda)\beta^{\lambda-1}}\int_0^\infty \left(\frac{u\beta}{\lambda}\right)^{\lambda-1} e^{-u}\partial u \tag{13}$$

The density function defined in Equation 5 is clearly a valid family of distributions, as evidenced by this.

$$\frac{1}{\Gamma(\lambda)} \times \Gamma(\lambda) = 1 \tag{14}$$

The following are the primary reasons for employing the NE-G family in practice: (i) to give symmetrical distributions a skewness; (ii) to model real data with heavy-tailed distributions that aren't longer-tailed; (iii) under the same baseline distribution, to provide consistently better fits than other generated models

2.3. Expansion for NE-G Density and Distribution Function

Using generalized binomial and taylor expansion, one may obtain

$$f(x) = \frac{2\lambda^{\lambda}\alpha g(x)\left[1-e^{-\alpha\frac{G(x)}{1-G(x)}}\right]^{2\lambda-1}}{\Gamma(\lambda)\beta^{\lambda}\left[1-G(x)\right]^{2}e^{-2\lambda\alpha\left(\frac{G(x)}{1-G(x)}\right)}}\sum_{k=0}^{\infty}\frac{(-1)^{k}}{k!}\left[\frac{\lambda}{\beta}\left(\frac{1-e^{-\alpha\left(\frac{G(x)}{1-G(x)}\right)}}{e^{-\alpha\left(\frac{G(x)}{1-G(x)}\right)}}\right)^{2}\right]^{k} \tag{15}$$

$$= \frac{2\lambda^{\lambda+k}\alpha g(x)\left[1-e^{-\alpha\frac{G(x)}{1-G(x)}}\right]^{2\lambda+2k-1}}{\Gamma(\lambda)\beta^{\lambda+k}\left[1-G(x)\right]^{2}}\sum_{k=0}^{\infty}\frac{(-1)^{k}}{k!}\mathrm{e}^{\alpha[2\lambda+2k]\left(\frac{G(x)}{1-G(x)}\right)} \tag{16}$$

$$\left[1-e^{-\alpha\frac{G(x)}{1-G(x)}}\right]^{2\lambda+2k-1} = \sum_{i=0}^{\infty}(-1)^{i}\binom{2\lambda+2k-1}{i}e^{-i\alpha\left(\frac{G(x)}{1-G(x)}\right)}$$

$$= \frac{2\lambda^{\lambda+k}\alpha g(x)}{\Gamma(\lambda)\beta^{\lambda+k}\left[1-G(x)\right]^{2}}\sum_{k,i=0}^{\infty}\frac{(-1)^{k+i}}{k!}\binom{2\lambda+2k-1}{i}\mathrm{e}^{\alpha[2\lambda+2k-i]\left(\frac{G(x)}{1-G(x)}\right)} \tag{17}$$

$$= \frac{2\lambda^{\lambda+k}\alpha g(x)}{\Gamma(\lambda)\beta^{\lambda+k}}\sum_{k,i,j,p=0}^{\infty}\frac{(-1)^{k+i+p}}{k!p!}\binom{2\lambda+2k-1}{i}\binom{j+p+1}{p}\alpha^{j}[2\lambda+2k-i]^{j}G(x)^{j+p} \tag{18}$$

reduced

$$f(x) = \sum_{k,i,j,p=0}^{\infty}\kappa_{k,i,j,p}h_{j+p+1}(x) \tag{19}$$

where

$$\kappa_{k,i,j,p} = \frac{2\lambda^{\lambda+k}\alpha}{\Gamma(\lambda)\beta^{\lambda+k}}\frac{(-1)^{k+i+p}}{k!p!}\binom{2\lambda+2k-1}{i}\binom{j+p+1}{p}\frac{\alpha^{j}[2\lambda+2k-i]^{j}}{[j+p+1]}$$

and

$$h_{j+p+1}(x) = (j+p+1)g(x)G(x)^{j+p}$$

We get by integrating from equation 19 with respect to x.

$$F(x) = \sum_{k,i,j,p=0}^{\infty}\kappa_{k,i,j,p}H_{j+p+1}(x) \tag{20}$$

where

$$H_{j+p+1}(x) = G(x)^{j+p+1}$$

2.4. Properties of the NE-G Distribution

We establish certain mathematical features of the NE-G family in this section.

2.4.1. Quantile Function

The inverse distribution function is the most popular and simplest method for producing random variates. The qf of the NE-G family can be obtained by inverting Equation 4 and then solve the equation numerically. We can utilize the following method:

$$u = F(x) = \frac{1}{\Gamma(\lambda)}\gamma\left[\lambda, \frac{\lambda}{\beta}\left(\frac{1-e^{-\alpha\left(\frac{G(x)}{1-G(x)}\right)}}{e^{-\alpha\left(\frac{G(x)}{1-G(x)}\right)}}\right)^2\right] \tag{21}$$

$$G(x) = \frac{\frac{1}{\alpha}log\left\{\left\{\frac{\beta}{\lambda}\gamma^{-1}\left[\lambda, u\Gamma(\lambda)\right]\right\}^{1/2}+1\right\}}{1+\frac{1}{\alpha}log\left\{\left\{\frac{\beta}{\lambda}\gamma^{-1}\left[\lambda, u\Gamma(\lambda)\right]\right\}^{1/2}+1\right\}} \tag{22}$$

2.5. Moment and Moment Generating Function

Moments are crucial in statistical analysis. Moments can be used to investigate some of the most important characteristics of a distribution.

2.5.1. Moment

The r^{th} ordinary moment of X is given by

$$E(X^r) = \mu'_r = \int_0^{\infty} x^r f(x)\partial x \tag{23}$$

The following can be derived from equation 19:

$$E(X^r) = \mu'_r = \sum_{k,i,j,p=0}^{\infty} \kappa_{k,i,j,p} E(Y_{j+p+1}^r) \tag{24}$$

Y_{j+p+1} represents the Exp-G distribution with power parameter (j+p + 1). Choosing r = 1 in equation 24, We now have the mean of X.

2.5.2. Moment Generating Function

The moment generating function of X say, $M_X(t) = E(e^{tX})$ is given by

$$M_X(t) = \sum_{r=0}^{\infty}\frac{t^r}{r!}\mu'_r = \sum_{k,i,j,p,r=0}^{\infty}\frac{t^r\kappa_{k,i,j,p}}{r!}E(Y_{j+p+1}^r) \tag{25}$$

2.5.3. Incomplete Moments

The k^{th} incomplete moments, say $\rho_k(t)$, is given by

$$\rho_k(t) = \sum_{r=0}^{\infty}\kappa_{k,i,j,p}\int_{-\infty}^{t} h_{j+p+1}(x)\partial x \tag{26}$$

2.5.4. Entropy

The Rényi entropy of a random variable X is defined mathematically as follows:

$$I_R(\sigma) = \frac{1}{1-\sigma} log \left(\int_0^\infty f^\sigma(x) \partial x \right) \tag{27}$$

Where $\sigma > 0$ and $\sigma \neq 1$. Based on $f(x)$ of any distribution. From equation 5

$$f^\sigma(x) = \left\{ \frac{2\lambda^\lambda \alpha g(x) \left[1 - e^{-\alpha \frac{G(x)}{1-G(x)}}\right]^{2\lambda-1}}{\Gamma(\lambda)\beta^\lambda [1-G(x)]^2 e^{-2\lambda\alpha\left(\frac{G(x)}{1-G(x)}\right)}} e^{-\frac{\lambda}{\beta}\left(\frac{1-e^{-\alpha\left(\frac{G(x)}{1-G(x)}\right)}}{e^{-\alpha\left(\frac{G(x)}{1-G(x)}\right)}} \right)^2} \right\}^\sigma \tag{28}$$

$$f^\sigma(x) = \left(\frac{2\lambda^\lambda}{\Gamma(\lambda)\beta^\lambda}\right)^\sigma \left(\frac{\sigma\lambda}{\beta}\right)^k \sum_{k,i,j,p=0}^\infty \binom{(2\lambda-1)\sigma + 2k}{i} \binom{2\sigma + j + p - 1}{p} \alpha^j \left(i - (2\lambda\sigma + 2k)\right)^j$$
$$g(x)^\sigma G(x)^{j+p} \tag{29}$$

reduced

$$f^\sigma(x) = \sum_{k,i,j,p=0}^\infty \Lambda_{k,i,j,p} g(x)^\sigma G(x)^{j+p} \tag{30}$$

where

$$\Lambda_{k,i,j,p} = \left(\frac{2\lambda^\lambda}{\Gamma(\lambda)\beta^\lambda}\right)^\sigma \left(\frac{\sigma\lambda}{\beta}\right)^k \binom{(2\lambda-1)\sigma + 2k}{i} \binom{2\sigma + j + p - 1}{p} \alpha^j \left(i - (2\lambda\sigma + 2k)\right)^j$$

$$I_R(\sigma) = \frac{1}{1-\sigma} log \left(\int_0^\infty \sum_{k,i,j,p=0}^\infty \Lambda_{k,i,j,p} g(x)^\sigma G(x)^{j+p} \partial x \right) \tag{31}$$

2.5.5. Order Statistics

Let $x_1, x_2 \ldots, x_n$ be independent random sample from a distribution function, $F(x)$, with an associated probability density function, $f(x)$. Then, the probability density function of the i^{th} order statistics, $x_{(i)}$, is given by:

$$f_{x_{(j)}}(x) = \frac{n!}{(r-1)!(n-r)!} \sum_{z=0}^{n-r} (-1)^z \binom{n-r}{z} f_X(x) \left[F_X(x)\right]^{z+r-1} \tag{32}$$

The *pdf* of i^{th} order statistic from NE-G distribution is obtained by substituting equation 19 and 20 into 32

$$f_{x_{(j)}}(x) = \frac{n!}{(r-1)!(n-r)!} \sum_{z=0}^{n-r} \sum_{k,i,j,p=0}^\infty (-1)^z \binom{n-r}{z} \kappa_{k,i,j,p} h_{j+p+1}(x) \left[\sum_{k,i,j,p=0}^\infty \kappa_{k,i,j,p} H_{j+p+1}(x) \right]^{z+r-1} \tag{33}$$

2.6. Maximum Likelihood Estimator

The maximum likelihood method is used here to estimate the unknown parameters of the NE-G family. When constructing confidence intervals, MLEs have desirable properties and provide simple approximations that work well in finite samples.
The log-likelihood function $\ell(\Theta)$ for the vector of parameters $\Theta = (\lambda, \beta, \xi)^T$ from n observations $(x_1, \cdots, x_n)$ has the form

$$\ell(\Theta) = n\ln(2) + n\lambda\ln(\lambda) + \sum_{i=0}^{n}\ln(g(x_i,\xi)) + (2\lambda-1)\sum_{i=0}^{n}\ln\left[1-\mathrm{e}^{-\alpha\left(\frac{G(x_i,\xi)}{1-G(x_i,\xi)}\right)}\right] - \frac{\lambda}{\beta}\sum_{i=0}^{n}\left(\frac{1-\mathrm{e}^{-\alpha\frac{G(x_i,\xi)}{1-G(x_i,\xi)}}}{\mathrm{e}^{-\alpha\frac{G(x_i,\xi)}{1-G(x_i,\xi)}}}\right)^2$$
$$- n\ln(\Gamma(\lambda)) - n\lambda\ln(\beta) - 2\sum_{i=0}^{n}\ln\left[1-G(x_i,\xi)\right] + 2\lambda\alpha\sum_{i=0}^{n}\left(\frac{G(x_i,\xi)}{1-G(x_i,\xi)}\right) \quad (34)$$

The maximum likelihood estimators can be obtained by numerically solving the following equations

$$\frac{\partial\ell(\Theta)}{\partial\lambda} = n + n\ln(\lambda) + 2\sum_{i=0}^{n}\ln\left[1-\mathrm{e}^{-\alpha\left(\frac{G(x_i,\xi)}{1-G(x_i,\xi)}\right)}\right] - \frac{1}{\beta}\sum_{i=0}^{n}\left(\frac{1-\mathrm{e}^{-\alpha\frac{G(x_i,\xi)}{1-G(x_i,\xi)}}}{\mathrm{e}^{-\alpha\frac{G(x_i,\xi)}{1-G(x_i,\xi)}}}\right)^2 - n\frac{\Gamma'(\lambda)}{\Gamma(\lambda)} - n\ln(\beta)$$
$$+ 2\alpha\sum_{i=0}^{n}\left(\frac{G(x_i,\xi)}{1-G(x_i,\xi)}\right) \quad (35)$$

$$\frac{\partial\ell(\Theta)}{\partial\beta} = \frac{\lambda}{\beta^2}\sum_{i=0}^{n}\left(\frac{1-\mathrm{e}^{-\alpha\frac{G(x_i,\xi)}{1-G(x_i,\xi)}}}{\mathrm{e}^{-\alpha\frac{G(x_i,\xi)}{1-G(x_i,\xi)}}}\right)^2 - \frac{n\lambda}{\beta} \quad (36)$$

$$\frac{\partial\ell(\Theta)}{\partial\xi} = \sum_{i=0}^{n}\frac{g(xi,\xi)'}{g(xi,\xi)} + (2\lambda-1)\sum_{i=0}^{n}\frac{\alpha G(x_i,\xi)'\mathrm{e}^{-\alpha\left(\frac{G(x_i,\xi)}{1-G(x_i,\xi)}\right)}}{(1-G(x_i,\xi))^2\left[1-\mathrm{e}^{-\alpha\left(\frac{G(x_i,\xi)}{1-G(x_i,\xi)}\right)}\right]} - \frac{2\alpha\lambda}{\beta}\sum_{i=0}^{n}\frac{G(x_i,\xi)'}{(1-G(x_i,\xi))^2}\times$$
$$\left[\frac{1-\mathrm{e}^{-\alpha\left(\frac{G(x_i,\xi)}{1-G(x_i,\xi)}\right)}}{\mathrm{e}^{-2\alpha\left(\frac{G(x_i,\xi)}{1-G(x_i,\xi)}\right)}}\right] + 2\sum_{1=0}^{n}\frac{G(x_i,\xi)'}{1-G(x_i,\xi)} + 2\lambda\alpha\sum_{i=0}^{n}\frac{G(x_i,\xi)'}{(1-G(x_i,\xi))^2} \quad (37)$$

where $g(x_i,\xi)' = \frac{\partial g(x_i,\xi)}{\partial\xi}$ and $G(x_i,\xi)' = \frac{\partial G(x_i,\xi)}{\partial\xi}$

2.7. The Nakagami Exponential Uniform (NE-U) Distribution

The cdf and pdf of our baseline distribution, the uniform distribution with parameters $(0,\vartheta)$ are given by:

$$G(x;\vartheta) = \frac{x}{\vartheta}$$

and

$$g(x;\vartheta) = \frac{1}{\vartheta}, 0 < x < \vartheta$$

By plugging $g(x;\vartheta)$ and $G(x;\vartheta)$ into Equation 5, we get the pdf of the NE-U distribution.

$$f(x) = \frac{2\lambda^\lambda\alpha}{\vartheta\Gamma(\lambda)\beta^\lambda\left(\frac{\vartheta-x}{\vartheta}\right)^2}\frac{\left[1-e^{-\alpha\left(\frac{x}{\vartheta-x}\right)}\right]^{2\lambda-1}}{e^{-2\lambda\alpha\left(\frac{x}{\vartheta-x}\right)}}e^{\frac{-\lambda}{\beta}\left(\frac{1-e^{-\alpha\left(\frac{x}{\vartheta-x}\right)}}{e^{-\alpha\left(\frac{x}{\vartheta-x}\right)}}\right)^2} \quad (38)$$

2.8. Investigation of the Proposed NE-U Distribution

$$\int_0^\infty \frac{2\lambda^\lambda \alpha}{\vartheta \Gamma(\lambda)\beta^\lambda \left(\frac{\vartheta - x}{\vartheta}\right)^2} \frac{\left[1 - e^{-\alpha\left(\frac{x}{\vartheta - x}\right)}\right]^{2\lambda - 1}}{e^{-2\lambda\alpha\left(\frac{x}{\vartheta - x}\right)}} e^{\frac{-\lambda}{\beta}\left(\frac{1 - e^{-\alpha\left(\frac{x}{\vartheta - x}\right)}}{e^{-\alpha\left(\frac{x}{\vartheta - x}\right)}}\right)^2} \partial x = 1 \tag{39}$$

let

$$u = \frac{\lambda}{\beta}\left(\frac{1 - e^{-\alpha\left(\frac{x}{\vartheta - x}\right)}}{e^{-\alpha\left(\frac{x}{\vartheta - x}\right)}}\right)^2 \tag{40}$$

$$\partial x = \frac{\beta(\vartheta - x)^2 \mathrm{e}^{-\frac{2\alpha x}{\vartheta - x}}}{2\lambda\alpha\vartheta\left(1 - \mathrm{e}^{-\frac{\alpha x}{\vartheta - x}}\right)} \partial u \tag{41}$$

substituting equation 41 and 40 into equation 39 yield

$$\frac{\lambda^{\lambda - 1}}{\Gamma(\lambda)\beta^{\lambda - 1}} \int_0^\infty \left(\frac{\beta u}{\lambda}\right)^{\lambda - 1} \mathrm{e}^{-u} \partial u \tag{42}$$

$$\int_0^\infty f(x)\partial x = \frac{1}{\Gamma(\lambda)} \times \Gamma(\lambda) = 1 \tag{43}$$

Hence Nakagami Exponential Uniform Distribution is pdf.

2.8.1. Cdf and Survival and Hazard Function of the NE-U Distribution

The distribution function of NE-U has the form

$$F(x) = \gamma_1\left(\lambda, \frac{\lambda}{\beta}\left(\mathrm{e}^{\alpha\left(\frac{x}{\vartheta - x}\right)} - 1\right)^2\right) \tag{44}$$

The survival function of NE-U has the form

$$R(x) = 1 - \gamma_1\left(\lambda, \frac{\lambda}{\beta}\left(\mathrm{e}^{\alpha\left(\frac{x}{\vartheta - x}\right)} - 1\right)^2\right) \tag{45}$$

The hazard rate function of NE-U has the form

$$hrf(x) = \frac{\frac{2\lambda^\lambda \alpha}{\vartheta \Gamma(\lambda)\beta^\lambda \left(\frac{\vartheta - x}{\vartheta}\right)^2} \frac{\left[1 - e^{-\alpha\left(\frac{x}{\vartheta - x}\right)}\right]^{2\lambda - 1}}{e^{-2\lambda\alpha\left(\frac{x}{\vartheta - x}\right)}} e^{\frac{-\lambda}{\beta}\left(\frac{1 - e^{-\alpha\left(\frac{x}{\vartheta - x}\right)}}{e^{-\alpha\left(\frac{x}{\vartheta - x}\right)}}\right)^2}}{1 - \gamma_1\left(\lambda, \frac{\lambda}{\beta}\left(\mathrm{e}^{\alpha\left(\frac{x}{\vartheta - x}\right)} - 1\right)^2\right)} \tag{46}$$

2.9. Expansion for NE-U Distribution

In this part a simple form for the probability density function of NE-U distribution is derived. Using generalized binomial and taylor expansion in the equation 38 one can obtain

$$\mathrm{e}^{-\frac{\lambda}{\beta}\left(\frac{1 - e^{-\alpha\left(\frac{x}{\vartheta - x}\right)}}{e^{-\alpha\left(\frac{x}{\vartheta - x}\right)}}\right)^2} = \sum_{i=0}^{\infty} \frac{(-1)^i}{i!}\left(\frac{\lambda}{\beta}\right)^i \left(\frac{1 - e^{-\alpha\left(\frac{x}{\vartheta - x}\right)}}{e^{-\alpha\left(\frac{x}{\vartheta - x}\right)}}\right)^{2i} \tag{47}$$

Substituting 47 in pdf 38 then, the pdf of NE-U can be written as

$$f(x)=\frac{2\lambda^{\lambda}\alpha}{\vartheta\Gamma(\lambda)\beta^{\lambda}\left(\frac{\vartheta-x}{\vartheta}\right)^{2}}\frac{\left[1-e^{-\alpha\left(\frac{x}{\vartheta-x}\right)}\right]^{2\lambda-1}}{e^{-2\lambda\alpha\left(\frac{x}{\vartheta-x}\right)}}\sum_{i=0}^{\infty}\frac{(-1)^{i}}{i!}\left(\frac{\lambda}{\beta}\right)^{i}\left(\frac{1-e^{-\alpha\left(\frac{x}{\vartheta-x}\right)}}{e^{-\alpha\left(\frac{x}{\vartheta-x}\right)}}\right)^{2i} \quad (48)$$

$$\left[1-\left(1-e^{-\alpha\left(\frac{x}{\vartheta-x}\right)}\right)\right]^{-2(\lambda+i)}=\sum_{j=0}^{\infty}\binom{2(\lambda+i)+j-1}{j}\left(1-e^{-\alpha\left(\frac{x}{\vartheta-x}\right)}\right)^{j} \quad (49)$$

By inserting 49 in pdf 48 then, the pdf of NE-U can be written as

$$f(x)=\frac{2\lambda^{\lambda}\alpha}{\vartheta\Gamma(\lambda)\beta^{\lambda}\left(\frac{\vartheta-x}{\vartheta}\right)^{2}}\sum_{i,j=0}^{\infty}\frac{(-1)^{i}}{i!}\left(\frac{\lambda}{\beta}\right)^{i}\binom{2(\lambda+i)+j-1}{j}\left(1-e^{-\alpha\left(\frac{x}{\vartheta-x}\right)}\right)^{2\lambda+2i+j-1} \quad (50)$$

$$\left(1-e^{-\alpha\left(\frac{x}{\vartheta-x}\right)}\right)^{2\lambda+2i+j-1}=\sum_{k=0}^{\infty}(-1)^{k}\binom{2\lambda+2i+j-1}{k}e^{-k\alpha\left(\frac{x}{\vartheta-x}\right)} \quad (51)$$

Substituting 51 in pdf 50 then, the pdf of NE-U can be written as

$$f(x)=\frac{2\lambda^{\lambda}\alpha}{\vartheta\Gamma(\lambda)\beta^{\lambda}\left(\frac{\vartheta-x}{\vartheta}\right)^{2}}\sum_{i,j,k=0}^{\infty}\frac{(-1)^{i+k}}{i!}\left(\frac{\lambda}{\beta}\right)^{i}\binom{2(\lambda+i)+j-1}{j}\binom{2\lambda+2i+j-1}{k}e^{-k\alpha\left(\frac{x}{\vartheta-x}\right)} \quad (52)$$

Therefore, the NE-U distribution reduced to

$$f(x)=\sum_{i,j,k=0}^{\infty}\frac{\amalg_{i,j,k}}{\left(\frac{\vartheta-x}{\vartheta}\right)^{2}}\mathrm{e}^{\frac{-k\alpha x}{\vartheta-x}} \quad (53)$$

where

$$\amalg_{i,j,k}=\frac{2\lambda^{\lambda}\alpha}{\vartheta\Gamma(\lambda)\beta^{\lambda}}\frac{(-1)^{i+k}}{i!}\left(\frac{\lambda}{\beta}\right)^{i}\binom{2(\lambda+i)+j-1}{j}\binom{2(\lambda+i)+j-1}{k}$$

2.10. Quantile Function

It is not possible to obtain the qf of the NE-U distribution explicitly.

$$x=\frac{\frac{\vartheta}{\alpha}log\left\{\left\{\frac{\beta}{\lambda}\gamma^{-1}\left[\lambda,u\Gamma(\lambda)\right]\right\}^{1/2}+1\right\}}{1+\frac{1}{\alpha}log\left\{\left\{\frac{\beta}{\lambda}\gamma^{-1}\left[\lambda,u\Gamma(\lambda)\right]\right\}^{1/2}+1\right\}} \quad (54)$$

2.11. Parameters Estimation

In this section, the method of estimation employed was Maximum Likelihood estimation to estimate the parameters of the NE-U distribution. Let $x_1\cdots,x_n$ be a random sample from the NE-U, and the likelihood function be expressed as follows:

$$\prod_{i=1}^{n}f(x)=\prod_{i=1}^{n}\frac{2\lambda^{\lambda}\alpha}{\vartheta\Gamma(\lambda)\beta^{\lambda}\left(\frac{\vartheta-x}{\vartheta}\right)^{2}}\frac{\left[1-e^{-\alpha\left(\frac{x}{\vartheta-x}\right)}\right]^{2\lambda-1}}{e^{-2\lambda\alpha\left(\frac{x}{\vartheta-x}\right)}}e^{\frac{-\lambda}{\beta}\left(\frac{1-e^{-\alpha\left(\frac{x}{\vartheta-x}\right)}}{e^{-\alpha\left(\frac{x}{\vartheta-x}\right)}}\right)^{2}} \quad (55)$$

Now, in the equation 55, take the log of the likelihood function.

$$\ell = n\ln(2) + n\lambda\ln(\lambda) + n\ln(\alpha) + (2\lambda-1)\sum_{i=1}^{n}\ln\left[1-e^{-\alpha\left(\frac{x}{\vartheta-x}\right)}\right] - \frac{\lambda}{\beta}\sum_{i=1}^{n}\left\{\frac{\left[1-\mathrm{e}^{-\alpha\left(\frac{x}{\vartheta-x}\right)}\right]}{\mathrm{e}^{-\alpha\left(\frac{x}{\vartheta-x}\right)}}\right\}^{2}$$
$$- n\ln(\vartheta) - n\ln(\Gamma(\lambda)) - n\lambda\ln(\beta) - 2\sum_{i=1}^{n}\ln\left(\frac{x}{\vartheta-x}\right) + 2\lambda\alpha\sum_{i=1}^{n}\ln\left(\frac{x}{\vartheta-x}\right) \tag{56}$$

By obtaining the derivative of the equation 56 with respect to $\lambda, \beta, \alpha, \vartheta$ respectively,

$$\frac{\partial\ell}{\partial\lambda} = n\ln(\lambda) + n + 2\sum_{i=1}^{n}\ln\left[1-e^{-\alpha\left(\frac{x}{\vartheta-x}\right)}\right] - \frac{1}{\beta}\sum_{i=1}^{n}\left\{\frac{\left[1-\mathrm{e}^{-\alpha\left(\frac{x}{\vartheta-x}\right)}\right]}{\mathrm{e}^{-\alpha\left(\frac{x}{\vartheta-x}\right)}}\right\}^{2} - \frac{n\Gamma'(\lambda)}{\Gamma(\lambda)} - n\ln(\beta)$$
$$+ 2\alpha\sum_{i=1}^{n}\ln\left(\frac{x}{\vartheta-x}\right) \tag{57}$$

$$\frac{\partial\ell}{\partial\lambda} = \frac{\lambda}{\beta^{2}}\sum_{i=1}^{n}\left\{\frac{\left[1-\mathrm{e}^{-\alpha\left(\frac{x}{\vartheta-x}\right)}\right]}{\mathrm{e}^{-\alpha\left(\frac{x}{\vartheta-x}\right)}}\right\}^{2} - \frac{n\lambda}{\beta} \tag{58}$$

$$\frac{\partial\ell}{\partial\alpha} = \frac{n}{\alpha} + (2\lambda-1)\sum_{i=1}^{n}\frac{x\mathrm{e}^{-\alpha\left(\frac{x}{\vartheta-x}\right)}}{(\vartheta-x)\ln\left(1-\mathrm{e}^{-\alpha\left(\frac{x}{\vartheta-x}\right)}\right)} - \frac{2\lambda}{\beta}\sum_{i=1}^{n}\left\{\frac{x\left[1-\mathrm{e}^{-\alpha\left(\frac{x}{\vartheta-x}\right)}\right]}{(\vartheta-x)\mathrm{e}^{-2\alpha\left(\frac{x}{\vartheta-x}\right)}}\right\}$$
$$+ 2\lambda\sum_{i=1}^{n}\ln\left(\frac{x}{\vartheta-x}\right) \tag{59}$$

$$\frac{\partial\ell}{\partial\vartheta} = -(2\lambda-1)\sum_{i=1}^{n}\frac{x\alpha\mathrm{e}^{-\alpha\left(\frac{x}{\vartheta-x}\right)}}{(\vartheta-x)^{2}\ln\left(1-\mathrm{e}^{-\alpha\left(\frac{x}{\vartheta-x}\right)}\right)} + \frac{2\lambda\alpha}{\beta}\sum_{i=1}^{n}\frac{x\left[1-\mathrm{e}^{-\alpha\left(\frac{x}{\vartheta-x}\right)}\right]}{(\vartheta-x)^{2}\mathrm{e}^{-2\alpha\left(\frac{x}{\vartheta-x}\right)}} + \sum_{i=1}^{n}\left(\frac{2}{\vartheta-x}\right)$$
$$- \sum_{i=1}^{n}\left(\frac{2\lambda\alpha}{\vartheta-x}\right) \tag{60}$$

equate equations 57 to 60 to zero and solve them using any numerically iterative techniques.

3. NE-U Performance

The proposed NE-U model is evaluated in two ways in this section. The performance of the MLE's was examined using a simulation study. Secondly, the goodness of the fit of the NE-U was evaluated in relation to the other existing distributions.

3.1. Monte Carlo Simulation

The properties of maximum likelihood estimators for the parameters of the NE-U distribution were investigated using simulation in this section. The Average Bias and MSE of the parameters were measured. To generate random samples from the NE-U distribution, the quantile function given in equation 54 was employed. The simulation experiment was repeated N = 10000 times with sample sizes of n = 25, 50, 75, 100, 125, and parameter values of $\lambda, \beta, \alpha, \vartheta$ = (0.5, 0.9, 2, 1) and $\lambda, \beta, \alpha, \vartheta$ = (0.5, 0.9, 3, 1).

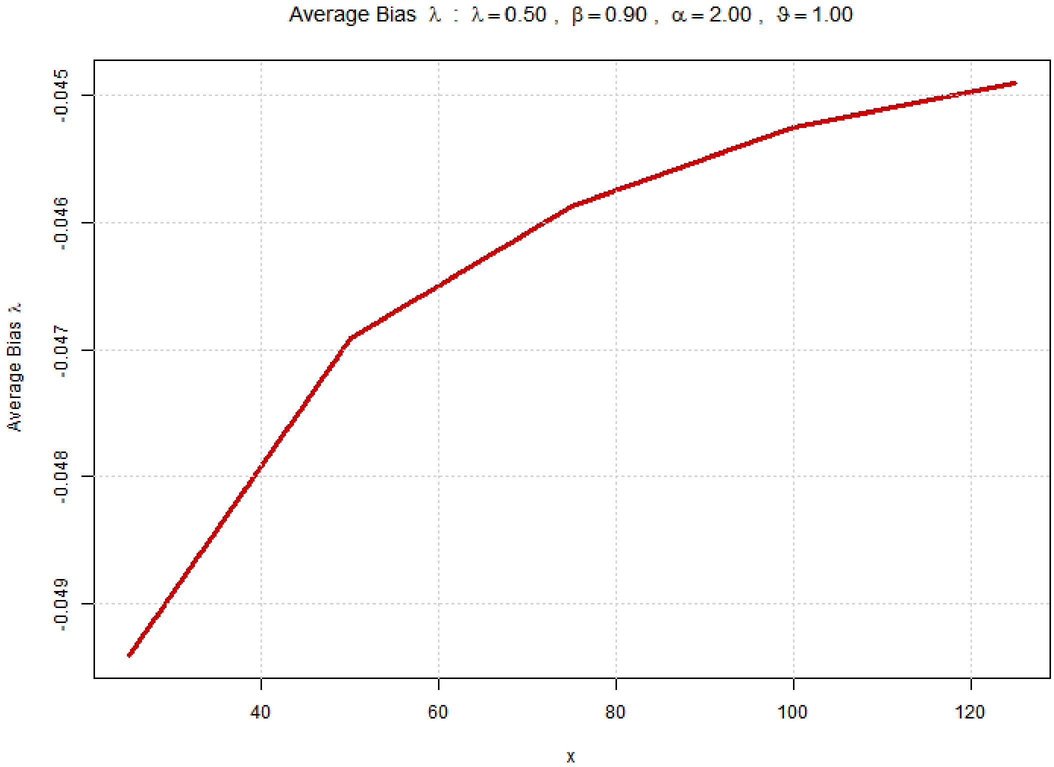

Fig. 5. Bias Lambda for $\lambda = 0.5, \beta = 0.9, \alpha = 2,$ and $\vartheta = 1$

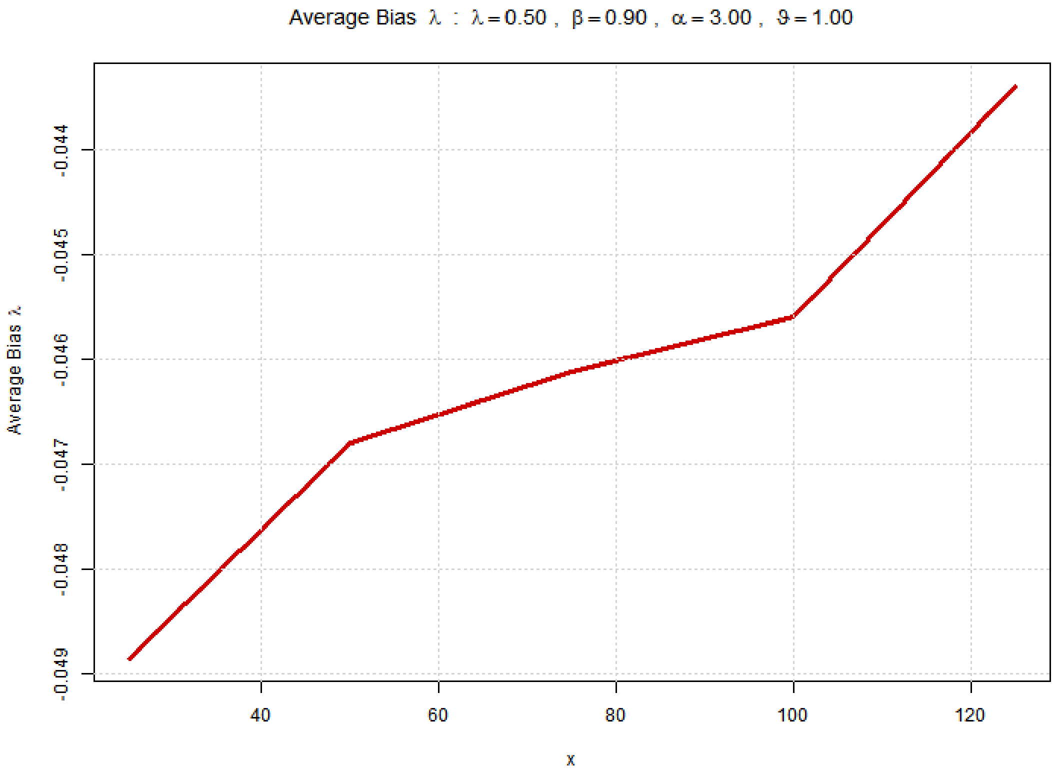

Fig. 6. Bias Lambda for $\lambda = 0.5, \beta = 0.9, \alpha = 3,$ and $\vartheta = 1$

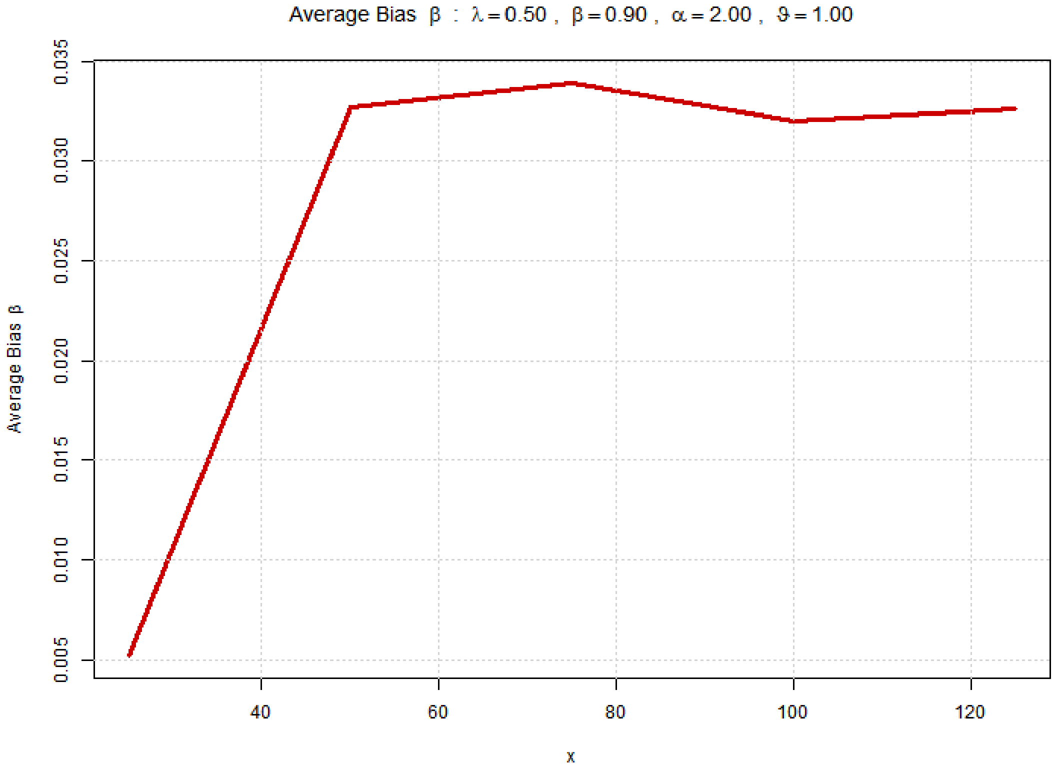

Fig. 7. Bias Beta for $\lambda = 0.5, \beta = 0.9, \alpha = 2,$ and $\vartheta = 1$

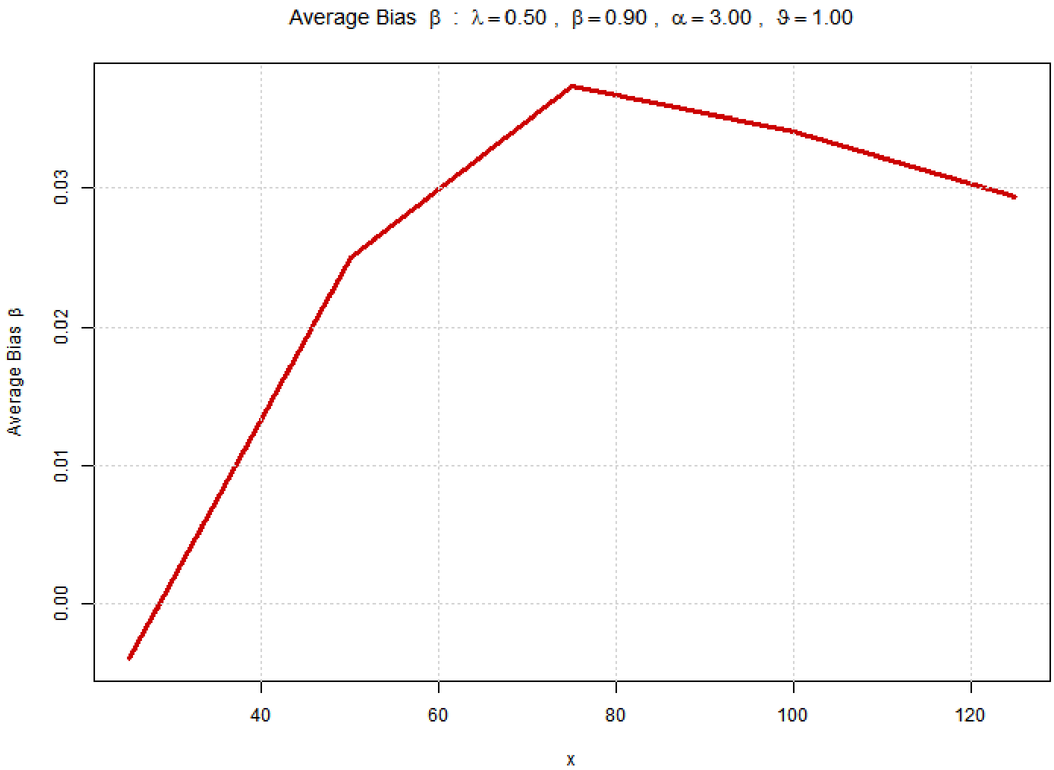

Fig. 8. Bias Beta for $\lambda = 0.5, \beta = 0.9, \alpha = 3,$ and $\vartheta = 1$

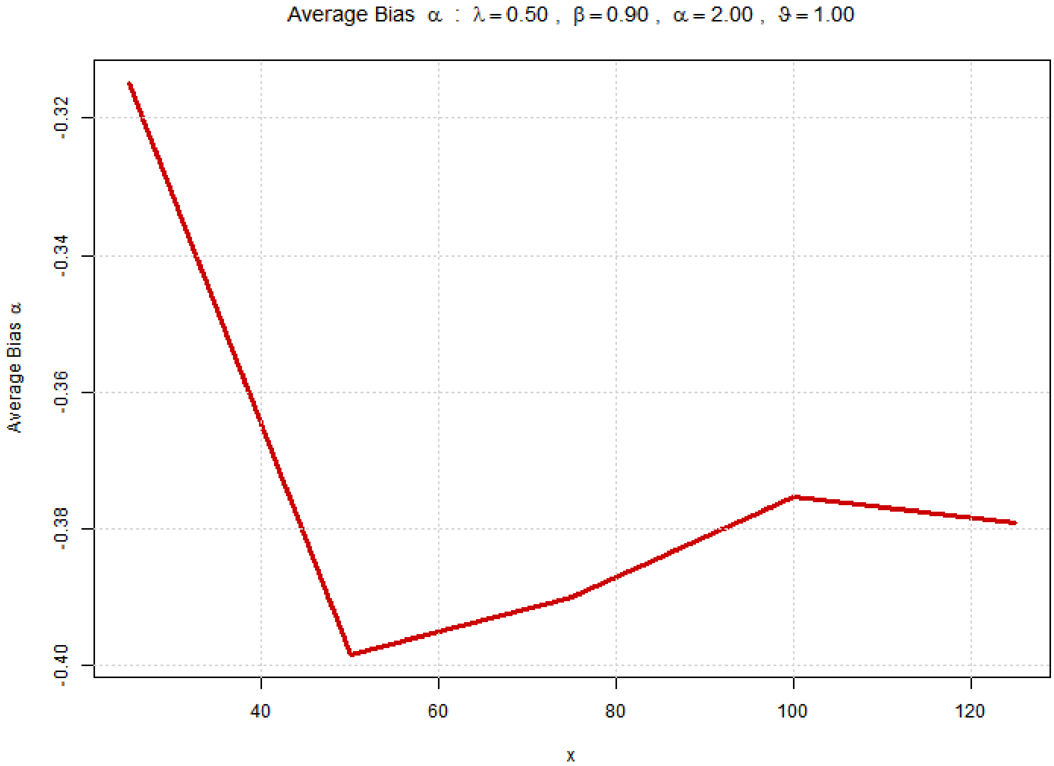

Fig. 9. Bias Alpha for $\lambda = 0.5, \beta = 0.9, \alpha = 2,$ and $\vartheta = 1$

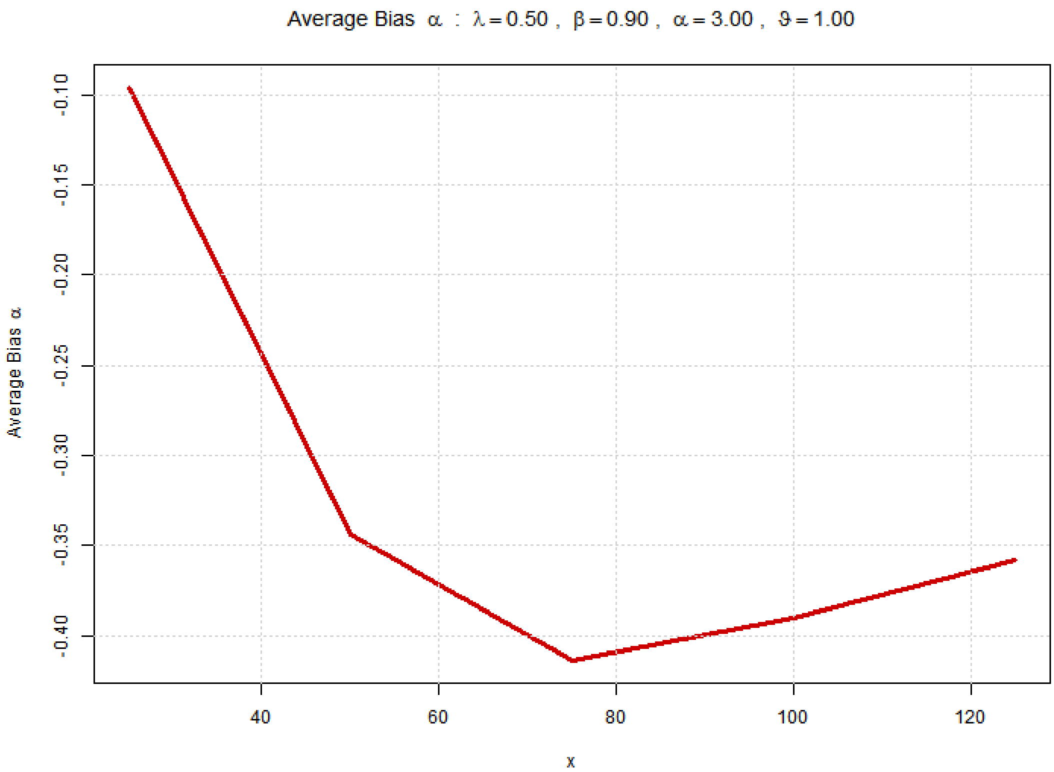

Fig. 10. Bias Alpha for $\lambda = 0.5, \beta = 0.9, \alpha = 3,$ and $\vartheta = 1$

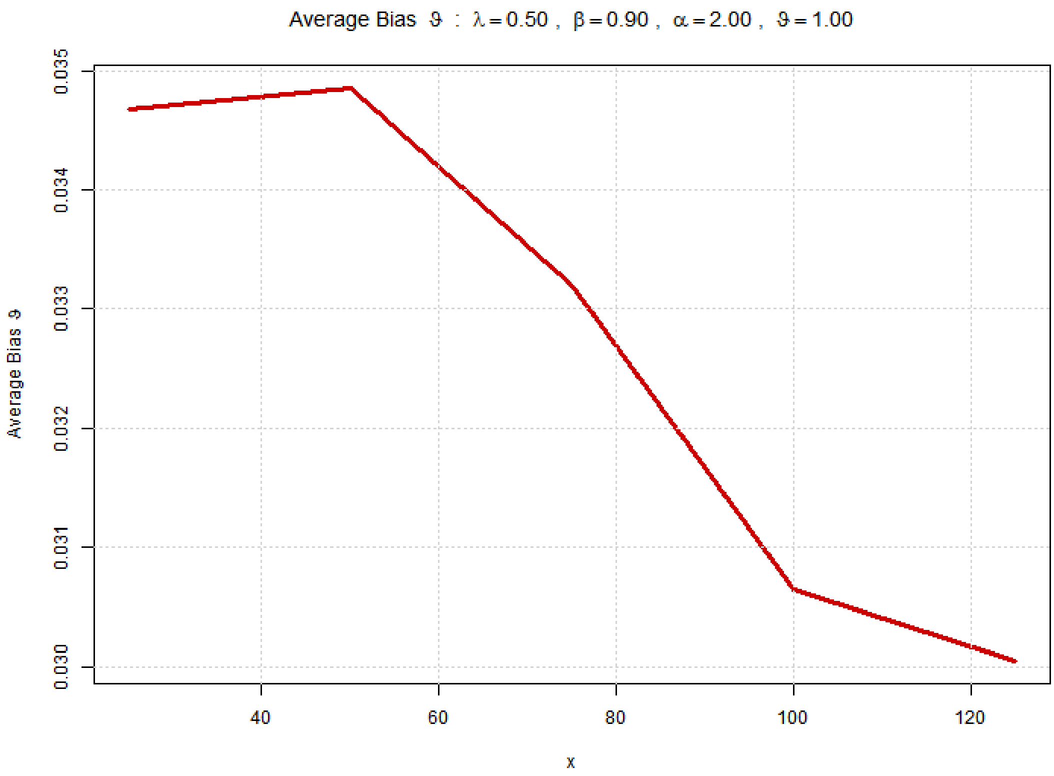

Fig. 11. Bias Vartheta for $\lambda = 0.5, \beta = 0.9, \alpha = 2,$ and $\vartheta = 1$

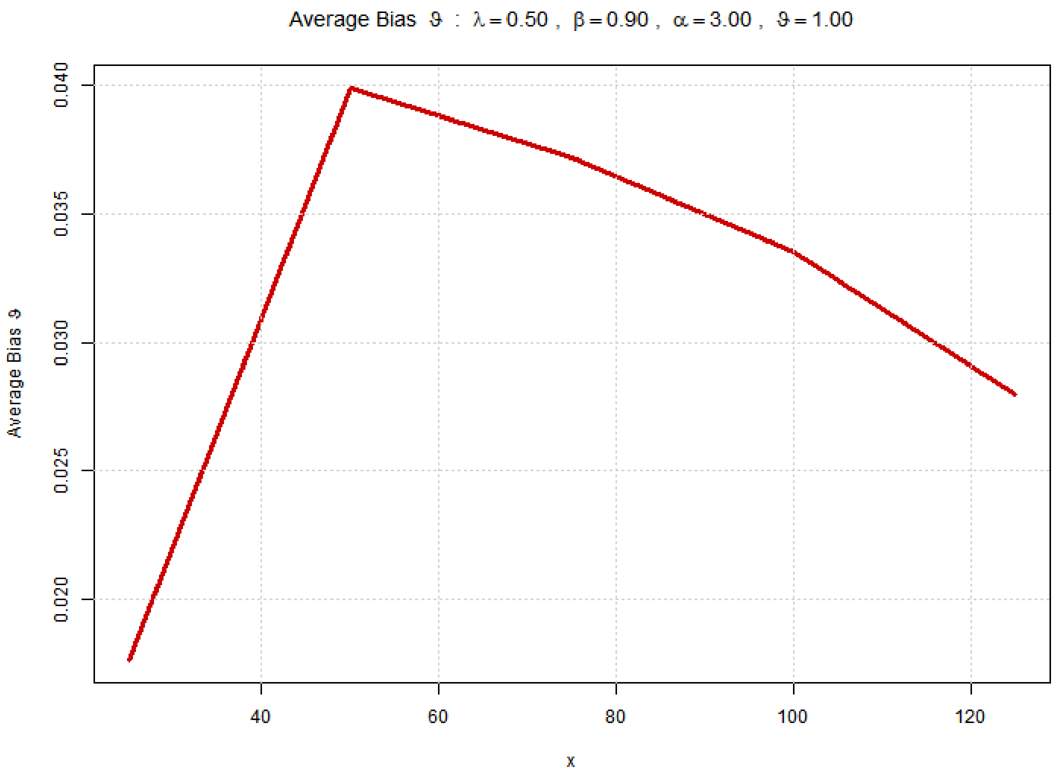

Fig. 12. Bias Vartheta for $\lambda = 0.5, \beta = 0.9, \alpha = 3,$ and $\vartheta = 1$

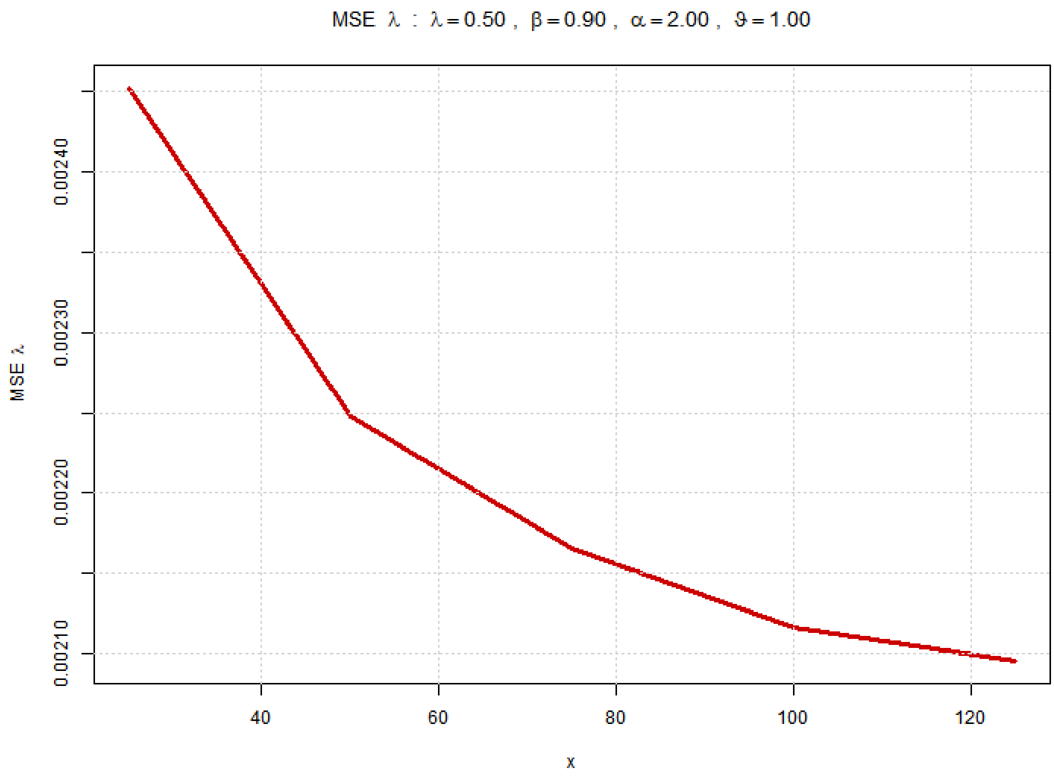

Fig. 13. MSE Lambda for $\lambda = 0.5, \beta = 0.9, \alpha = 2,$ and $\vartheta = 1$

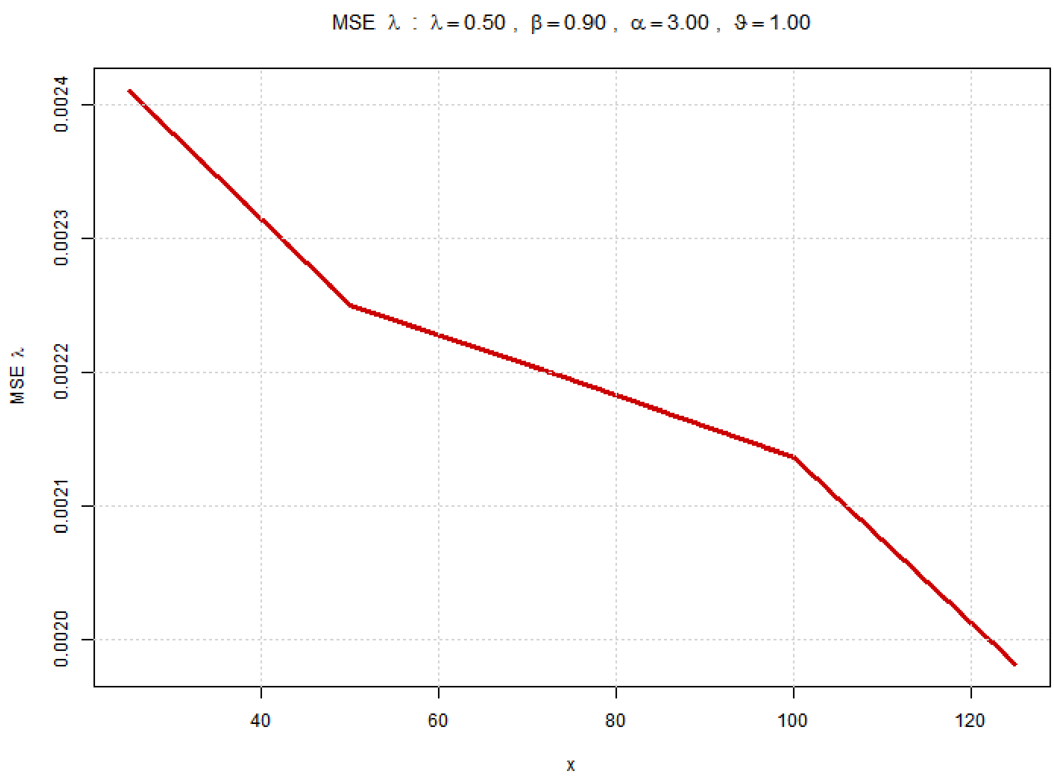

Fig. 14. MSE Lambda for $\lambda = 0.5, \beta = 0.9, \alpha = 3,$ and $\vartheta = 1$

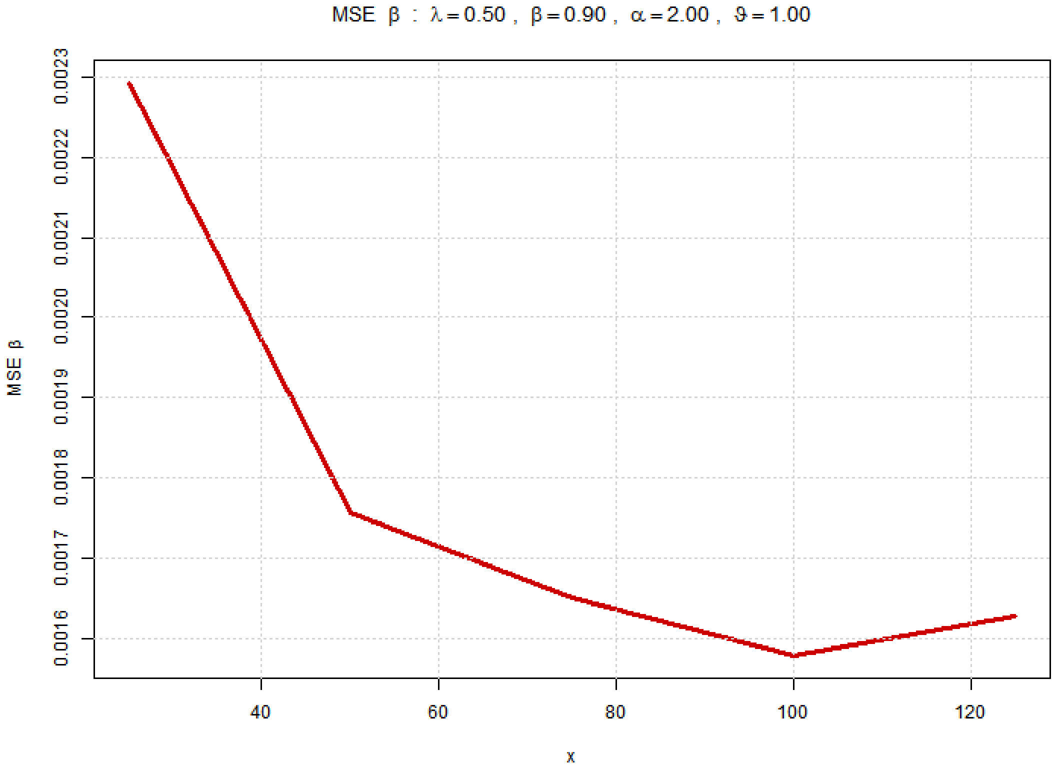

Fig. 15. MSE Beta for $\lambda = 0.5, \beta = 0.9, \alpha = 2,$ and $\vartheta = 1$

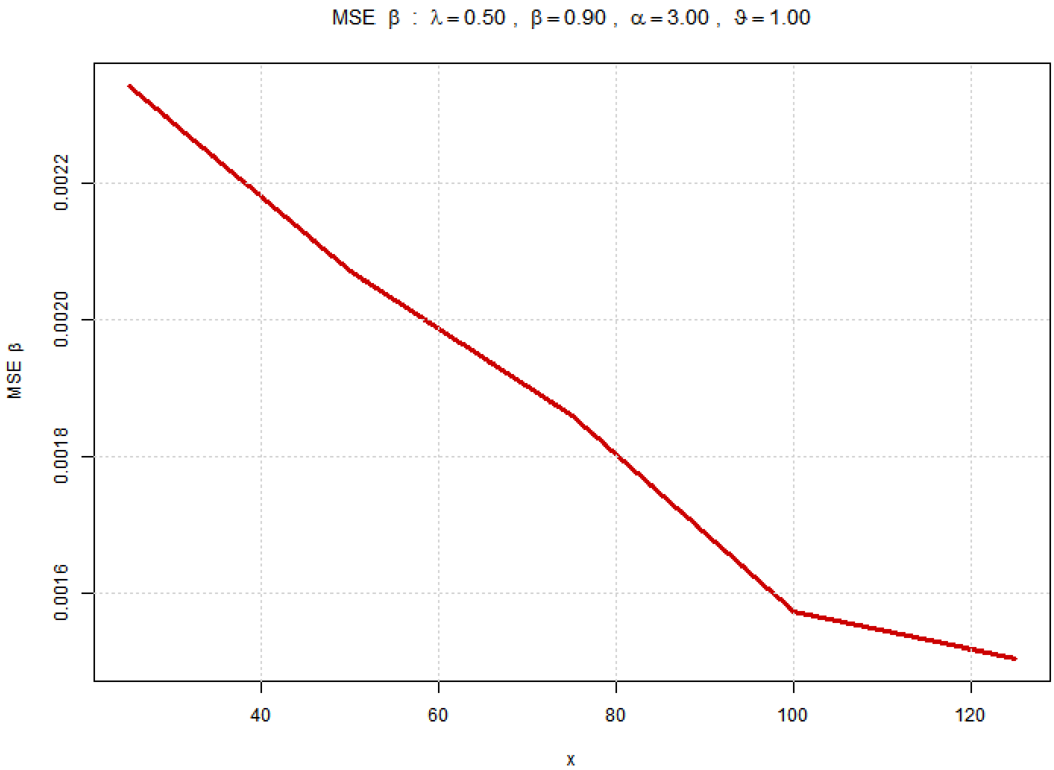

Fig. 16. MSE Beta for $\lambda = 0.5, \beta = 0.9, \alpha = 3,$ and $\vartheta = 1$

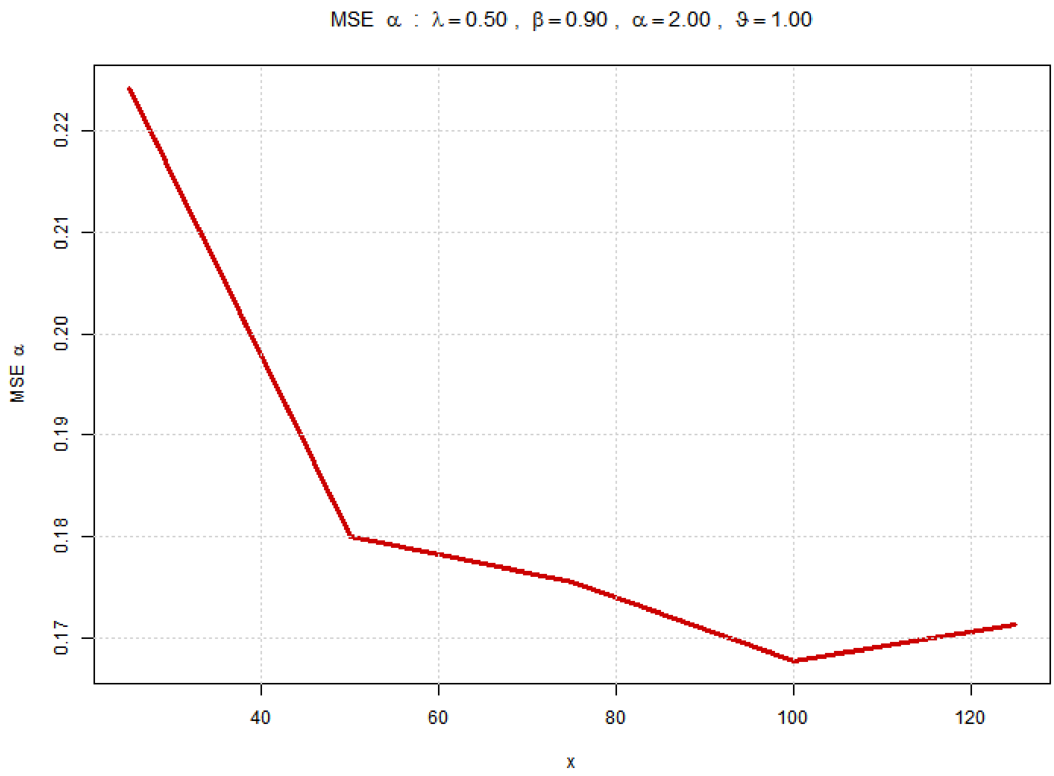

Fig. 17. MSE Alpha for $\lambda = 0.5, \beta = 0.9, \alpha = 2,$ and $\vartheta = 1$

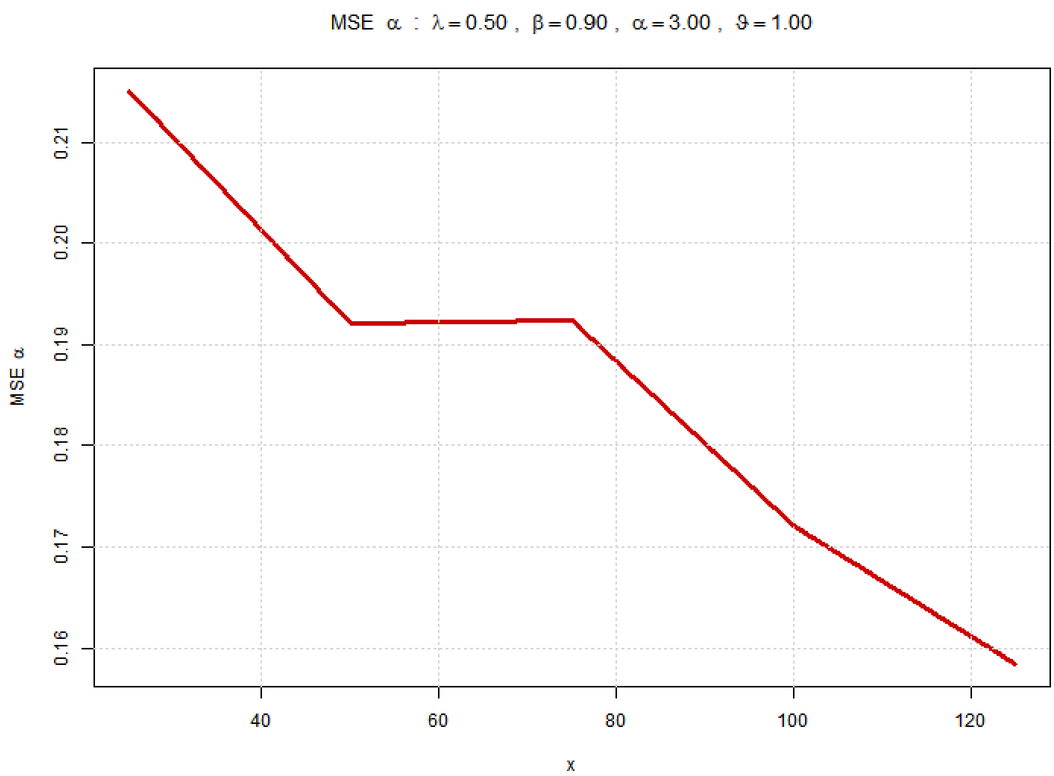

Fig. 18. MSE Alpha for $\lambda = 0.5, \beta = 0.9, \alpha = 3,$ and $\vartheta = 1$

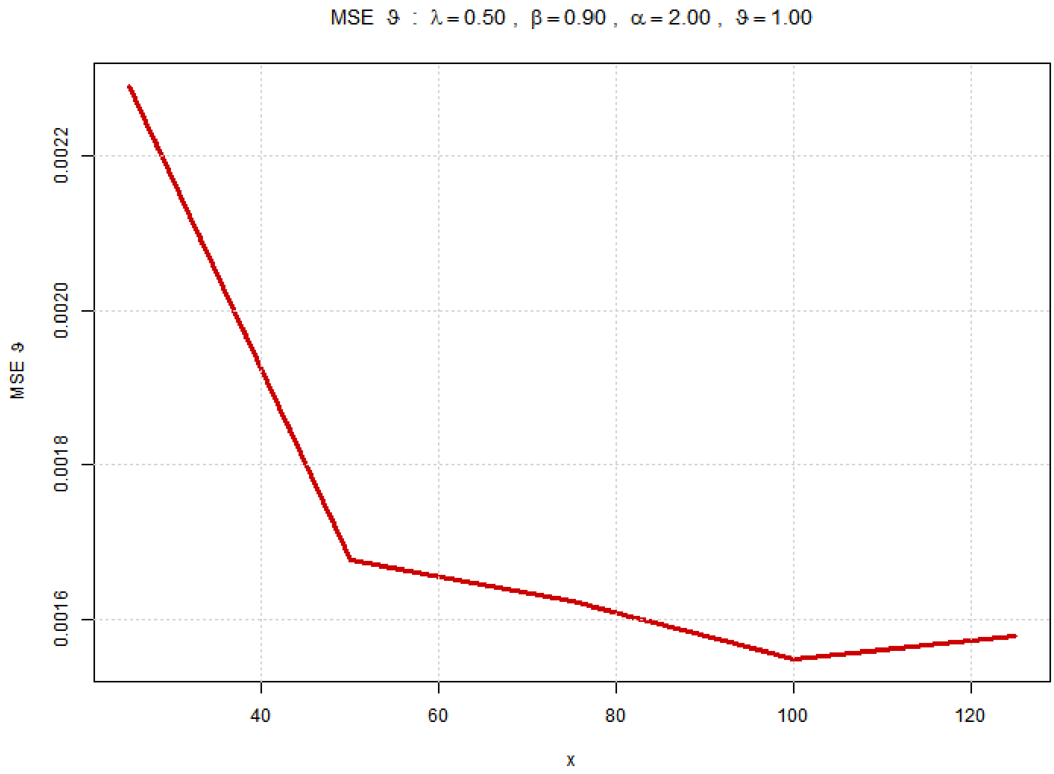

Fig. 19. MSE Vartheta for $\lambda = 0.5, \beta = 0.9, \alpha = 2,$ and $\vartheta = 1$

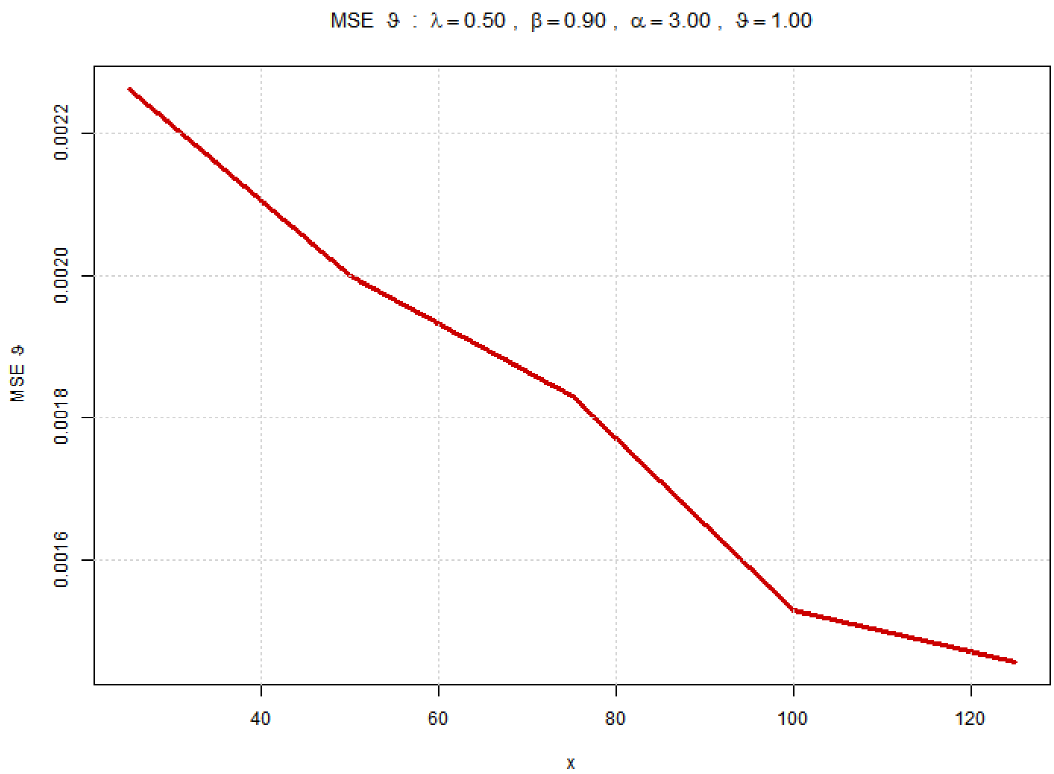

Fig. 20. MSE Vartheta for $\lambda = 0.5, \beta = 0.9, \alpha = 3,$ and $\vartheta = 1$

Figure [5-20] respectively show as the sample size grows, the average bias for the parameter estimators fluctuates upward and downward. The MSE for the parameter estimators, on the other hand, revealed a declining pattern as the sample size increased.

4. Applications

In this section, we provide application to real data sets to demonstration the applicability of the NE-G family. The real-world data set was collected on the breaking stress of carbon fibres with a length of 50 mm (GPa). The data has already been used by [16] and [17]. The following is the data set:

0.55, 0.93, 1.25, 1.36, 1.49, 1.52, 1.58, 1.61, 1.64, 1.68, 1.73, 1.81, 2,0.74, 1.04, 1.27, 1.39, 1.49, 1.53, 1.59, 1.61, 1.66,1.68, 1.76, 1.82, 2.01, 0.77, 1.11, 1.28, 1.42, 1.5,1.54, 1.6, 1.62, 1.66, 1.69, 1.76, 1.84,2.24, 0.81, 1.13, 1.29, 1.48, 1.5, 1.55, 1.61, 1.62,1.66, 1.7, 1.77, 1.84, 0.84, 1.24, 1.3, 1.48, 1.51, 1.55, 1.61, 1.63, 1.67, 1.7, 1.78, 1.89.

Table 1. MLEs and Goodness-of-fit measures for real data set

Model	MLE	$-\ell$	W	A	Ks	P-value
NE-U	λ=1.3844747 β= 0.3061201 α= 2.6127508 ϑ=21.1906288	85.97571	0.08519182	0.518155	0.088342	0.6816
Nak-Wei	λ=1.6103057 β= 1.1390558 α=0.2809454 ϑ=0.8761429	86.19047	0.09335068	0.5278914	0.10898	0.4133
GIK-Exp	λ= 4.0944733 β=0.8866774 θ=6.6609265 α=0.5132424	89.55029	0.1992844	1.069601	0.12743	0.2342
Exp.-Wei	λ= 0.5379012 β=1.8126305 α=0.3763266 ϑ= 1.8069314	91.99278	0.1818074	0.9721329	0.15906	0.07089
GOG-Exp	λ= 2.9664896 β=1.5056397 α=0.6131095	86.58091	0.1057304	0.6069994	0.094865	0.5925
OGG-Wei	λ= 1.9006879 β= 0.4242168 α=1.5138327 ϑ= 0.7524188	159.4275	0.18397049	0.6766763	0.62739	2.2e-16
Exp.	α= 2.9664896	132.9944	0.2462793	1.33359	0.35813	8.883e-08
Bet-Exp	λ=7.6786602 β=7.2017403 α=0.2758384	91.4858	0.2527494	1.369781	0.13384	0.1878

A summary of the fitted information criteria and MLEs is shown in Table 1. With the minimum of Cramér-von Misses (W), Anderson Darling (A), and Kolmogorov-Smirnov test (Ks) and the maximum value of log-likelihood, the proposed Nakagami exponential-uniform distribution has been sorted. As you can see, all the criteria pointed to the NE-U as the best model. Notably, NE-U's P-Value is higher than that of every other distribution.

5. Conclusion

This study proposes the appropriate NE-G family of distribution for any parent continuous distribution G. Quantile functions, moments, moments-generating functions, incomplete moments, entropy, and order statistics are some of the statistical and mathematical aspects of the new generator studied. The maximum likelihood estimates of model parameters are derived. We finally fitted the proposed NE-U model, among others, to real-life data and found that the Nakagami Exponential Uniform distribution outperformed its competitors. We anticipate that this generalisation will lead to other statistical applications.

Author Contributions

This work was equally contributed by all the writers. The authors read and approved the last version of the paper.

Conflicts of Interest

There are no conflicts of interest declared by the authors.

Acknowledgement

The Tertiary Education Trust Fund (TETFund) of Yobe State University in Nigeria financed this research.

References

[1] N. Eugene, C. Lee, F. Famoye, *Beta-Normal Distribution and Its Applications*, Communications in Statistics-Theory and Methods 31 (4) (2002) 497–512.

[2] M. A. R. De Pascoa, E. M. M. Ortega, G. M. Cordeiro, *The Kumaraswamy Generalized Gamma Distribution with Application in Survival Analysis*, Statistical methodology 8 (5) (2011) 411–433.

[3] G. M. Cordeiro, E. M. M. Ortega, D. C. C. da Cunha, *The Exponentiated Generalized Class of Distributions*, Journal of Data Science 11 (1) (2013) 1–27.

[4] H. Torabi, N. H. Montazeri, *The Logistic-Uniform Distribution and Its Applications*, Communications in Statistics-Simulation and Computation 43 (10) (2014) 2551–2569.

[5] M. M. Ristić, N. Balakrishnan, *The Gamma-Exponentiated Exponential Distribution*, Journal of Statistical Computation and Simulation 82 (8) (2012) 1191–1206.

[6] C. Alexander, G. M. Cordeiro, E. M. M. Ortega, J. M. Sarabia, *Generalized Beta-Generated Distributions*, Computational Statistics & Data Analysis 56 (6) (2012) 1880–1897.

[7] M. Amini, S. M. T. K. MirMostafaee, J. Ahmadi, *Log-Gamma-Generated Families of Distributions*, Statistics 48 (4) (2014) 913–932.

[8] A. S. Hassan, S. E. Hemeda, *A New Family of Additive Weibull-Generated Distributions*, rn 55 (2016) 7.

[9] M. Alizadeh, G. M. Cordeiro, E. De Brito, C. G. B. Demétrio, *The Beta Marshall-Olkin Family of Distributions*, Journal of Statistical Distributions and Applications 2 (1) (2015) 4.

[10] B. Hosseini, M. Afshari, M. Alizadeh, *The Generalized Odd Gamma-G Family of Distributions: Properties and Applications*, Austrian Journal of Statistics 47 (2) (2018) 69–89.

[11] H. Torabi, N. M. Hedesh, *The Gamma-Uniform Distribution and Its Applications*, Kybernetika 48 (1) (2012) 16–30.

[12] M. H. Tahir, M. Zubair, M. Mansoor, G. M. Cordeiro, M. Alizadehk, G. G. Hamedani, *A New Weibull-G Family of Distributions*, Hacettepe Journal of Mathematics and Statistics 45 (2) (2016) 629–647.

[13] A. Z. Afify, G. Cordeiro, F. Jamal, M. Elgarhy, M. Nasir, *The Marshall-Olkin Odd Burr III-G Family of Distributions: Theory, Estimation and Applications*.

[14] Z. Azam, A. Ahmad Saeed, J. Riffat, *A New Exponentiated Generalized Power Function Distribution*, Advances and Applications in Statistics 61 (1) (2020) 33–63.

[15] I. Abdullahi, J. Obalowu, *The Generalized Odd Nakagami-G Family of Distributions: Properties and Applications*, Naturengs 1 (2) (2020) 1–16.

[16] M. D. Nichols, W. J. Padgett, *A Bootstrap Control Chart for Weibull Percentiles*, Quality and reliability engineering international 22 (2) (2006) 141–151.

[17] P. E. Oguntunde, O. S. Balogun, H. I. Okagbue, S. A. Bishop, *The Weibull-Exponential Distribution: Its Properties and Applications*, Journal of Applied Sciences 15 (11) (2015) 1305–1311.

Journal of
New Theory
ISSN: 2149-1402

39 (2022) 42-53
Journal of New Theory
https://dergipark.org.tr/en/pub/jnt
Open Access

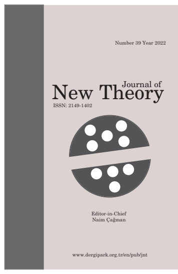

On the Multiplicative (Generalised) (α, α)-Derivations of Semiprime Rings

Handan Karahan[1], **Neşet Aydın**[2], **Didem Yeşil**[3]

Article Info
Received: 06 Jun 2022
Accepted: 28 Jun 2022
Published: 30 Jun 2022
doi:10.53570/jnt.1126644
Research Article

Abstract — The algebraic properties and identities of a semiprime ring are investigated with the help of the multiplicative (generalised)-(α, α)-reverse derivation on the non-empty ideal of the semiprime ring.

Keywords — *Semiprime ring, derivation, reverse derivation, generalised derivation, generalised reverse derivation*

Mathematics Subject Classification (2020) — 16N60, 16W25

1. Introduction

Many authors have investigated the relationship between the commutativity of a ring and the act of derivations(reverse derivation, (α, β)-reverse derivation, multiplicative reverse derivation, multiplicative (generalised) - (α, β)-reverse derivation etc.) defined on ring. Herstein was the first to introduce the concept of reverse derivation [1]. He shows that if R is a prime ring, and d is a nonzero reverse derivation of R, then R is a commutative integral domain, and d is a derivation. Firstly, Samman and Alyamani extended the result of Herstein to semiprime rings and investigated some more properties of reverse derivations in [2]. Asma and Bano inquired into some identities involving multiplicative (generalised) reverse derivation and demonstrated some theorems in which we characterise these mappings in [3]. Sandhu and Kumar investigate some properties of multiplicative reverse derivations on prime rings in [4]. Tiwari et al. described multiplicative (generalised) reverse derivation in [5]. The paper, as mentioned earlier, substantiated the commutativity of semiprime rings getting a multiplicative (generalised) reverse derivation satisfying some identities. Alhaidary and Majeed [6] proved commutativity of prime ring admitting a multiplicative (generalised) (α, β) reverse derivation such that α and β are automorphism on the prime ring, satisfying some identities. Further, they investigate some more properties of multiplicative (generalised)-(α, β)-reverse derivation of prime rings on square closed Lie ideals in [7]. The present paper study is directly motivated by the studies mentioned earlier and the work of Ulutaş and Gölbaşı [8]. We aim to investigate some identities with multiplicative (generalised) - (α, α)- reverse derivation on a nonzero ideal of a semiprime ring. Thus, we proved the following theorem:

[1]handankarahan1709@gmail.com; [2]neseta@comu.edu.tr; [3]dyesil@comu.edu.tr(Corresponding Author)
[1,2,3] Department of Mathematics, Faculty of Arts and Sciences, Çanakkale Onsekiz Mart University, Çanakkale, Turkiye

Theorem 1.1. Let R be a semiprime ring, α is an anti-epimorphism of R, $I \subsetneq Ker\alpha$ is a nonzero ideal of R and F is a nonzero multiplicative (generalised)-(α,α)-reverse derivation with the map d of R. If one of the following conditions holds,

i. $F([x,y]) = 0$,

ii. $F(xoy) = 0$,

iii. $F([x,y]) = \pm\alpha([x,y])$,

iv. $F(xoy) = \pm\alpha(xoy)$,

v. $F([x,y]) = \pm\alpha(xoy)$,

vi. $F(xoy) = \pm\alpha([x,y])$,

vii. $F([x,y]) = \pm\alpha([F(x),y])$,

viii. $F(xoy) = \pm\alpha(F(x)ox)$,

ix. $F(xy) = F(x)F(y)$,

x. $F(xy) + F(x)F(y) = 0$,

for all $x,y \in I$, then $[\alpha(x),d(x)] = 0$ for all $x \in I$.

2. Preliminaries

If the ring R satisfies the condition, $a = 0$ while $aRa = (0)$ for $a \in R$, it is called a semiprime ring. An additive mapping $d : R \to R$ is called (α,α) −derivation if $d(xy) = d(x)\alpha(y) + \alpha(x)d(y)$ holds for all $x,y \in R$, where α is automorphism of R. An additive mapping $d : R \to R$ is a reverse derivation, if $d(xy) = d(y)x + yd(x)$ for all $x,y \in R$. Let $d : R \to R$ be a map. If for all $x,y \in R$, $d(xy) = d(y)\alpha(x) + \alpha(y)d(x)$ such that α is an anti-epimorphism of R, then d is called multiplicative-(α,α)-reverse derivation. Let $F : R \to R$ be a mapping and d be a multiplicative (α,α)-reverse derivation . If for all $x,y \in R$,

$$F(xy) = F(y)\alpha(x) + \alpha(y)d(x)$$

then F is a called multiplicative (generalised)-(α,α)-reverse derivation associated with d. Hence the concept of multiplicative (generalised)-(α,α)-reverse derivation involves the concept of multiplicative (α,α)-reverse derivation and multiplicative generalised reverse derivation. Below, a multiplicative (generalised)-(α,α)-reverse derivation which is not multiplicative (generalised)-(α,α)-derivation and multiplicative (generalised)-(α,α)-derivation, which is not multiplicative (generalised)-(α,α)-reverse derivation examples, are given, respectively.

Example 2.1. Let $(R,+,.)$ be a commutative ring, and $(S,\oplus,\odot)$ be a noncommutative ring. Now let's consider operation $\circledast : S \times S \to S$, $a \circledast b = b \odot a$. With these operations $(S,\oplus,\circledast)$ called opposite ring and it is shown S^{op}.

$\alpha : S^{op} \to S^{op}$ is identity mapping, $d : S^{op} \to S^{op}$ is a multiplicative (α,α)-derivation, and $F : S^{op} \to S^{op}$ is a multiplicative (generalised)-(α,α)- derivation of R associated with a nonzero mapping d of R. Define the maps $\mu,\phi,\varphi : R \times S^{op} \to R \times S^{op}$ as follows: $\mu(a,x) = (a,F(x))$, $\phi(a,x) = (a,d(x))$ and $\varphi(a,x) = (a,\alpha(x))$. φ is an anti-homomorphism of R, and ϕ is multiplicative (φ,φ)-reverse derivation.

Then it is straightforward to verify that μ is a multiplicative (generalised)-(φ,φ)-reverse derivation associated with ϕ, but μ is not a multiplicative (generalised)-(φ,φ)-derivation of R.

Example 2.2. Now, define the maps $\mu,\phi,\varphi : R \times S^{op} \to R \times S^{op}$ as follows: $\mu(a,x) = (F(a),x)$, $\phi(a,x) = (d(a),x)$ and $\varphi(a,x) = (\alpha(a),x)$. ϕ is multiplicative (φ,φ)-derivation, and φ is an anti-homomorphism of R.

It is easy to see that μ is a multiplicative (generalised)-(φ,φ)-derivation if there exists a mapping ϕ, but μ is not a multiplicative (generalised)-(φ,φ)- reverse derivation of R.

3. Main Results

As of now on, R refers a semiprime ring, α is an anti-epimorphism of R, I is a nonzero ideal of R such that $I \subsetneq Ker(\alpha)$ and F is a nonzero multiplicative (generalised)-(α, α)-reverse derivation with the map d of R unless otherwise mentioned.

Lemma 3.1. d is a multiplicative -(α, α)-reverse derivation, that is, $d(xy) = d(y)\alpha(x) + \alpha(y)d(x)$ for all $x, y \in R$.

PROOF. By our assumption, we have

$$F(xz) = F(z)\alpha(x) + \alpha(z)d(x) \text{ for all } x, z \in R. \tag{1}$$

We put $x = xy$, $y \in R$ in (1), and since α is an anti-epimorphism of R,

$$F((xy)z) = F(z)\alpha(y)\alpha(x) + \alpha(z)d(xy) \text{ for all } x, y, z \in R. \tag{2}$$

Since $(xy)z = x(yz)$ and F is a multiplicative (generalised)-(α, α)-reverse derivation associated with the map d, that is

$$F(x(yz)) = F(z)\alpha(y)\alpha(x) + \alpha(z)d(y)\alpha(x) + \alpha(yz)d(x) \text{ for all } x, y, z \in R. \tag{3}$$

Subtracting (3) from (2), we obtain

$$\alpha(z)(d(xy) - d(y)\alpha(x) - \alpha(y)d(x)) = 0 \text{ for all } x, y, z \in R.$$

That is,

$$\alpha(R)(d(xy) - d(y)\alpha(x) - \alpha(y)d(x)) = 0 \text{ for all } x, y \in R.$$

Since α is an anti-epimorphism of R, $\alpha(R) = R$ and hence from above we have

$$R(d(xy) - d(y)\alpha(x) - \alpha(y)d(x)) = 0 \text{ for all } x, y \in R. \tag{4}$$

Left multipliying (4) by $d(xy) - d(y)\alpha(x) - \alpha(y)d(x)$, we get

$d(xy) - d(y)\alpha(x) - \alpha(y)d(x)R(d(xy) - d(y)\alpha(x) - \alpha(y)d(x)) = 0$ for all $x, y \in R$. Since R is a semiprime ring, we have

$$d(xy) - d(y)\alpha(x) - \alpha(y)d(x) = 0 \text{ for all } x, y \in R.$$

□

Lemma 3.2. $F(0) = 0$.

PROOF. From the definition of F, we get

$$F(xz) = F(z)\alpha(x) + \alpha(z)d(x) \text{ for all } x, z \in R. \tag{5}$$

Taking $x = 0$ and $z = 0$ in (5), one can obtain

$$F(0) = F(0)\alpha(0) + \alpha(0)d(0). \tag{6}$$

Since α is an additive map of R, it gives us $F(0) = 0$. □

Theorem 3.3. If $F([x,y]) = 0$ for all $x, y \in I$, then $[\alpha(x), d(x)] = 0$ for all $x \in I$.

PROOF. From our assumption,

$$F([x,y]) = 0 \text{ for all } x, y \in I. \tag{7}$$

If we write yx instead of x in (7), we get

$$0 = F([yx,y]) = F(y[x,y] + [y,y]x) \text{ for all } x, y \in I. \tag{8}$$

Besides, since F is a nonzero multiplicative (generalised)-(α,α)-reverse derivation with the map d, we have

$$F([x,y])\alpha(y) + \alpha([x,y])d(y) = 0 \text{ for all } x, y \in I. \tag{9}$$

When editing the last equation, we obtained

$$\alpha([x,y])d(y) = 0 \text{ for all } x, y \in I. \tag{10}$$

That is,

$$[\alpha(x), \alpha(y)]d(y) = 0 \text{ for all } x, y \in I. \tag{11}$$

Since α is an anti-epimorphism of R,

$$[z, \alpha(y)]d(y) = 0 \text{ for all } y \in I, z \in J, \tag{12}$$

where $J = \alpha(I)$ a nonzero ideal of R. We put $z = rz$, where $z \in J$, $r \in R$ in (12),

$$[r, \alpha(y)]zd(y) = 0 \text{ for all } y \in I, z \in J, r \in R. \tag{13}$$

We put $z = z\alpha(y)$ in (13),

$$[r, \alpha(y)]z\alpha(y)d(y) = 0 \text{ for all } y \in I, z \in J, r \in R. \tag{14}$$

Right multipliying (13) by $\alpha(y)$,

$$[r, \alpha(y)]zd(y)\alpha(y) = 0 \text{ for all } y \in I, z \in J, r \in R. \tag{15}$$

Subtracting (15) from (14),

$$[r, \alpha(y)]z[d(y), \alpha(y)] = 0 \text{ for all } y \in I, z \in J, r \in R. \tag{16}$$

Replacing r by $d(y)$ in (16),

$$[d(y), \alpha(y)]z[d(y), \alpha(y)] = 0 \text{ for all } y \in I, z \in J, r \in R,$$

where $J = \alpha(I)$ a semiprime ring, we get the required result. □

Theorem 3.4. If $F(xoy) = 0$ for all $x, y \in I$, then $[\alpha(x), d(x)] = 0$ for all $x \in I$.

PROOF. From the hypothesis,

$$F(xoy) = 0 \text{ for all } x, y \in I. \tag{17}$$

Substituting y by yx in (17),

$$\alpha(xoy)d(x) = 0 \text{ for all } x, y \in I. \tag{18}$$

Replacing y by zy, $z \in I$ in (18), and using α is an anti-epimorphism of R, we get

$$[\alpha(x), w]td(x) = 0 \text{ for all } x \in I, w, t \in J. \tag{19}$$

Replacing w by $wd(x)$ in (19),

$$w[\alpha(x), d(x)]td(x) = 0 \text{ for all } x \in I, w, t \in J. \tag{20}$$

Right multiplying (20) by $\alpha(x)$,

$$w[\alpha(x), d(x)]td(x)\alpha(x) = 0 \text{ for all } x \in I, w, t \in J. \tag{21}$$

We put $t = t\alpha(x)$ in (20),

$$w[\alpha(x), d(x)]t\alpha(x)d(x) = 0 \text{ for all } x \in I, w, t \in J. \tag{22}$$

Subtracting (22) from (21),

$$w[\alpha(x), d(x)]t[\alpha(x), d(x)] = 0 \text{ for all } x \in I, w, t \in J. \tag{23}$$

Replacing t by w in (23),

$$w[\alpha(x), d(x)]tw[\alpha(x), d(x)] = 0 \text{ for all } x \in I, w, t \in J,$$

where $J = \alpha(I)$ is semiprime ring, we get the required result. □

Theorem 3.5. If $F([x, y]) = \pm\alpha([x, y])$ for all $x, y \in I$, then $[\alpha(x), d(x)] = 0$ for all $x \in I$.

PROOF. By our assumption,

$$F([x, y]) = \pm\alpha([x, y]) \text{ for all } x, y \in I. \tag{24}$$

Replacing x with yx in (24),

$$\alpha([x, y])d(x) = 0 \text{ for all } x, y \in I.$$

Using the same arguments after (10) in the proof of Theorem 3.3, the desired result is obtained. □

Theorem 3.6. If $F(xoy) = \pm\alpha(xoy)$ for all $x, y \in I$, then $[\alpha(x), d(x)] = 0$ for all $x \in I$.

PROOF. From the assumption,

$$F(xoy) = \pm\alpha(xoy) \text{ for all } x, y \in I. \tag{25}$$

Substituting x by yx in (25),

$$\alpha(xoy)d(y) = 0 \text{ for all } x, y \in I.$$

Since the last case is the same as the equation (10) and using the similar argument as used in the Theorem 3.4, the desired result is obtained. □

Theorem 3.7. If $F([x,y]) = \pm\alpha(xoy)$ for all $x, y \in I$, then $[\alpha(x), d(x)] = 0$ for all $x \in I$.

PROOF. By the assumption,

$$F([x,y]) = \pm\alpha(xoy) \ for \ all \ x, y \in I. \tag{26}$$

Replacing x with yx in (26),

$$\alpha([x,y])d(y) = 0 \text{ for all } x, y \in I.$$

The last expression is the same as the relation (10) and hence using the similar argument as used in Theorem 3.3, we get the required result. □

Theorem 3.8. If $F(xoy) = \pm\alpha([x,y])$ for all $x, y \in I$, then $[\alpha(x), d(x)] = 0$ for all $x \in I$.

PROOF. Substituting yx instead of x in hypothesis,

$$\alpha(xoy)d(y) = 0 \text{ for all } x, y \in I.$$

Since the last expression is the same as the equation (18), the desired result is obtained by the following similar steps in the Theorem 3.4, □

Theorem 3.9. If $F([x,y]) = \pm\alpha([F(x), y])$ for all $x, y \in I$, then $[\alpha(x), d(x)] = 0$ for all $x \in I$.

PROOF. By the supposition, we have

$$F([x,y]) = \pm\alpha([F(x), y]) \ for \ all \ x, y \in I. \tag{27}$$

We put $y = xy$ in (27),

$$\alpha([x,y])d(x) \ = \pm\alpha(y)\alpha([F(x), x]) \ for \ all \ x, y \in I. \tag{28}$$

Replacing x in place of y in (27),

$$\pm\,\alpha([F(x), x]) = 0 \ for \ all \ x \in I. \tag{29}$$

Appliying (29), (28) yields that

$$\alpha([x,y])d(x) = 0 \text{ for all } x, y \in I.$$

The equation is same as the equation (10) in Theorem 3.3, thus we proceed in the same way as in Theorem 3.3 and we get the required result. □

Theorem 3.10. If $F(xoy) = \pm\alpha(F(x)ox)$ for all $x, y \in I$, then $[\alpha(x), d(x)] = 0$ for all $x \in I$.

PROOF. By the hypothesis,

$$F(xoy) = \pm\alpha(F(x)ox) \; for \; all \; x, y \in I. \tag{30}$$

Replacing y with xy in (30),

$$\alpha(xoy)d(x) = \pm\alpha(y)\alpha([F(x), x]) \; for \; all \; x, y \in I. \tag{31}$$

Substituting yr, $r \in R$ for y in (31) and using this equation,

$$\alpha([x, r])\alpha(y)d(x) = 0 \; for \; all \; x, y \in I, r \in R. \tag{32}$$

Seeing α is an anti-epimorphism of R,

$$[\alpha(x), r]zd(x) = 0 \text{ for all } x \in I, z \in J, r \in R.$$

The last expression is the same as the relation (13) and hence using the similar argument as used in Theorem 3.3, we get the required result. □

Theorem 3.11. If $F(xy) = F(x)F(y)$ for all $x, y \in I$, then $[\alpha(x), d(x)] = 0$ for all $x \in I$.

PROOF. By the hypothesis,

$$F(xy) = F(x)F(y) \text{ for all } x, y \in I. \tag{33}$$

Then replacing y with xy in (33),

$$F(x(xy)) = F(xy)\alpha(x) + F(x)\alpha(y)d(x) \text{ for all } x, y \in I. \tag{34}$$

Since F is a nonzero multiplicative generalised-(α, α)-reverse derivation associated with a nonzero mapping d of R, it follows that

$$F(x(xy)) = F(xy)\alpha(x) + \alpha(xy)d(x) \text{ for all } x, y \in I. \tag{35}$$

Subtracting (35) from (34),

$$(\alpha(xy) - F(x)\alpha(y))d(x) = 0 \text{ for all } x, y \in I. \tag{36}$$

Substituting yr, $r \in R$ for y in (36) and since α is an anti-epimorphism of R,

$$(r\alpha(xy) - F(x)r\alpha(y))d(x) = 0 \text{ for all } x, y \in I, r \in R. \tag{37}$$

Replacing r with $F(z)$, where $z \in I$, in (37),

$$(F(z)\alpha(xy) - F(x)F(z)\alpha(y))d(x) = 0 \text{ for all } x, y, z \in I. \tag{38}$$

Left multiplying (36) by $F(z)$ and then subracting from (38),

$$(F(zx) - F(xz))\alpha(y)d(x) = 0 \text{ for all } x, y, z \in I. \tag{39}$$

Replacing xz in place of z in (39),

$$\alpha([z, x])d(x)\alpha(y)d(x) = 0 \text{ for all } x, y, z \in I. \tag{40}$$

Since for $r \in R$, $[z, x]r \in I$, we put $y = [z, x]r$ in (40) and α is an anti-epimorphism of R,

$$\alpha([z, x])d(x)R\alpha([z, x])d(x) = 0 \text{ for all } x, z \in I. \tag{41}$$

Since R is a semiprime ring,

$$\alpha([z, x])d(x) = 0 \text{ for all } x, z \in I. \tag{42}$$

Replacing z with zr, where $r \in R$, in (42),

$$[\alpha(r), \alpha(x)]\alpha(z)d(x) = 0 \text{ for all } x, z \in I, r \in R. \tag{43}$$

Right multiplying (43) by $\alpha(x)$,

$$[\alpha(r), \alpha(x)]\alpha(z)d(x)\alpha(x) = 0 \text{ for all } x, z \in I, r \in R. \tag{44}$$

Replacing xz in place of z in (43) and then subracting from (44),

$$[\alpha(r), \alpha(x)]\alpha(z)[d(x), \alpha(x)] = 0 \text{ for all } x, z \in I, r \in R. \tag{45}$$

Since α is an anti-epimorphism of R, $\alpha(R) = R$ and hence from above,

$$[r, \alpha(x)]\alpha(I)[d(x), \alpha(x)] = 0 \text{ for all } x \in I, r \in R. \tag{46}$$

We put $r = d(x)$ in (46) and since α is an anti-epimorphism of R,

$$[d(x), \alpha(x)]\alpha(I)[d(x), \alpha(x)] = 0 \text{ for all } x \in I. \tag{47}$$

Since $\alpha(I)$ is a semiprime ring,

$$[d(x), \alpha(x)] = 0 \text{ for all } x \in I.$$

□

Theorem 3.12. If $F(xy) + F(x)F(y) = 0$ for all $x, y \in I$, then $[\alpha(x), d(x)] = 0$ for all $x \in I$.

Proof. If F is a nonzero multiplicative generalised-(α,α)-reverse derivation associated with a nonzero map d, then $-F$ is a nonzero multiplicative generalised-(α,α)-reverse derivation associated with a nonzero map $-d$. We get the results by replacing F with $-F$ and d with $-d$ in Theorem 3.11. □

Theorem 3.13. If $F(xy) = F(y)F(x)$ for all $x, y \in I$, then $\alpha(I)d(I) = 0$ and $[F(y), \alpha(y)] = 0$ for all $y \in I$.

PROOF. We have

$$F(xy) = F(y)F(x) \text{ for all } x, y \in I. \tag{48}$$

Then replacing x with xz in (48), where $z \in I$,

$$F((xz)y) = F(zy)\alpha(x) + F(y)\alpha(z)d(x) \text{ for all } x, y, z \in I. \tag{49}$$

Since F is a nonzero multiplicative generalised-(α, α)-reverse derivation associated with a nonzero map d of R,

$$F(x(zy)) = F(zy)\alpha(x) + \alpha(y)\alpha(z)d(x) \text{ for all } x, y, z \in I. \tag{50}$$

Subtracting (49) from (50),

$$(F(y) - \alpha(y))\alpha(z)d(x) = 0 \text{ for all } x, y, z \in I. \tag{51}$$

Substituting z by zr, $r \in R$ in (51) and since α is an anti-epimorphism of R,

$$(F(y) - \alpha(y))R\alpha(z)d(x) = 0 \text{ for all } x, y, z \in I. \tag{52}$$

We put $x = y$ in (52),

$$(F(y) - \alpha(y))R\alpha(z)d(y) = 0 \text{ for all } y, z \in I. \tag{53}$$

Left multiplying (53) by $F(z)$, that is

$$F(z)(F(y) - \alpha(y))R\alpha(z)d(y) = 0 \text{ for all } x, y, z \in I. \tag{54}$$

Again, from (48) we can write $F(z)\alpha(y) + \alpha(z)d(y) = F(z)F(y)$ for all $x, y, z \in I$, that is

$$F(z)(F(y) - \alpha(y)) = \alpha(z)d(y) \ for \ all \ x, y, z \in I. \tag{55}$$

Let's substitute (55) in (54), we get $F(z)(F(y) - \alpha(y))RF(z)(F(y) - \alpha(y)) = 0$ for all $y, z \in I$. Moreover $\alpha(z)d(y)R\alpha(z)d(y) = 0$ for all $x, z \in I$ where R is semiprime ring, we conclude that $\alpha(z)d(y) = 0$ $for \ all \ x, z \in I$, that is $\alpha(I)d(I) = 0$ and $F(z)(F(y) - \alpha(y)) = 0$ for all $y, z \in I$. Thus we have

$$F(xy) = F(y)\alpha(x) \text{ for all } x, y \in I.$$

Now putting $z = yz$ and $y = y^2$ in $F(z)(F(y) - \alpha(y)) = 0$ for all $y, z \in I$,

$$F(z)\alpha(y)(F(y) - \alpha(y)) = 0 \ for \ all \ y, z \in I. \tag{56}$$

and

$$F(z)(F(y)\alpha(y) - \alpha(y)^2) = 0 \ for \ all \ y, z \in I. \tag{57}$$

Subtracting (57) from (56),

$$F(z)[F(y),\alpha(y)] = 0 \; for \; all \; y,z \in I. \tag{58}$$

We put $z = xz$ in (58),

$$F(z)\alpha(x)[F(y),\alpha(y)] = 0 \text{ for all } x,y,z \in I. \tag{59}$$

Then replacing z with z^2 in (59) and since α is an anti-epimorphism of R,

$$F(z)\alpha(z)\alpha(x)[F(y),\alpha(y)] = 0 \text{ for all } x,y,z \in I. \tag{60}$$

We put $x = xz$ in (59), we obtain

$$F(z)\alpha(z)\alpha(x)[F(y),\alpha(y)] = 0 \text{ for all } x,y,z \in I. \tag{61}$$

Left multiplying (59) by $\alpha(z)$, that is

$$\alpha(z)F(z)\alpha(x)[F(y),\alpha(y)] = 0 \text{ for all } x,y,z \in I. \tag{62}$$

Subtracting (61) from (62), we obtain

$$[F(z),\alpha(z)]\alpha(x)[F(y),\alpha(y)] = 0 \text{ for all } x,y,z \in I. \tag{63}$$

Then replacing x with xr, $r \in R$ in (63), and since α is an anti-epimorphism of R,

$$[F(z),\alpha(z)]R\alpha(x)[F(y),\alpha(y)] = 0 \text{ for all } x,y,z \in I. \tag{64}$$

Left multiplying (64) by $\alpha(x)$, we obtain

$$\alpha(x)[F(z),\alpha(z)]R\alpha(x)[F(y),\alpha(y)] = 0 \text{ for all } x,y,z \in I. \tag{65}$$

We put $y = z$ in (65), for all $x,y,z \in I$

$$\alpha(x)[F(z),\alpha(z)]R\alpha(x)[F(z),\alpha(z)] = 0 \text{ for all } x,z \in I,$$

is obtained.Since F and $\alpha(I)$ is semiprime ring, we conclude that $[F(y),\alpha(y)] = 0$ for all $y \in I$. □

Theorem 3.14. If $F(xy) + F(y)F(x) = 0$ for all $x,y \in I$, then $\alpha(I)d(I) = 0$ and $[F(y),\alpha(y)] = 0$ for all $y \in I$.

Proof. If F is a nonzero multiplicative generalised-(α,α)-reverse derivation associated with a nonzero map d, then $-F$ is a nonzero multiplicative (generalised)-(α,α)-reverse derivation associated with a nonzero map d. Thus replacing F with $-F$ and d with $-d$ in Theorem 3.13. □

4. Conclusions

We have shown some properties of a nonzero ideal of a semiprime ring with multiplicative (generalised) (α, α)-reverse derivation. Moreover, when R is a semiprime ring, α is an anti-epimorphism of R, I is a nonzero ideal of R such that $I \subsetneq Ker(\alpha)$ and $F : R \to R$ is a nonzero multiplicative (generalised) (α, α)-reverse derivation, we investigated the commutativity of semiprime rings. Also, we give examples for each multiplicative (generalised) (α, α)-reverse derivation and generalised (α, α)-reverse derivation. Furthermore, we adapt some well-known results in reverse derivation to (α, α)-reverse derivation. The commutativity of a ring can be investigated in the sense of this article and the articles in [9–13].

Author Contributions

This study was derived from the master's thesis of the Handan Karahan. Neşet Aydın posed the problem and supervised this work's findings. Handan Karahan and Neşet Aydın wrote the manuscript in consultation with Didem Yeşil. Didem Yeşil reviewed and edited the manuscript. They all read and approved the last version of the paper.

Conflicts of Interest

The authors declare no conflict of interest.

References

[1] I. N. Herstein, *Jordan Derivations of Prime Rings*, Proceedings of the American Mathematical Society 8 (6) (1957) 1104–1110.

[2] M. S. Samman, and N. Alyamani, *Derivations and Reverse Derivations in Semiprime Rings*, International Mathematical Forum 2 (39) (2007) 1895–1902.

[3] A. Asma, and A. Bano, *Multiplicative (Generalized) Reverse Derivations on Semiprime Ring*, European Journal of Pure and Applied Mathematics 11 (3) (2018) 717–729.

[4] G. S. Gurninder, and D. Kumar, *Annihilator Conditions of Multiplicative Reverse Derivation on Prime Rings*, International Electronic Journal of Algebra 25 (2019) 87–103.

[5] S. K. Tiwari, R. K. Sharma, and B. Dhara, *Some theorems of commutativity on semiprime rings with mappings*, Southeast Asian Bulletin of Mathematics 42 (2) (2018) 279–292.

[6] Z. S. M. Alhaidary, and A. H. Majeed, *Commutativity Results for Multiplicative (Generalized) (α, β)-Reverse Derivations on Prime Rings*, Iraqi Journal of Science 62 (9) (2021) 3102–3113.

[7] Z. S. M. Alhaidary, and A. H. Majeed, *Square Closed Lie Ideals and Multiplicative (Generalised) (α, β)-Reverse Derivation of Prime Rings*, Journal of Discrete Mathematical Sciences & Cryptography 24 (7) (2021) 2037–2046.

[8] E. Ulutas, and Ö. Gölbası, *Results On Multiplicative Generalized (α, α)-Derivations*, International Journal of Open Problems in Computer Science & Mathematics 13 (3) (2020) 128–135.

[9] S. Türkmen, and N. Aydın, *Generalized *-Lie ideal of *-Prime Ring*, Turkish Journal of Mathematics 41 (4) (2017) 841–853.

[10] N. Aydın, E. Koç, and Ö Gölbaşı, *On *-(σ, τ)-Lie Ideals of *-Prime Rings with Derivation*, Hacettepe Journal of Mathematics and Statics 47 (5) (2018) 1240–1247.

[11] B. Albayrak, and N. Aydın, *Reverse and Jordan-biderivation on Prime and semiprime Rings*, Adıyaman University Journal of Science 9 (1) (2019) 149–164.

[12] B. Albayrak, and D. Yeşil, *A Generalized Study on Closed Lie İdeals with* (α, α)*-derivations*, Eskişehir Technical University Journal of Science and Technology B - Theoretical Sciences 7 (2) (2019) 195–203.

[13] B. Albayrak, and D. Yeşil, *Closed Lie Ideals of Prime Rings with Generalized* α*-Derivations*, International Journal of Mathematics Trends and Technology 65 (7) (2019) 101–109.

Journal of New Theory
ISSN: 2149-1402

39 (2022) 54-83
Journal of New Theory
https://dergipark.org.tr/en/pub/jnt
Open Access

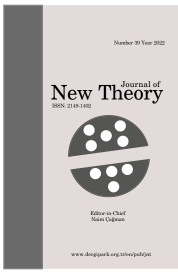

Diagnosing COVID-19, Prioritizing Treatment, and Planning Vaccination Priority via Fuzzy Parameterized Fuzzy Soft Matrices

Zeynep Parla Parmaksız[1], Burak Arslan[2], Samet Memiş[3], Serdar Enginoğlu[4]

Article Info
Received: 09 Jun 2022
Accepted: 30 Jun 2022
Published: 30 Jun 2022
doi:10.53570/jnt.1128289
Research Article

Abstract — In the fight against the COVID-19 pandemic, it is vital to rapidly diagnose possible contagions, treat patients, plan follow-up procedures with correct and effective use of resources and ensure the formation of herd immunity. The use of machine learning and statistical methods provides great convenience in dealing with too many data produced during research. Since access to the PCR test used for the diagnosis of COVID-19 may be limited, the test is relatively too slow to yield results, the cost is high, and its reliability is controversial; thus, making a symptomatic classification before the PCR is timesaving and far less costly. In this study, by modifying a state-of-the-art classification method, namely Comparison Matrix-Based Fuzzy Parameterized Fuzzy Soft Classifier (FPFS-CMC), an effective method is developed for a rapid diagnosis of COVID-19. The paper then presents the accuracy, sensitivity, specificity, and F1-score values that represent the diagnostic performances of the modified method. The results show that the modified method can be adopted as a competent and accurate diagnosis procedure. Afterwards, a tirage study is performed by calculating the patients' risk scores to manage inpatient overcrowding in healthcare institutions. In the subsequent section, a vaccine priority algorithm is proposed to be used in the case of a possible crisis until the supply shortage of a newly developed vaccine is over if a possible variant of COVID-19 that is highly contagious is insensitive to the vaccine. The accuracy of the algorithm is tested with real-life data. Finally, the need for further research is discussed.

Keywords – *Medical diagnosing, prioritizing treatment, planning vaccination priority, fpfs-matrices, soft decision-making*

Mathematics Subject Classification (2020) – 03E72, 68Q32

1. Introduction

1.1. Diagnosis of COVID-19

The severe acute respiratory syndrome coronavirus (SARS-CoV-2) has affected our lives for the past two years. Rapid diagnosis of possible contagions, planning of follow-up treatment, and effective use of resources have vital importance in the fight against the COVID-19 pandemic. The use of machine learning and statistical methods provides great convenience to deal with these difficulties. In the literature, there are several common

[1]zeynepparlaparmaksiz@gmail.com (Corresponding Author); [2]tburakarslan@gmail.com; [3]samettmemis@gmail.com; [4]serdarenginoglu@gmail.com
[1]Beşiktaş Arts and Sciences Centre, İstanbul, Turkiye
[2,4]Department of Mathematics, Faculty of Arts and Sciences, Çanakkale Onsekiz Mart University, Çanakkale, Turkiye
[3]Department of Computer Engineering, Faculty of Engineering and Natural Sciences, İstanbul Rumeli University, İstanbul, Turkiye

classifiers, such as Support Vector Machine (SVM) [1], Fuzzy k-Nearest Neighbour (Fuzzy kNN) [2], AdaBoost [3], Decision Tree (DT) [4], Fuzzy Soft Set Classifier (FSSC) [5], Fuzzy Soft Set Classifier Using Distance-Based Similarity Measure (FussCyier) [6], and Hamming Distance-Based Fuzzy Soft Set Classifier (HDFSSC) [7]. Recently, a novel classifier, i.e., Compare-Matrix Based Fuzzy Parameterized Fuzzy Soft Classifier (FPFS-CMC) [8,9] that produces high scores in “Breast Cancer”, “Parkinsons[sic]”, and “Parkinson’s Diseases” datasets provided in UCI Machine Learning Repository [10], has been prominent among the aforesaid classifiers in medical diagnosis. However, it has not been applied to COVID-19 yet. Therefore, it is worth studying to diagnose COVID-19 via the classifier. This study, firstly, detects whether the individual is COVID-19 positive by utilizing a state-of-the-art classification method FPFS-CMC.

COVID-19: SARS-CoV-2 was first reported in Wuhan, China, in December 2019 and spread rapidly worldwide. COVID-19 formed a clade within the subgenus sarbecovirus, Orthocoronavirinae subfamily. This virus is a droplet infection [11]. The available research on COVID-19 has been increasing [12-18]. Moreover, several datasets related to COVID-19 have been shared in data repositories, such as UCI and Kaggle. This study uses the datasets titled “Symptoms and COVID Presence (May 2020 data)”, “Covid-19 Symptoms”, and “Brazilian Covid Symptomatic Patients Data” [19-21], provided in Kaggle Data Repository to diagnose COVID-19 by using a classification method (classifier).

Classifiers: Supervised learning is a sub-field of machine learning which is commonly used in various fields, particularly defense industry, meteorology, psychology, finance, medicine, astronomy, and space sciences. Classification is a supervised learning technique that learns a predictive model from the training data to make an accurate prediction of a datum’s label [22]. Classifiers utilize the information of the training set, whose labels are known, and predict the class label of a sample with an unknown label. So far, many classifiers have been produced, such as SVM, Fuzzy kNN, AdaBoost, DT, FSSC, FussCyier, and HDFSSC.

Lately, a state-of-the-art classifier FPFS-CMC, which employs the modeling capability of fuzzy parameterized fuzzy soft matrices (*fpfs*-matrices) [23] in real-world problems containing uncertainties, has been proposed. FPFS-CMC produces high scores than the aforesaid classifiers in “Breast Cancer”, “Parkinsons[sic]”, and “Parkinson’s Disease” datasets provided in UCI Machine Learning Repository [10]. Therefore, this study utilizes FPFS-CMC to diagnose COVID-19.

1.2. Follow-Up Treatment Priority in COVID-19 Patients

Designing an algorithm to calculate each patient’s risk score is crucial for hospitals to provide better follow-up methods and treatment services. These unique risk scores for patients who have tested positive for COVID-19 have significance to compare the severity levels of the disease in patients. This study secondly determines how severely the patient will recover from the virus by comparing risk scores.

Comorbidities: Comorbidities can negatively affect patients’ conditions during COVID-19 [13,14,17,18]. This study focuses on the common comorbidities during COVID-19 – namely, hypertension, cardiovascular diseases, cancer, chronic kidney failure, and diabetes.

1.3. Vaccination Priority Planning

Furthermore, the COVID-19 vaccination priority planning is essential to overcoming a possible crisis until the supply shortage of a newly developed vaccine is over in the case a possible highly contagious variant of COVID-19 is insensitive to the vaccine. Besides, planning for booster doses is another issue that needs to be considered when an inadequate number of vaccines are available. This study thirdly produces a ranking order among individuals who are willing to get vaccinated based on their vaccination priority scores. Finally, it discusses the need for further research.

Current Vaccination Applications: Currently, several criteria are being utilized in the vaccination process. While planning for vaccination, the Turkish Ministry of Health [16] focused on systemic diseases, age, and occupation of an individual who will be vaccinated. This study expands these criteria to make a more specific analysis of the vaccination process. It considers seven criteria, i.e., systemic disease, age, presence of risk group individuals in the immediate vicinity, presence of COVID-19 history, province-district, transportation preference, and occupation, to make a better priority planning. The framework in this study is shown in Fig. 1.

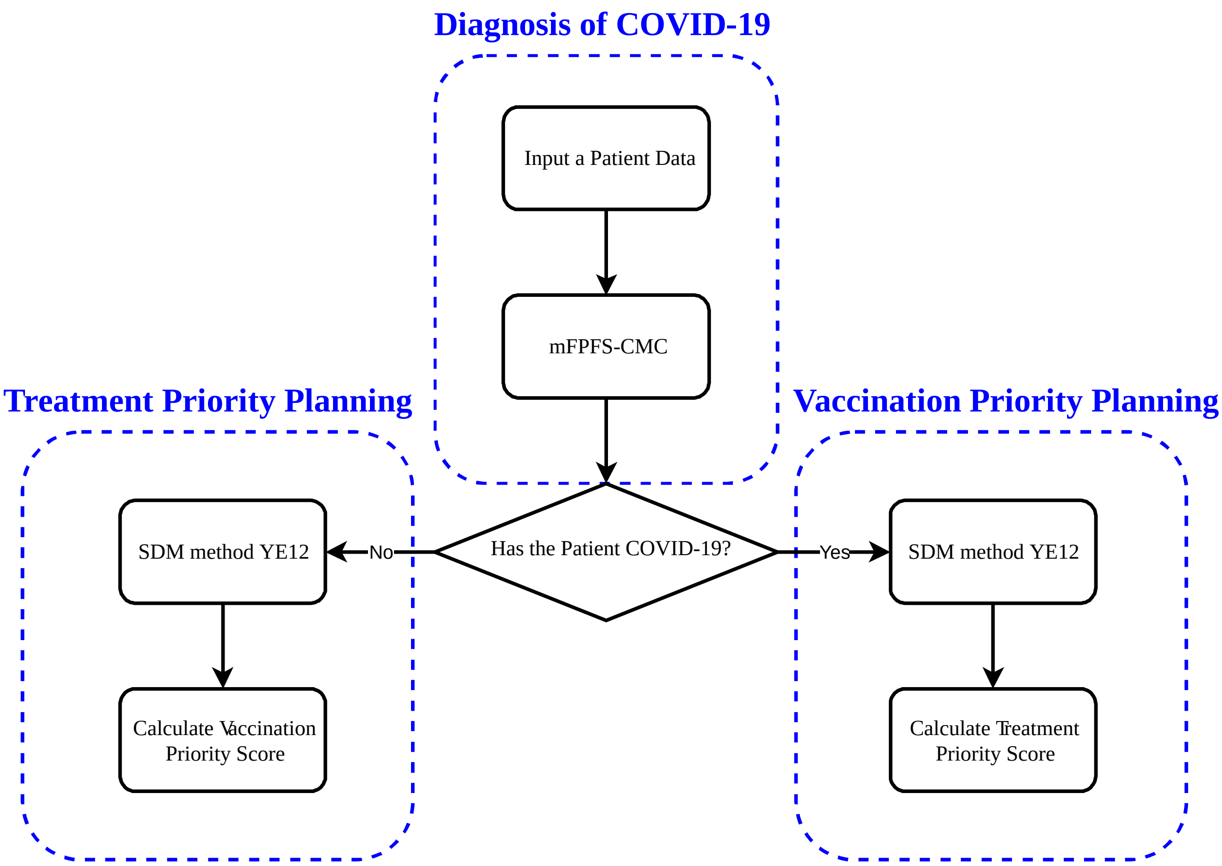

Fig. 1. Flowchart of the proposed work

2. Hypotheses:

This study considers the following hypotheses:

i. If FPFS-CMC is used in medical diagnosis, then whether the individual has COVID-19 can be determined.

ii. If the risk score of the patient can be calculated by looking at the patient's age and systemic diseases, then the follow-up treatment priorities of patients can be compared.

iii. If such parameters as systemic disease history, age, presence of risk-group individuals in the immediate vicinity, presence of COVID-19 history, province-district, transportation preference, and occupation can be obtained, then individuals' vaccination priority scores can be calculated.

3. Preliminaries

This study presents some of the basic definitions required in the next sections. Throughout this study, let E be a parameter set, U be a universal set, $F(E)$ be the set of all the fuzzy sets over E, and $\mu \in F(E)$. Here, $\mu := \{{}^{\mu(x)}x : x \in E\}$.

Definition 1. [24] Let U be a universal set, $\mu \in F(E)$, and α be a function from μ to $F(U)$. Then, the set $\left\{\left({}^{\mu(x)}x, \alpha\left({}^{\mu(x)}x\right)\right) \mid x \in E\right\}$, being the graphic of α, is called a fuzzy parameterized fuzzy soft set (*fpfs*-set) parameterized via E over U (or briefly over U).

Moreover, the set of all the *fpfs*-sets parameterized via E over U is denoted by $FPFS_E(U)$.

Definition 2. [23] Let $\alpha \in FPFS_E(U)$. Then, $[a_{ij}]$ is called *fpfs*-matrix of α and is defined by

$$[a_{ij}] = \begin{bmatrix} a_{01} & a_{02} & a_{03} & \cdots & a_{0n} & \cdots \\ a_{11} & a_{12} & a_{13} & \cdots & a_{1n} & \cdots \\ \vdots & \vdots & \vdots & \ddots & \vdots & \vdots \\ a_{m1} & a_{m2} & a_{m3} & \cdots & a_{mn} & \cdots \\ \vdots & \vdots & \vdots & \ddots & \vdots & \ddots \end{bmatrix}$$

such that for $i \in \{0,1,2,\cdots\}$ and $j \in \{1,2,\cdots\}$,

$$a_{ij} := \begin{cases} \mu(x_j), & i = 0 \\ \alpha\left({}^{\mu(x_j)}x_j\right)(u_i), & i \neq 0 \end{cases}$$

Here, if $|U| = m - 1$ and $|E| = n$, then $[a_{ij}]$ has order $m \times n$. Moreover, the set of all the *fpfs*-matrices parameterized via E over U is denoted by $FPFS_E[U]$.

Definition 3. Let $u, v \in \mathbb{R}^n$. Then, the function $P: \mathbb{R}^n \times \mathbb{R}^n \to [-1,1]$ defined by

$$P(u,v) := \frac{n\sum_{i=1}^{n} u_i v_i - \left(\sum_{i=1}^{n} u_i\right)\left(\sum_{i=1}^{n} v_i\right)}{\sqrt{\left[n\sum_{i=1}^{n} u_i^2 - \left(\sum_{i=1}^{n} u_i\right)^2\right]\left[n\sum_{i=1}^{n} v_i^2 - \left(\sum_{i=1}^{n} v_i\right)^2\right]}}$$

Definition 4. [25] Let D_{train} with $m_1 \times n$ and $C_{m_1 \times 1}$ be a training matrix and the class column vector of D_{train}. Then, fw is called the feature weight vector based on the Pearson correlation coefficient of D_{train} and is denoted by

$$fw_{1j} := \left|P\left(D_{train-j}, C\right)\right|, \quad j \in I_n := \{1, 2, 3, \cdots, n\}$$

Definition 5. Let $u \in \mathbb{R}^n$. Then, the vector $\hat{u} \in \mathbb{R}^n$ defined by

$$\hat{u}_i := \begin{cases} \dfrac{u_i - \min\limits_{k \in I_n}\{u_k\}}{\max\limits_{k \in I_n}\{u_k\} - \min\limits_{k \in I_n}\{u_k\}}, & \max\limits_{k \in I_n}\{u_k\} \neq \min\limits_{k \in I_n}\{u_k\} \\ 1, & \max\limits_{k \in I_n}\{u_k\} = \min\limits_{k \in I_n}\{u_k\} \end{cases}, \quad i \in I_n$$

is called normalizing vector of u.

Definition 6. Let $u \in \mathbb{R}^n$. Then, the standard deviation of u is defined by

$$\text{std}(u) \coloneqq \sqrt{\frac{\sum_{i=1}^{n}\left(u_i - \frac{1}{n}\sum_{i=1}^{n} u_i\right)}{n-1}}$$

Definition 7. [25] Let $D = [d_{ij}]_{m\times(n+1)}$ be a data matrix, $i \in I_m$, and $j \in I_n$. Then, the matrix $\widetilde{D} = [\tilde{d}_{ij}]_{m\times n}$ defined by

$$\tilde{d}_{ij} \coloneqq \begin{cases} \dfrac{d_{ij} - \min\limits_{k\in I_m}\{d_{kj}\}}{\max\limits_{k\in I_m}\{d_{kj}\} - \min\limits_{k\in I_m}\{d_{kj}\}}, & \max\limits_{k\in I_m}\{d_{kj}\} \neq \min\limits_{k\in I_m}\{d_{kj}\} \\ 1, & \max\limits_{k\in I_m}\{d_{kj}\} = \min\limits_{k\in I_m}\{d_{kj}\} \end{cases}$$

is called column normalized matrix (feature-fuzzification matrix) of D.

Definition 8. [25] Let $(D_{train})_{m_1\times n}$ be a training matrix obtained from $D = [d_{ij}]_{m\times(n+1)}$. Then, the matrix $\widetilde{D}_{train} = [\tilde{d}_{ij-train}]_{m_1\times n}$ defined by

$$\tilde{d}_{ij-train} \coloneqq \begin{cases} \dfrac{d_{ij-train} - \min\limits_{k\in I_m}\{d_{kj}\}}{\max\limits_{k\in I_m}\{d_{kj}\} - \min\limits_{k\in I_m}\{d_{kj}\}}, & \max\limits_{k\in I_m}\{d_{kj}\} \neq \min\limits_{k\in I_m}\{d_{kj}\} \\ 1, & \max\limits_{k\in I_m}\{d_{kj}\} = \min\limits_{k\in I_m}\{d_{kj}\} \end{cases}, \qquad i \in I_{m_1} \text{ and } j \in I_n$$

is called column normalized matrix (feature-fuzzification matrix) of D_{train}.

Definition 9. [25] Let $(D_{test})_{m_2\times n}$ be a training matrix obtained from $D \coloneqq [d_{ij}]_{m\times(n+1)}$. Then, the matrix $\widetilde{D}_{test} = [\tilde{d}_{ij-test}]_{m_2\times n}$ defined by

$$\tilde{d}_{ij-test} \coloneqq \begin{cases} \dfrac{d_{ij-test} - \min\limits_{k\in I_m}\{d_{kj}\}}{\max\limits_{k\in I_m}\{d_{kj}\} - \min\limits_{k\in I_m}\{d_{kj}\}}, & \max\limits_{k\in I_m}\{d_{kj}\} \neq \min\limits_{k\in I_m}\{d_{kj}\} \\ 1, & \max\limits_{k\in I_m}\{d_{kj}\} = \min\limits_{k\in I_m}\{d_{kj}\} \end{cases}, \qquad i \in I_{m_2} \text{ and } j \in I_n$$

is called column normalized matrix (feature-fuzzification matrix) of D_{test}.

Definition 10. [25] Let $[a_{ij}]_{m\times n}, [b_{ij}]_{m\times n} \in FPFS_E[U]$ and $p \in \mathbb{Z}^+$. Then, the mapping $s_M^p: FPFS_E[U] \times FPFS_E[U] \to \mathbb{R}$ defined by

$$s_M^p([a_{ij}],[b_{ij}]) = 1 - \frac{1}{\sqrt[p]{(m-1)n}}\left(\sum_{i=1}^{m-1}\sum_{j=1}^{n}\left|a_{0j}a_{ij} - b_{0j}b_{ij}\right|^p\right)^{\frac{1}{p}}$$

is a pseudo-similarity over $FPFS_E[U]$ and is called Minkowski pseudo-similarity. Here, s_M^1 is referred to as Hamming pseudo-similarity and is denoted by s_H. Moreover, s_M^2 is referred to as Euclidean pseudo-similarity and is denoted by s_E.

Definition 11. [25] Let $[a_{ij}]_{m\times n}, [b_{ij}]_{m\times n} \in FPFS_E[U]$ and $p \in \mathbb{Z}^+$. Then, the mapping $s_{Hs}^p: FPFS_E[U] \times FPFS_E[U] \to \mathbb{R}$ defined by

$$s_{Hs}^p([a_{ij}],[b_{ij}]) = 1 - \frac{1}{\sqrt[p]{m-1}}\left(\sum_{i=1}^{m-1} \max_{j\in I_n}\left\{\left|a_{0j}a_{ij} - b_{0j}b_{ij}\right|^p\right\}\right)^{\frac{1}{p}}$$

is a pseudo-similarity over $FPFS_E[U]$ and is called p-Hausdorff pseudo-similarity. Here, s_{Hs}^1 is referred to as Hausdorff pseudo-similarity and is denoted by s_{Hs}.

Definition 12. [25] Let $[a_{ij}]_{m\times n}, [b_{ij}]_{m\times n} \in FPFS_E[U]$. Then, the mapping $s_C: FPFS_E[U] \times FPFS_E[U] \to \mathbb{R}$ defined by

$$s_C([a_{ij}],[b_{ij}]) = 1 - \max_{i\in I_{m-1}}\left\{\max_{j\in I_n}\left\{\left|a_{0j}a_{ij} - b_{0j}b_{ij}\right|\right\}\right\}$$

is a pseudo-similarity over $FPFS_E[U]$ and is called Chebyshev pseudo-similarity.

4. Method

This study

- ➢ diagnoses COVID-19 by employing the classification method mFPFS-CMC,
- ➢ calculates the follow-up treatment priority of individuals with COVID-19 by risk scores,
- ➢ computes COVID-19 vaccination priority scores.

4.1. Safety

This study does not include vertebrate animals, potentially hazardous biological agents (microorganisms, rDNA, and tissues, including blood and blood products), and hazardous substances and devices.

The survey studies provided herein do not require any personal data while gathering information about individuals’ views about the vaccination process, and their criteria points. By not recording any name, gender, or e-mail address, the respective patient is anonymized. Thus, it stores the received data anonymously so that they cannot be associated with real people.

All the participants have explicit consent to the following to be used for academic reasons:

- ➢ participants’ views on vaccination priority planning
- ➢ their information about their systemic disease, age, and occupation
- ➢ whether they live in the immediate vicinity
- ➢ presence of their COVID-19 history
- ➢ the population of their current province and district
- ➢ their transportation preferences

Participants are aware of the potential risks of the study:

- ➢ an outside source may be tampered when using the internet for collecting information.
- ➢ there is always a possibility of hacking or other security breaches that could threaten the confidentiality of their responses while the confidentiality of participants’ responses will be protected once the data are downloaded from the internet.

The surveys declare that the participants are free not to answer any questions. All the responses are deleted from the online survey. No personal or electronic identifier is kept. The data file is stored on a password-protected computer.

4.2. Experimentation

4.2.1. Diagnosis of COVID-19

This subsection presents a classification algorithm to diagnose COVID-19.

FPFS-CMC: FPFS-CMC firstly utilizes the Pearson correlation coefficient between each column, corresponding to parameters, and the last column, manifesting the class labels, in the considered dataset to calculate feature weights based on the impact of parameters on classification. Then, using feature fuzzification of the training and testing samples and feature weights, it creates two *fpfs*-matrices: a training *fpfs*-matrix and a testing *fpfs*-matrix. It then creates a comparison matrix based on the pseudo-similarities between the training and testing *fpfs*-matrices. After that, it calculates the standard deviation of each column of the comparison matrix to produce the parameter weights and then merges the parameter weights and the matrix to generate the comparison *fpfs*-matrix. The ideal training sample is obtained by applying the soft decision-making (SDM) method sMBR01 on the comparison *fpfs*-matrix. Finally, the testing sample is given the class label of the optimum training sample. The same procedures are applied for all the test samples. However, FPFS-CMC has a disadvantage in terms of running time compared to the aforesaid classifiers herein. To overcome this drawback, this study modifies FPFS-CMC by employing the SDM method EMK19 [26,27] instead of sMBR01 [28]. Thus, the modified FPFS-CMC (mFPFS-CMC) produces a running time advantage of up to 70% over FPFS-CMC. The pseudocode of mFPFS-CMC is as follows:

Algorithm 1. Pseudocode of mFPFS-CMC

Input: $(D_{train})_{m_1 \times n}$, $C_{m_1 \times 1}$, and $(D_{test})_{m_2 \times n}$
Output: $T'_{m_2 \times 1}$

procedure mFPFS-CMC(D_{train}, C, D_{test})
    Compute fw using D_{train} and C
    Compute feature fuzzification of D_{train} and D_{test}, namely $\widetilde{D}_{train}$ and $\widetilde{D}_{test}$
    for i from 1 to m_2 **do**
        Compute the training *fpfs*-matrix $[a_{ij}]$ using fw and $\widetilde{D}_{j-train}$
        for *j* from 1 to m_1 **do**
            Compute the testing *fpfs*-matrix $[b_{ij}]$ using fw and $\widetilde{D}_{i-test}$
            $F_{j1} \leftarrow s_H([a_{ij}],[b_{ij}])$
            $F_{j2} \leftarrow s_C([a_{ij}],[b_{ij}])$
            $F_{j3} \leftarrow s_E([a_{ij}],[b_{ij}])$
            $F_{j4} \leftarrow s_{Hs}([a_{ij}],[b_{ij}])$
            $F_{j5} \leftarrow s_M^3([a_{ij}],[b_{ij}])$
        end for
        for *j* from 1 to 5 **do**
            $sd_j \leftarrow \text{std}(F_{.j})$
        end for
        $nw \leftarrow 1 - \widehat{sd}$
        Compute comparison *fpfs*-matrix $[g_{ij}]$ using pw and F
        $[[s_{k1}],[dm_{k1}],[op_{k1}]] \leftarrow \text{EMK19}([g_{ij}])$
        $t'_{i1} \leftarrow C(op_{11}, 1)$
    end for
return $T'_{m_2 \times 1}$
end procedure

SDM Methods: The related literature offers many SDM methods operating *fpfs*-matrices [23,29-34]. The SDM methods employ single, double, or multiple *fpfs*-matrix/matrices. In FPFS-CMC, sMBR01 working with a single *fpfs*-matrix is used. Another SDM method EMK19, employing a single *fpfs*-matrix, provides the best advantage in running time of FPFS-CMC over the others. For this reason, this study has chosen EMK19 to modify FPFS-CMC.

Real-Life Interpretation: This study firstly applies FPFS-CMC to the datasets Symptoms and COVID Presence (May 2020 data) [19], Covid-19 Symptoms [20], and Brazilian Covid Symptomatic Patients Data [21] provided in Kaggle Data Repository utilizing MATLAB R2021b software and a laptop with I(R) Core(TM) i5-10210U CPU @ 1.60GHz 2.11 GHz and 8.00 GB. Moreover, it compares them with kNN, Fuzzy kNN, and SVM. In the simulation process, to split the datasets as training and testing, 5-fold cross-validation is used (for more details about k-fold cross-validation, see [35-37]). The simulation results in Table 1 show that FPFS-CMC can be successfully applied to diagnose COVID-19. However, the results also manifest that the classifier has a running time disadvantage. To overcome this difficulty, this study employs the SDM method EMK19 instead of sMBR01 used in a step of the classifier FPFS-CMC. Here, FPFS-CMC with EMK19 is denoted by mFPFS-CMC.

Table 1. Simulation results of the classifiers for the considered dataset

Datasets' References	Classifiers	Acc∓SD	Sen∓SD	Spe∓SD	F1∓SD	RT ∓SD
[19]	kNN	96.8273∓0.0044	83.7574∓0.0220	99.9566∓0.0010	91.0564∓0.0134	1.7714∓0.6284
	Fuzzy kNN	96.8237∓0.0042	83.6718∓0.0211	99.9772∓0.0005	91.0489∓0.0129	0.5669∓0.2851
	SVM	96.7667∓0.0046	85.8218∓0.0388	99.3908∓0.0081	91.1028∓0.0138	0.8290∓0.5427
	FPFS-CMC	96.8182∓0.0041	83.6434∓0.0207	99.9772∓0.0005	91.0326∓0.0127	964.4258∓122.9805
	mFPFS-CMC	96.8182∓0.0041	83.6434∓0.0207	99.9772∓0.0005	91.0326∓0.0127	286.2255∓40.8747
[20]	kNN	84.8850∓0.0351	96.9331∓0.0312	30.0278∓0.1534	91.3102∓0.0203	0.0460∓0.0060
	Fuzzy kNN	84.7990∓0.0296	95.5320∓0.0368	35.8611∓0.1578	91.1349∓0.0181	0.0009∓0.0004
	SVM	86.8589∓0.0366	95.9630∓0.0318	45.3333∓0.1828	92.2945∓0.0212	0.0214∓0.0045
	FPFS-CMC	87.3923∓0.0314	94.9915∓0.0370	52.6944∓0.1460	92.4903∓0.0195	0.2757∓0.0159
	mFPFS-CMC	87.0406∓0.0318	94.9915∓0.0370	50.7222∓0.1589	92.3014∓0.0195	0.2902∓0.0223
[21]	kNN	96.1174∓0.0081	92.1834∓0.0215	98.0516∓0.0064	93.9858∓0.0129	0.5669∓0.0101
	Fuzzy kNN	96.5564∓0.0070	94.1915∓0.0187	97.7187∓0.0065	94.7402∓0.0110	0.1055∓0.0018
	SVM	86.5061∓0.0116	71.7255∓0.0247	93.7736∓0.0103	77.7876∓0.0200	0.2278∓0.0184
	FPFS-CMC	96.4052∓0.0071	94.4757∓0.0189	97.3536∓0.0081	94.5396∓0.0110	130.4978∓0.1860
	mFPFS-CMC	96.4052∓0.0071	94.4757∓0.0189	97.3536∓0.0081	94.5396∓0.0110	50.4621∓0.2595

Acc, Sen, Spe, and F1 and their standard deviations (SD) are presented in percentage. Running time and its SD are presented in seconds.

In medical diagnosis, accuracy, sensitivity, specificity, and F1-score are vital and expected to occur close to 100%. According to the results in Table 1, although mFPFS-CMC's result of sensitivity for the dataset in [19] and the results of accuracy and specificity for the dataset in [20] are less than 90%, its other results are above 90%. As seen in Table 2, since the considered datasets are imbalanced, some results are lower than 90%. Moreover, $O((m-1)^2n)$ and $O\big((m-1)nt\big)$ represent the computational complexities of sMBR01 and EMK19, respectively, such that $m-1$, n, and t denote the number of samples, the number of attributes, and the number of matrices, respectively. Here, since mFPFS-CMC utilizes one matrix, $t=1$. Because the computational complexity of sMBR01 is higher than the computational complexity of EMK19, mFPFS-CMC has a running time advantage of up to 70% over FPFS-CMC. To this end, improving mFPFS-CMC is worth studying. Consequently, mFPFS-CMC is reliable and practical in medical diagnosis.

Table 2. Details of the considered datasets (# represents "the number of")

No.	Reference	Sample #	Attribute #	Class #	Class Labels	Samples' Distribution	Balanced/Imbalanced
1.	[19]	5434	20	2	No and Yes	1051 (No) 4383 (Yes)	Imbalanced
2.	[20]	227	31	2	0 and 1	214 (0) 13 (1)	Imbalanced
3.	[21]	2779	10	2	0 and 1	916 (0) 1863 (1)	Imbalanced

Here, the mathematical notations of the performance metrics, namely accuracy (acc), sensitivity (sen), specificity (spe), and F1-score (F1) [38,39], are as follows: Let $D_{test}=\{x_1,x_2,\cdots,x_n\}$, $T=\{T_1,T_2,\cdots,T_n\}$, $T'=\{T'_1,T'_2,\cdots,T'_n\}$, and $I_n\coloneqq\{1,2,3,\cdots,n\}$ be the set of n samples to be classified, the set of ground truth classes of the samples, the set of prediction class of the samples, and an index set, respectively. Then,

$$\text{Accuracy}(T,T')\coloneqq\frac{TP+TN}{TP+TN+FP+FN}$$

$$\text{Sensitivity}(T,T')\coloneqq\frac{TP}{TP+FN}$$

$$\text{Specificity}(T,T')\coloneqq\frac{TN}{TN+FP}$$

$$\text{F1}-\text{Score}(T,T')\coloneqq\frac{2TP}{2TP+FP+FN}$$

where TP, TN, FP, and FN are the number of true positive, true negative, false positive, and false negative, respectively, and their mathematical notations are as follows:

$$TP\coloneqq|\{x_k:1\in T_k\wedge 1\in T'_k,k\in I_n\}|$$

$$TN\coloneqq|\{x_k:0\in T_k\wedge 0\in T'_k,k\in I_n\}|$$

$$FP\coloneqq|\{x_k:0\in T_k\wedge 1\in T'_k,k\in I_n\}|$$

$$FN\coloneqq|\{x_k:1\in T_k\wedge 0\in T'_k,k\in I_n\}|$$

Furthermore, Table 3 shows the mean values TP, FN, TN, and FP for each fold of cross-validation obtained in ten runs by classifiers for the considered datasets.

Table 3. Mean of TP, FN, TN, and FP values obtained in ten runs

		[19]				[20]				[21]			
Classifiers	k-fold	TP	FN	TN	FP	TP	FN	TN	FP	TP	FN	TN	FP
kNN	Fold 1	176.9	33.1	875.3	0.7	36.3	0.7	1.7	6.3	169.5	13.5	364.9	7.1
	Fold 2	178.7	32.3	875.8	0.2	37	1	2.3	5.7	169.7	14.3	365.4	6.6
	Fold 3	175.7	34.3	876.6	0.4	35.8	1.2	3.5	5.5	168.1	14.9	365.8	7.2
	Fold 4	173.7	36.3	876.8	0.2	35.5	1.5	2.4	5.6	167.4	15.6	364.5	8.5
	Fold 5	175.3	34.7	876.6	0.4	35.7	1.3	2.5	5.5	169.7	13.3	366.1	6.9
Fuzzy kNN	Fold 1	176.5	33.5	875.9	0.1	35.8	1.2	2.1	5.9	173.4	9.6	363.4	8.6
	Fold 2	178.5	32.5	875.8	0.2	36.7	1.3	2.7	5.3	174.4	9.6	363.1	8.9
	Fold 3	175.5	34.5	876.6	0.4	34.8	2.2	4.1	4.9	171.8	11.2	364.4	8.6
	Fold 4	173.5	36.5	876.8	0.2	35.2	1.8	3.3	4.7	170.8	12.2	364.3	8.7
	Fold 5	175.4	34.6	876.9	0.1	35.2	1.8	2.6	5.4	172.4	10.6	365.3	7.7
SVM	Fold 1	181.3	28.7	870.4	5.6	35.5	1.5	3	5	132.6	50.4	349.7	22.3
	Fold 2	183.7	27.3	870.4	5.6	36.8	1.2	4.2	3.8	131	53	348.7	23.3
	Fold 3	179.5	30.5	871.9	5.1	35.2	1.8	5.1	3.9	130.1	52.9	352.3	20.7
	Fold 4	178.5	31.5	870.7	6.3	35.6	1.4	3.2	4.8	132.3	50.7	346.9	26.1
	Fold 5	179	31	872.9	4.1	35.4	1.6	3.2	4.8	131	52	349.4	23.6
FPFS-CMC	Fold 1	176.5	33.5	875.9	0.1	35.5	1.5	3.7	4.3	173.9	9.1	361.2	10.8
	Fold 2	178.2	32.8	875.8	0.2	36.7	1.3	4.5	3.5	174.3	9.7	362.4	9.6
	Fold 3	175.5	34.5	876.6	0.4	34.5	2.5	5.6	3.4	172.5	10.5	363.1	9.9
	Fold 4	173.5	36.5	876.8	0.2	35.1	1.9	4.1	3.9	171.4	11.6	364	9
	Fold 5	175.4	34.6	876.9	0.1	34.9	2.1	3.8	4.2	173.3	9.7	363	10
mFPFS-CMC	Fold 1	176.5	33.5	875.9	0.1	35.5	1.5	3.4	4.6	173.9	9.1	361.2	10.8
	Fold 2	178.2	32.8	875.8	0.2	36.7	1.3	4.2	3.8	174.3	9.7	362.4	9.6
	Fold 3	175.5	34.5	876.6	0.4	34.5	2.5	5.5	3.5	172.5	10.5	363.1	9.9
	Fold 4	173.5	36.5	876.8	0.2	35.1	1.9	3.9	4.1	171.4	11.6	364	9
	Fold 5	175.4	34.6	876.9	0.1	34.9	2.1	3.9	4.1	173.3	9.7	363	10

4.2.2. Follow-Up Treatment Priority in COVID-19 Patients

This subsection proposes a treatment priority algorithm to utilize in follow-up treatment priority in COVID-19 patients.

Risk Scores: This study calculates risk scores for age and the aforesaid comorbidities by using the following functions:

Age: The odds ratios of individuals' ages provided in [14,17] show that the age criterion affects the death rates caused by COVID-19. Therefore, this study considers the death rates of COVID-19 patients per 100,000 people in the last 7 days by age group in Table 4 provided in [15]. It then determines a priority score for individuals according to their ages. Hence, the age risk score function f_A is as follows:

$$f_A : P \to [0,1]$$

$$x \to f_A(x) = \chi(x, i)$$

such that $\chi(x,i) = the\ value\ corresponding\ to\ i^{th}\ age\ range\ that\ x\ belongs\ in.$ Here, $A = \{x_1, x_2, x_3, x_4, x_5, x_6\}$ is a set of age ranges such that x_1 = "0-14", x_2 = "15-24", x_3 = "25-49", x_4 = "50-64", x_5 = "65-79", and x_6 = ">80" and P is a set of patents. To illustrate, if a patient x belongs in the age range 15-24, then the priority score $f_A(x) = \chi(x, 2) = 0.0013$.

Table 4. Normalized death rates according to age range

Age Ranges	0-14	15-24	25-49	50-64	65-79	>80
Scores	0.0130	0.0013	0.0100	0.1037	0.4552	1

The scores are obtained by normalizing and merging the ranges < 2, 2-4, and 5-14 as 0-14.

Hypertension: In Turkiye, approximately 80% of hypertension patients have primary hypertension and the remaining 20% have secondary hypertension [40]. Therefore, this study considers the basic risk scores 0.8 and 0.2 for primary and secondary hypertensions, respectively. Moreover, it adds the effect of transmitting factors to basic risk scores, i.e., excessive alcohol intake, smoking, sedentary life, polysystem, non-steroidal anti-inflammatories, and low potassium intake. Hence, the hypertension risk score function is as follows:

$$f_H : P \to [0,1]$$

$$x \to f_H(x) = \begin{cases} 0.8 + \frac{1}{30}\sum_{i=1}^{6}\chi(i), & x\ has\ primary\ hypertension \\ 0.2 + \frac{1}{30}\sum_{i=1}^{6}\chi(i), & x\ has\ secondary\ hypertension \end{cases}$$

such that $\chi(i) = \begin{cases} 1, & x\ has\ h_i \\ 0, & x\ has\ not\ h_i \end{cases}$. Here, $H = \{h_1, h_2, h_3, h_4, h_5, h_6\}$ is a set of transmitting factors such that h_1 = "excessive alcohol intake", h_2 = "smoking", h_3 = "sedentary life", h_4 = "polysystem", h_5 = "non-steroidal anti-inflammatories", and h_6 = "low potassium intake" and P is a set of patients. To illustrate, if the patient x has primary hypertension and three transmitting factors h_1, h_2, and h_6, then the hypertension risk score of x is $f_H(x) = 0.8 + \frac{1}{30}(1 + 1 + 0 + 0 + 0 + 1) = 0.9$.

Cardiovascular Diseases: In Turkiye, the mortality rate because of cardiovascular disease is 42% [41]. Therefore, this study calculates the cardiovascular risk score by using the rate 42% and interactive risk score

$R(x)$, obtained by the interactive form provided in [42,43]. Hence, the cardiovascular risk score function is as follows:

$$f_{Cr} : P \to [0,1]$$
$$x \to f_{Cr}(x) = \begin{cases} 0.42 + R(x), & R(x) \leq 0.58 \; doesn't \; have \; cardiovascular \; disease \\ 1, & otherwise \end{cases}$$

Here, P is a set of patients.

Cancer: This study determines cancer risk scores by using Table 5 provided as cited in [44, 45]. Hence, the cancer risk score function is as follows:

$$f_C : P \to [0,1]$$
$$x \to f_C(x) = 1 - \chi(x,i,j)$$

such that $\chi(x,i,j) = the\ 5 - year\ lifetimes\ rate\ of\ i^{th}\ cancer\ type\ and\ j^{th}\ stage\ that\ x\ has$. Here, $C = \{x_1, x_2, x_3, x_4, x_5, x_6, x_7\}$ is a set of cancer types such that x_1 = "breast cancer", x_2 = "colorectal cancer", x_3 = "non-Hodgkin lymphoma cancer", x_4 = "lung cancer ", x_5 = "testicular cancer ", x_6 = "bladder cancer", and x_7 = "uterine cancer ", $S = \{s_1, s_2, s_3\}$ is a set of stages such that s_1 = "early", s_2 = "local forward", and s_3 = "metastatic", and P is a set of patients. To illustrate, if a patient x has lung cancer in the metastatic stage, then the cancer risk score $f_C(x) = 1 - \chi(x, 4, 3) = 1 - 0.04 = 0.96$.

Table 5. Five-year lifetime rates for different cancer types and stages [as cited in 44]

Cancer Types/Stages	Early	Local Forward	Metastatic
Breast Cancer	0.99	0.85	0.26
Colorectal Cancer	0.90	0.71	0.13
Non-Hodgkin Lymphoma Cancer	0.82	0.74	0.62
Lung Cancer	0.55	0.27	0.04
Testicular Cancer	0.99	0.96	0.74
Bladder Cancer	0.70	0.34	0.05
Uterine Cancer	0.95	0.68	0.17

Chronic Kidney Failure: This study determines chronic kidney failure risk scores by using the stage number of the disease in Table 6 provided in [46]. Hence, the chronic kidney failure risk score function is as follows:

$$f_{Ch} : P \to [0,1]$$
$$x \to f_{Ch}(x) = \frac{S(x)}{5}$$

such that $S(x)$ is the stage of the disease shown in Table 6. Here, P is a set of patients. To illustrate, if the patient is in the third stage, then his/her chronic kidney failure risk score is $\frac{3}{5} = 0.6$.

Table 6. Stages of chronic kidney failure [46]

Stage	Glomerular Filtration Rate	Description	Treatment Stage
1	90+	Normal kidney function but urine findings or structural abnormalities or genetic trait point to kidney disease	Observation, control of blood pressure
2	60-89	Mildly reduced kidney function, and other findings (as for stage 1) point to kidney disease	Observation, control of blood pressure and risk factor
3	30-59	Moderately reduced kidney function	Observation, control of blood pressure and risk factor
4	15-29	Severely reduced kidney function	Planning for end-stage renal failure
5	<15 or on dialysis	Very severe or end-stage kidney failure (sometimes call established renal failure)	Treatment choices

Diabetes: This study determines diabetes risk scores by using the group number of the disease $G(x)$ in Table 7 provided in [47]. Moreover, it considers whether the individual has a cardiovascular disease because cardiovascular diseases significantly increase the risk of diabetes [48]. Hence, the diabetes risk score function is as follows:

$$f_D : P \to [0,1]$$

$$x \to f_D(x) = \frac{9 - G(x)}{10} + 0.2\,\chi(x)$$

such that

$$\chi(x) = \begin{cases} 1, & x \text{ has a cardiovascular disease} \\ 0, & \text{otherwise} \end{cases}$$

To illustrate, if the patient is in the second group and he/she has a cardiovascular disease, then his/her diabetes risk score is $\frac{9-2}{10} + 0.2 = 0.9$.

Table 7. Types of diabetes [47]

Group	Description
1	Classic type-1 diabetes, a severe immune system disease
2	A type of diabetes caused by severe insulin deficiency
3	Severe insulin resistance
4	A type of diabetes caused by obesity
5	Moderate diabetes

COVID-19 Death Correlation Score: This study calculates the death correlation score, for the aforesaid comorbidities, using mean death rates in Table 8. Moreover, the death correlation score for age criterion is obtained to be 0.26 by the mean of values in Table 4. The death rates of the patients with comorbidities who died from COVID-19 are obtained from [11,12,18,49].

Table 8. COVID-19-induced death rates of the patients with comorbidities

Group	Chen et al., 2020	Çoktaş, 2020	Erol, 2020	Zhou et al., 2020	Mean
Hypertension	0.58	N\A	0.76	0.45	0.60
Cardiovascular diseases	0.70	N\A	0.63	N\A	0.67
Cancer	N\A	0.89	N\A	0	0.45
Chronic kidney failure	N\A	N\A	0.93	1	0.97
Diabetes	N\A	N\A	0.73	0.47	0.60

N\A: Not Available

Calculation of risk score: This study computes the total risk score of a patient with COVID-19 via age and comorbidities risk scores with the death correlation scores corresponding to each risk score. Hence, the treatment priority score function is as follows:

$$f_{TPS} : P \to [0,1]$$

$$x \to f_{TPS}(x) = \frac{1}{\sum_{i=1}^{6} r_i}\left(f_A(x)r_1 + f_H(x)r_2 + f_{Cr}(x)r_3 + f_C(x)r_4 + f_{Ch}(x)r_5 + f_D(x)r_6\right)$$

Here, $MDR = \{r_1, r_2, r_3, r_4, r_5, r_6\}$ is a set of the mean death rates in Table 7 such that $r_1 = 0.26$, $r_2 = 0.60$, $r_3 = 0.67$, $r_4 = 0.45$, $r_5 = 0.97$, and $r_6 = 0.60$ and P is a set of patients. To illustrate, if the risk scores of a patient x are $f_A(x) = 0.65$, $f_H(x) = 0.4$, $f_{Cr}(x) = 0.52$, $f_C(x) = 0.34$, $f_{Ch}(x) = 0.18$, and $f_D(x) = 0$, then the treatment priority score of x is as follows:

$$f_{TPS}(x) = \frac{0.65 \cdot 0.26 + 0.4 \cdot 0.60 + 0.52 \cdot 0.67 + 0.34 \cdot 0.45 + 0.18 \cdot 0.97 + 0 \cdot 0.60}{0.26 + 0.60 + 0.67 + 0.45 + 0.97 + 0.60} = \frac{1.085}{3.55} = 0.3056$$

A Hypothetical Scenario: This study considers scores provided in Table 9 for ten patients to illustrate the aforesaid treatment priority score function's performance and performance of the SDM method YE12 employing a single matrix [50,51]. Let $P = \{x_1, x_2, x_3, x_4, x_5, x_6, x_7, x_8, x_9, x_{10}\}$ be a set of patients and $E = \{e_1, e_2, e_3, e_4, e_5, e_6\}$ be a set of parameters such that $e_1 =$ "age", $e_2 =$ "hypertension", $e_3 =$ "cardiovascular diseases", $e_4 =$ "cancer", $e_5 =$ "chronic kidney failure", and $e_6 =$ "diabetes". Here, the weights of parameters are $r_1 = 0.26$, $r_2 = 0.60$, $r_3 = 0.67$, $r_4 = 0.45$, $r_5 = 0.97$, and $r_6 = 0.60$, respectively. Then, the *fpfs*-matrix $[a_{ij}]_{11\times 6}$ constructed by these weights and the data in Table 9 is as follows:

$$[a_{ij}] = \begin{bmatrix} 0.26 & 0.60 & 0.67 & 0.45 & 0.97 & 0.60 \\ 0.0130 & 0.84 & 0.54 & 0.39 & 0.6 & 0.7 \\ 0.4552 & 0.26 & 0.72 & 0.73 & 0.2 & 0.3 \\ 0.0100 & 0.90 & 0.64 & 0.66 & 0.4 & 0.9 \\ 0.0130 & 0.87 & 1 & 0.26 & 0.6 & 0.4 \\ 1 & 0.93 & 0.48 & 0.87 & 0.2 & 0 \\ 0.1037 & 0.27 & 0.82 & 0.96 & 0.8 & 0.3 \\ 0.0130 & 0.35 & 0.74 & 0.38 & 0.8 & 0.6 \\ 0.4552 & 0.36 & 0.42 & 0.83 & 0.2 & 0.4 \\ 0.0013 & 0.24 & 0.60 & 0.66 & 0.4 & 0.8 \\ 0.0013 & 0.34 & 0.80 & 0.01 & 0.4 & 0.1 \end{bmatrix}$$

Then, this study applies the SDM method YE12 to $[a_{ij}]$. Thus, the decision set, score matrix, and ranking order produced by YE12, respectively, are as follows:

$$\{{}^{0.5765}x_1, {}^{0.4111}x_2, {}^{0.6187}x_3, {}^{0.6012}x_4, {}^{0.4859}x_5, {}^{0.5990}x_6, {}^{0.5679}x_7, {}^{0.4009}x_8, {}^{0.4821}x_9, {}^{0.3360}x_{10}\}$$

$$[s_{i1}] = [0.5765 \quad 0.4111 \quad 0.6187 \quad 0.6012 \quad 0.4859 \quad 0.5990 \quad 0.5679 \quad 0.4009 \quad 0.4821 \quad 0.3360]^T$$

and

$$x_{10} \prec x_8 \prec x_2 \prec x_9 \prec x_5 \prec x_7 \prec x_1 \prec x_6 \prec x_4 \prec x_3$$

Here,

$$s_{41} = f_{TPS}(x_4) = \frac{0.0130 \cdot 0.26 + 0.87 \cdot 0.60 + 1 \cdot 0.67 + 0.26 \cdot 0.45 + 0.6 \cdot 0.97 + 0.4 \cdot 0.60}{0.26 + 0.60 + 0.67 + 0.45 + 0.97 + 0.60} = \frac{2.1344}{3.55} = 0.6012$$

Table 9. Priority scores for 10 individuals

Individuals / Criteria	Age	Hypertension	Cardiovascular Diseases	Cancer	Chronic Kidney Failure	Diabetes
x_1	0.0130	0.84	0.54	0.39	0.6	0.7
x_2	0.4552	0.26	0.72	0.73	0.2	0.3
x_3	0.0100	0.90	0.64	0.66	0.4	0.9
x_4	0.0130	0.87	1	0.26	0.6	0.4
x_5	1	0.93	0.48	0.87	0.2	0
x_6	0.1037	0.27	0.82	0.96	0.8	0.3
x_7	0.0130	0.35	0.74	0.38	0.8	0.6
x_8	0.4552	0.36	0.42	0.83	0.2	0.4
x_9	0.0013	0.24	0.60	0.66	0.4	0.8
x_{10}	0.0013	0.34	0.80	0.01	0.4	0.1

4.2.3. Vaccination Priority Planning

This subsection proposes a vaccine priority algorithm to employ in a possible vaccine crisis and for the planning of booster doses.

Survey Criteria Scores: This study applies an online form, conducted through Google Forms, to 200 people to gain insight into people's understanding of the importance of the aforesaid seven criteria in vaccination priority and planning. This survey asks participants to rank the seven criteria from least to most important and calculates survey criterion points by arithmetic average. For the survey's safety, see Section 4.1. the means of values determined by 200 participants for the aforesaid seven criteria, i.e., systemic disease, age, presence of risk group individuals in the immediate vicinity, presence of COVID-19 history, province-district, transportation preference, and occupation, provided in Table 10 are denoted by S_{Sd}, S_A, S_{IV}, S_{CH}, S_{PD}, S_{TP}, and S_O, respectively.

Table 10. Survey results

Abbreviations	Survey Criteria	Mean Values	Normalized Mean Values
Sd	Systemic disease	$S_{Sd} = 3.0825$	$NS_{Sd} = 1$
A	Age	$S_A = 2.805$	$NS_A = 0.9100$
IV	Presence of risk group individuals in the immediate vicinity	$S_{IV} = 3.0575$	$NS_{IV} = 0.9919$
CH	Presence of COVID-19 history	$S_{CH} = 2.705$	$NS_{CH} = 0.8775$
PD	Province-district	$S_{PD} = 1.765$	$NS_{PD} = 0.5726$
TP	Transportation preference	$S_{TP} = 2.27$	$NS_{TP} = 0.7364$
O	Occupation	$S_O = 2.2725$	$NS_O = 0.7372$

Individual Priority Scores: This study details the aforesaid seven criteria to make a more individual-specific vaccination planning and assigns a score to each criterion.

Systemic Disease: Scientific studies observe that cases of COVID-19 with systemic diseases have a higher death rate than cases without systemic diseases. Therefore, this study considers mean percentage values of mortality rates in Table 11 provided in [11,12,18,49]. Moreover, it determines a priority score for individuals with systemic disease. Hence, the systemic disease priority score function f_{Sd} is as follows:

$$f_{Sd} : I \to [0,1]$$
$$x \to f_{Sd}(x) = \begin{cases} \chi(x,i), & i^{th} \text{ systemic disease that } x \text{ has} \\ 0, & x \text{ has no systemic disease} \end{cases}$$

such that $\chi(x,i) = the\ value\ corresponding\ to\ i^{th}\ systemic\ disease\ that\ x\ has$. Here, $Sd = \{x_1, x_2, x_3, x_4, x_5, x_6\}$ is a set of systemic diseases such that $x_1 =$ "kidney failure (dialysis)", $x_2 =$ "chronic lung disease", $x_3 =$ "cardiovascular disease", $x_4 =$ "diabetes", $x_5 =$ "cancer", and $x_6 =$ "no" and I is a set of individuals. To illustrate, if an individual x has diabetes, then the systemic disease priority score $f_{Sd}(x) = \chi(x,5) = 0.60$.

Table 11. Systemic diseases and the respective vaccination scores

Systemic Diseases	[44]	[12]	[11]	[18]	Mean
Chronic lung disease	N\A	N\A	0.80	0.67	0.74
Cardiovascular diseases	0.70	N\A	0.63	N\A	0.67
Cancer	N\A	0.89	N\A	0	0.45
Chronic kidney failure	N\A	N\A	0.93	1	0.97
Diabetes	N\A	N\A	0.73	0.47	0.60

Age: This study considers the number of new COVID-19 patients per 100,000 people in the last 7 days by age group in Table 12 provided in [15]. It then determines a priority score for individuals according to their ages. Hence, the age priority score function f_A is as follows:

$$f_A : I \rightarrow [0,1]$$
$$x \rightarrow f_A(x) = \chi(x,i)$$

such that $\chi(x,i) = the\ value\ corresponding\ to\ i^{th}\ age\ range\ that\ x\ belongs.$ Here, $A = \{x_1, x_2, x_3, x_4, x_5, x_6\}$ is a set of age ranges such that x_1 = "0-14", x_2 = "15-24", x_3 = "25-49", x_4 = "50-64", x_5 = "65-79", and x_6 = ">80" and I is a set of individuals. To illustrate, if an individual x belongs in the age range 15-24, then the age priority score $f_A(x) = \chi(x, 2) = 0.8$.

Table 12. Normalized case distribution according to age range

Age Ranges	0-14	15-24	25-49	50-64	65-79	>80
Scores	0.39	0.80	1.00	0.92	0.85	0.76

The scores are obtained by normalizing and merging the ranges < 2, 2-4, and 5-14 as 0-14.

Presence of risk group individuals in the immediate vicinity: This study assigns priority scores in Table 13 according to immediate vicinity levels of individuals that live in the same house. Hence, it sets a priority score for individuals that live in the same house. Hence, the immediate vicinity priority score function f_{IV} is as follows:

$$f_{IV} : I \rightarrow [0,1]$$
$$x \rightarrow f_{IV}(x) = \begin{cases} \chi(x,i), & i^{th}\ immediate\ vicinity\ type\ that\ x\ lives\ with \\ 0, & x\ does\ not\ live\ with\ any\ immediate\ vicinities \end{cases}$$

such that $\chi(x,i) = the\ value\ corresponding\ to\ i^{th}\ immediate\ vicinity\ type\ that\ x\ lives\ in.$ Here, $IV = \{x_1, x_2, x_3, x_4\}$ is a set of immediate vicinities such that x_1 = "with chronic elderly patients", x_2 = "with chronic young patients", x_3 = "with elders", and x_4 = "with more than ten non-risky individuals" and I is a set of individuals. To illustrate, if an individual x lives with elders, then the immediate vicinity priority score $f_{IV}(x) = \chi(x, 3) = 0.4$.

Table 13. Vicinity and risk relation

Immediate Vicinities	Scores
With chronic elderly patients	0.8
With chronic young patients	0.6
With elders	0.4
With > ten non-risky individuals	0.2

Presence of COVID-19 History: How severely an individual with a history of COVID-19 presents symptoms is related to vaccination priority. This study determines priority scores in Table 14 according to their COVID-19 histories. Thus, the COVID-19 histories priority score function f_{CH} is as follows:

$$f_{CH} : I \rightarrow [0,1]$$
$$x \rightarrow f_{CH}(x) = \chi(x,i)$$

such that $\chi(x,i) = the\ value\ corresponding\ to\ i^{th}\ COVID-19\ history\ type\ that\ x\ has$. Here, $CH = \{x_1, x_2, x_3, x_4, x_5\}$ is a set of COVID-19 history types such that x_1 = "patient with COVID-19 hospitalized in intensive care", x_2 = "individual who have not had COVID-19", x_3 = "patient with moderate symptoms with COVID-19", x_4 = "patient with mild symptoms of COVID-19", and x_5 = "patient with COVID-19 who did not show any symptoms" and I is a set of individuals. To illustrate, if an individual x has not contracted COVID-19, then the COVID-19 history priority score $f_{CH}(x) = \chi(x,2) = 0.6$.

Table 14. COVID-19 history and risk relation

COVID-19 History	Scores
Patient with COVID-19 hospitalized in intensive care	0.8
Individual with no COVID-19 history	0.6
Patient with moderate symptoms of COVID-19	0.5
Patient with mild symptoms of COVID-19	0.4
Patient with COVID-19 with no symptoms	0.3

Province-District: It is observed that COVID-19 cases increase in direct proportion to the region and the population of the region. Therefore, this study produces priority scores in Table 15 based on two criteria: province and district. Thereby, the province-district priority score function f_{PD} is as follows:

$$f_{PD} : I \to [0,1]$$
$$x \to f_{PD}(x) = \chi(x,i,j)$$

such that $\chi(x,i,j) = the\ value\ corresponding\ to\ i^{th}\ and\ j^{th}\ population\ ranges\ of\ the\ province\ and\ district\ where\ x\ lives$. Here, $P = \{x_1, x_2, x_3, x_4, x_5\}$ is a set of provinces' population ranges such that x_1 = "$< 10^6$", x_2 = "$10^6 - 3 \cdot 10^6$", x_3 = "$3 \cdot 10^6 - 5 \cdot 10^6$", x_4 = "$5 \cdot 10^6 - 7 \cdot 10^6$", and x_5 = "$\geq 7 \cdot 10^6$", $D = \{d_1, d_2, d_3, d_4, d_5\}$ is a set of districts' population ranges such that d_1 = "$10^4 - 10^5$", d_2 = "$10^5 - 2 \cdot 10^5$", d_3 = "$2 \cdot 10^5 - 3 \cdot 10^5$", d_4 = "$3 \cdot 10^5 - 4 \cdot 10^5$", and d_5 = "$\geq 4 \cdot 10^5$", and I is a set of individuals. To illustrate, if an individual x lives in a province and district with the populations $4 \cdot 10^6$ and $2.5 \cdot 10^5$, respectively, then the province-district priority score $f_{PD}(x) = \chi(x,3,3) = 0.64$.

Table 15. Province-district and risk relation

Province/District	$10^4 - 10^5$	$10^5 - 2 \cdot 10^5$	$2 \cdot 10^5 - 3 \cdot 10^5$	$3 \cdot 10^5 - 4 \cdot 10^5$	$\geq 4 \cdot 10^5$
$< 10^6$	0.40	0.42	0.44	0.46	0.48
$10^6 - 3 \cdot 10^6$	0.50	0.52	0.54	0.56	0.58
$3 \cdot 10^6 - 5 \cdot 10^6$	0.60	0.62	0.64	0.66	0.68
$5 \cdot 10^6 - 10^7$	0.70	0.72	0.74	0.76	0.78
$\geq 10^7$	0.80	0.82	0.84	0.86	0.88

Transportation Preferences: The transportation preferences of individuals affect the number of COVID-19 cases. Therefore, this study sets a score in Table 16 for each possible transportation preference. Thereafter, the transportation preference priority score function f_{TP} is as follows:

$$f_{TP} : I \to [0,1]$$
$$x \to f_{TP}(x) = \chi(x,i)$$

such that $\chi(x,i) = the\ value\ corresponding\ to\ i^{th}\ transporting\ type\ that\ x\ prefers$. Here, $TP = \{x_1, x_2, x_3, x_4, x_5\}$ is a set of transporting types such that x_1 = "using public transport 4+ per day", x_2 = "using public transport 4 times a day", x_3 = "using public transport 2 times a day", x_4 = "travelling by private vehicle", and x_5 = "not travelling" and I is a set of individuals. To illustrate, if an individual x travels by her/his own private vehicle, then the transportation preference priority score $f_{TP}(x) = \chi(x,4) = 0.2$.

Table 16. Transportation preferences and risk relation

Transportation Preferences	Scores
Using public transport 4+ per day	0.8
Using public transport 4 times a day	0.6
Using public transport 2 times a day	0.4
Using private vehicle	0.2
Not Travelling	0

Occupations: This study considers priority scores corresponding to the classification of occupations in Table 17 provided in [16]. Therefore, the occupation priority score function f_O is as follows:

$$f_O : I \to [0,1]$$
$$x \to f_O(x) = \chi(x,i)$$

such that $\chi(x,i) = the\ value\ corresponding\ to\ i^{th}\ occupation\ that\ x\ has$. Here, $O = \{x_1, x_2, x_3, x_4, x_5, x_6, x_7, x_8, x_9\}$ is a set of occupations such that x_1 = "health workers", x_2 = "nursing homes and protection homes", x_3 = "Ministry of National Defense, Ministry of Interior, individuals in strategic positions", x_4 = "municipal police, private security personal, Ministry of Justice, correctional facilities", x_5 = "education sector (teachers and faculty), food sector workers and bakeries, caterers, food and beverage processing plans, etc. registered with the Social Security Institution, transportation sector, workers registered with the Social Security Institution", x_6 = "workers in mass, crowded areas", x_7 = "businesses with less than ten employees", x_8 = "other/home-office", and x_9 = "unemployed" and I is a set of individuals. To illustrate, if an individual x is a teacher, then the occupation priority score $f_O(x) = \chi(x,5) = 0.5$.

Table 17. Vaccination group ranking

Type	Occupations	Scores
	Health Workers	1.0
	Nursing homes and Protection homes	0.8
A1, A2, A3	Ministry of National Defense, Ministry of Interior, Individuals in Strategic Positions	0.7
A4, A5, A6	Municipal Police, Private Security Personal, Ministry of Justice, Correctional Facilities	0.6
A7, A8, A9	Education Sector (Teachers and Faculty), Food Sector Workers and Bakeries, Caterers, Food and Beverage Processing Plans, etc. registered with the Social Security Institution, Transportation Sector, Workers registered with the Social Security Institution	0.5
A10	Workers in mass, crowded areas	0.4
A11	Businesses with less than ten employees	0.3
A12	Other/ Home-office	0.2
	Unemployed	0

The scores were assigned based on how crowded individuals' workspace is.

Calculation of Vaccination Priority Score: This study calculates the vaccination priority scores via the aforesaid scores in this subsection. Hence, the vaccination priority score function is as follows:

$$f_{VPS} : I \rightarrow [0,1]$$
$$x \rightarrow f_{VPS}(x) = \frac{NS_{Sd}f_{Sd}(x) + NS_A f_A(x) + NS_{IV} f_{IV}(x) + NS_{CH} f_{CH}(x) + NS_{PD} f_{PD}(x) + NS_{TP} f_{TP}(x) + NS_O f_O(x)}{NS_{Sd} + NS_A + NS_{IV} + NS_{CH} + NS_{PD} + NS_{TP} + NS_O}$$

Here, I is a set of individuals. To illustrate, if the total risk scores of an individual x are $f_{Sd}(x) = 0.82$, $f_A(x) = 0.92$, $f_{IV}(x) = 0.4$, $f_{CH}(x) = 0.5$, $f_{PD}(x) = 0.4$, $f_{TP}(x) = 0$, and $f_O(x) = 0.2$, then the vaccination priority score is as follows:

$$f_{VPS}(x) = \frac{1 \cdot 0.82 + 0.9100 \cdot 0.92 + 0.9919 \cdot 0.4 + 0.8775 \cdot 0.5 + 0.5726 \cdot 0.4 + 0.7364 \cdot 0 + 0.7372 \cdot 0.2}{1 + 0.9100 + 0.9919 + 0.8775 + 0.5726 + 0.7364 + 0.7372} = 0.4925$$

A Hypothetical Scenario: This study considers scores provided in Table 18 for ten individuals to illustrate the performances of the aforesaid vaccination priority score function and the SDM method YE12. Let $I = \{x_1, x_2, x_3, x_4, x_5, x_6, x_7, x_8, x_9, x_{10}\}$ be a set of individuals and $E = \{e_1, e_2, e_3, e_4, e_5, e_6, e_7\}$ be a set of parameters such that e_1 = "systemic disease", e_2 = "age", e_3 = "presence of risk group individuals in the immediate vicinity", e_4 = "presence of COVID-19 history", e_5 = "province-district", e_6 = "transportation preference", and e_7 = "occupation". Here, the weights of the parameters are $S_{Sd} = 1$, $S_A = 0.9100$, $S_{IV} = 0.9919$, $S_{CH} = 0.8775$, $S_{PD} = 0.5726$, $S_{TP} = 0.7364$, and $S_O = 0.7372$. Then, the *fpfs*-matrix $[a_{ij}]_{11\times 6}$ constructed by these weights and the data in Table 18 is as follows:

$$[a_{ij}] = \begin{bmatrix} 1 & 0.9100 & 0.9919 & 0.8775 & 0.5726 & 0.7364 & 0.7372 \\ 0.97 & 0.80 & 0.4 & 0.6 & 0.68 & 0.6 & 0.8 \\ 0.45 & 1 & 0.2 & 0.8 & 0.52 & 0.4 & 0.6 \\ 0.60 & 0.39 & 0.2 & 0.5 & 0.54 & 0.6 & 0 \\ 0.60 & 0.76 & 0.6 & 0.5 & 0.76 & 0.8 & 0.4 \\ 0.74 & 0.85 & 0.4 & 0.3 & 0.72 & 0 & 0.4 \\ 0.74 & 0.92 & 0.8 & 0.6 & 0.84 & 0.2 & 0.5 \\ 0.67 & 0.80 & 0.8 & 0.3 & 0.82 & 0.6 & 0.5 \\ 0.97 & 0.76 & 0.2 & 0.8 & 0.68 & 0.4 & 0.8 \\ 0.45 & 0.76 & 0.6 & 0.6 & 0.42 & 0.4 & 1 \\ 0.60 & 0.39 & 0.8 & 0.4 & 0.46 & 0.8 & 0.3 \end{bmatrix}$$

Then, this study applies the SDM method YE12 to $[a_{ij}]$. The decision set, score matrix, and ranking order produced by YE12, respectively, are as follows:

$$\{^{0.6939}x_1, {}^{0.5656}x_2, {}^{0.4022}x_3, {}^{0.6256}x_4, {}^{0.4945}x_5, {}^{0.6684}x_6, {}^{0.6411}x_7, {}^{0.6584}x_8, {}^{0.6069}x_9, {}^{0.5447}x_{10}\}$$

$$[s_{i1}] = [0.6939 \quad 0.5656 \quad 0.4022 \quad 0.6256 \quad 0.4945 \quad 0.6684 \quad 0.6411 \quad 0.6584 \quad 0.6069 \quad 0.5447]^T$$

and

$$x_3 \prec x_5 \prec x_{10} \prec x_2 \prec x_9 \prec x_4 \prec x_7 \prec x_8 \prec x_6 \prec x_1$$

Here,

$$s_{71} = f_{VPS}(x_7) = \frac{1 \cdot 0.67 + 0.9100 \cdot 0.8 + 0.9919 \cdot 0.8 + 0.8775 \cdot 0.3 + 0.5726 \cdot 0.82 + 0.7364 \cdot 0.6 + 0.7372 \cdot 0.5}{1 + 0.9100 + 0.9919 + 0.8775 + 0.5726 + 0.7364 + 0.7372} = 0.6411$$

Table 18. Priority scores for ten individuals

Individuals / Criteria	Systemic Disease	Age	Presence of risk group individuals in the immediate	Presence of COVID-19 History	Province-District	Transportation Preference	Occupation
x_1	0.97	0.80	0.4	0.6	0.68	0.6	0.8
x_2	0.45	1	0.2	0.8	0.52	0.4	0.6
x_3	0.60	0.39	0.2	0.5	0.54	0.6	0
x_4	0.60	0.76	0.6	0.5	0.76	0.8	0.4
x_5	0.74	0.85	0.4	0.3	0.72	0	0.4
x_6	0.74	0.92	0.8	0.6	0.84	0.2	0.5
x_7	0.67	0.80	0.8	0.3	0.82	0.6	0.5
x_8	0.97	0.76	0.2	0.8	0.68	0.4	0.8
x_9	0.45	0.76	0.6	0.6	0.42	0.4	1
x_{10}	0.60	0.39	0.8	0.4	0.46	0.8	0.3

Real-Life Interpretation: This study applies the SDM method YE12 to a real-life data derived from an online survey by Google Forms with 100 participants, 50 of whom are COVID-19 positive and the rest of whom are COVID-19 negative. The participants are asked to give information about their systemic diseases, ages, whether they are living in the immediate vicinity, the presence of their COVID-19 history, province-district they currently live in, their transportation preferences, and occupations. The results are provided in Table 19. To evaluate the performance of the SDM method YE12, this study utilizes the following validity function:

$$V : P \rightarrow [0,1]$$

$$x \rightarrow V(x) = \begin{cases} 1, & x \text{ is } COVID-19 \text{ positive and the order of } x < 75 \\ 1, & x \text{ is } COVID-19 \text{ negative and the order of } x > 25 \\ 0, & \text{otherwise} \end{cases}$$

Afterwards, it calculates the validity score $VS = \frac{1}{|P|}\sum_{x\in P} V(x)$. For this survey, the validity score is $VS = 0.96$. For example, for the second participant x_2, $V(x_2) = 1$ because he/she is COVID-19 positive and her/his order is less than 75. Similarly, for the participant x_{24}, $V(x_{24}) = 0$ because he/she is COVID-19 negative and her/his order is not greater than 25.

Table 19. Survey results for vaccination priority

Participants No / Criteria	Systemic disease	Age	Immediate vicinity	COVID-19 history	Province/ district	Transportation preference	Occupation	YE12's scores	COVID-19
1	0.97	0.85	0.8	0.8	0.48	0	0.7	0.6918	+
2	0.74	0.8	0.8	0.5	0.58	0.6	0.2	0.6217	+
3	0.6	0.8	0.2	0.6	0.88	0.8	0.4	0.5906	+
4	0.67	1	0	0.4	0.88	0.6	0.7	0.5824	+
5	0.6	0.92	0.8	0.5	0.46	0.2	0.4	0.5793	+
6	0.6	0.92	0.8	0.5	0.68	0.2	0.2	0.5757	+
7	0.67	0.92	0.4	0.6	0.82	0.2	0.4	0.5737	+
8	0.74	0.85	0.4	0.5	0.86	0.2	0.4	0.5636	+
9	0.6	1	0	0.5	0.78	0.6	0.4	0.5376	+
10	0.97	0.8	0	0.5	0.88	0.2	0.4	0.5292	+
11	0.74	1	0.2	0.5	0.58	0.2	0.4	0.5255	+
12	0.6	0.92	0.8	0.4	0.5	0.2	0	0.5176	+
13	0.67	1	0	0.6	0.46	0.6	0.2	0.5080	+
14	0.6	1	0	0.4	0.52	0.6	0.4	0.4970	+
15	0.6	0.85	0.8	0.4	0.4	0.2	0	0.4968	+
16	0.67	0.92	0	0.5	0.5	0.6	0.2	0.4843	+

17	0.6	0.85	0.4	0.4	0.42	0.6	0	0.4813	+
18	0.6	1	0	0.5	0.56	0.2	0.5	0.4781	+
19	0.6	0.85	0	0.4	0.88	0.2	0.5	0.4711	+
20	0.6	0.85	0	0.8	0.88	0.2	0	0.4680	+
21	0.6	1	0	0.5	0.7	0.2	0.3	0.4666	+
22	0.6	1	0	0.5	0.54	0.2	0.4	0.4635	+
23	0.67	0.92	0	0.5	0.54	0.2	0.4	0.4630	+
24	0	0.92	0	0.6	0.88	0.6	0.5	0.4597	-
25	0.6	0.92	0	0.5	0.88	0.2	0.2	0.4591	+
26	0.6	0.92	0.4	0.4	0.58	0.2	0	0.4573	+
27	0.6	0.92	0	0.8	0.4	0.2	0.2	0.4571	+
28	0.6	0.92	0	0.8	0.4	0.2	0.2	0.4571	+
29	0.74	1	0	0.4	0.88	0.2	0	0.4553	+
30	0.6	0.92	0	0.4	0.58	0.2	0.5	0.4525	+
31	0	1	0.4	0.5	0.78	0.2	0.4	0.4522	+
32	0.6	0.92	0	0.5	0.42	0.2	0.5	0.4519	+
33	0	0.85	0.8	0.6	0.88	0	0	0.4459	+
34	0.6	0.85	0	0.4	0.86	0	0.5	0.4438	+
35	0.6	0.92	0	0.8	0.52	0.2	0	0.4436	+
36	0.6	0.92	0	0.5	0.68	0.2	0.2	0.4394	+
37	0	1	0	0.6	0.5	0.6	0.5	0.4348	-
38	0.6	0.85	0	0.8	0.5	0.2	0	0.4307	+
39	0.6	0.92	0	0.3	0.88	0.2	0.2	0.4290	+
40	0	1	0	0.6	0.82	0.6	0.2	0.4283	-
41	0	1	0	0.6	0.4	0.6	0.5	0.4250	-
42	0.6	0.85	0	0.6	0.6	0	0.3	0.4231	+
43	0	0.92	0	0.5	0.78	0.2	0.8	0.4222	+

Table 19. (Continued) Survey results for vaccination priority

Participants No / Criteria	Systemic disease	Age	Immediate vicinity	COVID-19 history	Province/ district	Transportation preference	Occupation	YE12's scores	COVID-19
44	0	0.92	0	0.6	0.88	0.6	0.2	0.4217	-
45	0.74	0.85	0	0.3	0.4	0.6	0	0.4201	+
46	0	0.92	0	0.6	0.82	0.6	0.2	0.4158	-
47	0	1	0	0.6	0.88	0.6	0	0.4089	-
48	0	1	0	0.6	0.88	0.6	0	0.4089	-
49	0	1	0	0.6	0.62	0.6	0.2	0.4087	-
50	0.45	0.92	0	0.5	0.88	0.2	0	0.4080	+
51	0	0.8	0	0.6	0.5	0.6	0.5	0.4036	-
52	0	0.8	0	0.6	0.88	0.6	0.2	0.4030	-
53	0	0.92	0	0.6	0.4	0.6	0.4	0.3999	+
54	0	0.92	0.2	0.6	0.8	0.2	0.2	0.3974	-
55	0	1	0	0.6	0.5	0.6	0.2	0.3969	-
56	0	0.8	0	0.6	0.8	0.6	0.2	0.3951	-
57	0	1	0	0.5	0.86	0.2	0.4	0.3919	+
58	0.45	0.92	0	0.5	0.6	0.2	0	0.3805	+
59	0	1	0	0.6	0.84	0.2	0.2	0.3797	-
60	0	0.8	0	0.6	0.62	0.6	0.2	0.3774	-
61	0	1	0	0.6	0.42	0.2	0.5	0.3764	-
62	0	1	0	0.6	0.8	0.2	0.2	0.3758	-
63	0	0.8	0	0.6	0.84	0.6	0	0.3737	-
64	0	0.8	0	0.6	0.82	0.6	0	0.3718	-
65	0	0.8	0	0.6	0.62	0.2	0.5	0.3648	-
66	0	1	0	0.6	0.42	0.6	0	0.3637	-

67	0	0.92	0	0.4	0.82	0.2	0.4	0.3605	+
68	0	0.85	0	0.5	0.6	0.2	0.5	0.3556	+
69	0	1	0	0.4	0.52	0.2	0.4	0.3435	+
70	0	0.8	0	0.6	0.4	0.2	0.5	0.3432	-
71	0	1	0	0.6	0.62	0.2	0	0.3328	-
72	0	1	0	0.6	0.62	0.2	0	0.3328	-
73	0	1	0	0.6	0.6	0.2	0	0.3308	-
74	0	0.8	0	0.6	0.62	0.2	0.2	0.3269	-
75	0	0.85	0	0.6	0.4	0	0.5	0.3257	+
76	0	1	0.2	0.6	0.4	0	0	0.3199	-
77	0	1	0.2	0.6	0.4	0	0	0.3199	-
78	0	1	0	0.6	0.62	0	0	0.3075	-
79	0	1	0	0.6	0.6	0	0	0.3056	-
80	0	0.8	0	0.6	0.4	0.2	0.2	0.3052	-
81	0	0.92	0	0.6	0.46	0.2	0	0.3046	-
82	0	0.8	0	0.6	0.6	0.2	0	0.2996	-
83	0	0.92	0	0.6	0.4	0.2	0	0.2987	-
84	0	0.8	0	0.6	0.84	0	0	0.2979	-
85	0	0.92	0	0.6	0.62	0	0	0.2950	-
86	0	1	0	0.6	0.46	0	0	0.2918	-
87	0	1	0	0.6	0.46	0	0	0.2918	-
88	0	0.8	0	0.6	0.52	0.2	0	0.2917	-
89	0	0.8	0.2	0.6	0.4	0	0	0.2887	-
90	0	0.8	0	0.6	0.46	0.2	0	0.2858	-
91	0	0.8	0	0.6	0.46	0.2	0	0.2858	-

92	0	0.8	0	0.6	0.46	0.2	0	0.2858	-
93	0	0.92	0	0.6	0.52	0	0	0.2852	-
94	0	0.92	0	0.6	0.42	0	0	0.2754	-
95	0	0.8	0	0.6	0.6	0	0	0.2743	-
96	0	0.92	0	0.6	0.4	0	0	0.2734	-
97	0	0.85	0	0.6	0.5	0	0	0.2723	+
98	0	0.8	0	0.6	0.4	0	0	0.2547	-
99	0	0.8	0	0.6	0.4	0	0	0.2547	-
100	0	0.85	0	0.4	0.42	0	0	0.2343	+

5. Findings & Conclusions

This study successfully dealt with the rapid diagnosis of possible contagions, planning of follow-up methods and more developed treatment services, and planning an individual-specific vaccination priority by machine learning and statistical methods.

Diagnosis of COVID-19: This study employed mFPFS-CMC, the modified FPFS-CMC which is prominent among the well-known classifiers in medical diagnosis to diagnose COVID-19, and the dataset "Symptoms and COVID Presence (May 2020 data)" provided in Kaggle Data Repository. This is the first study to apply this classifier to COVID-19. The simulation results in Table 1 showed that mFPFS-CMC can be successfully applied to diagnose COVID-19 and it has a running time advantage of up to 70% over FPFS-CMC. This study then presented the accuracy, sensitivity, and specificity results of mFPFS-CMC. Although the sensitivity results of mFPFS-CMC are below 90%, its accuracy and specificity results are above 90%. The results showed that mFPFS-CMC is reliable and practical in medical diagnosis. Consequently, it has become more practical, timesaving, and far less costly to diagnose COVID-19 with the help of mFPFS-CMC.

Follow-Up Treatment Priority in COVID-19 Patients: This study constructed six risk score functions related to age, hypertension, cardiovascular disease, cancer, chronic kidney failure, and diabetes using the data provided in [11,12,14,15,17,18,40-47,49]. It then proposed a treatment priority score function to utilize in follow-up treatment priority in the presence of COVID-19 patients using the aforesaid six risk score functions. This study achieved developing a methodology that calculates each patient's risk score to provide better follow-up and treatment services. Afterward, it applied the SDM method YE12 to a hypothetical scenario. The results showed that the method herein is viable to rank COVID-19 patients in terms of treatment priority.

Vaccination Priority Planning: This study examined the vaccination process based on an individual-specific perspective via vaccination priority scores, calculated by considering the aforesaid seven criteria, i.e., systemic disease, age, presence of risk group individuals in the immediate vicinity, presence of COVID-19 history, province-district, transportation preference, and occupation. Moreover, it proposed a multi-dimensional vaccination priority algorithm to be used in a possible vaccine crisis in the case that a new variant that is insensitive to the vaccine or for booster dose planning. This study then presented a hypothetical and a real-life problem obtained by an online survey, conducted by Google Forms. The results manifested that this algorithm has 96% validity.

Suggestions: Although the first section of the project utilized three datasets consisting of 227, 2779, and 5434 patients, the others used the data of up to 200 participants. Increasing the number of participants can positively affect the validity of the results. Since the datasets herein are imbalanced, the sensitivity and specificity results can be improved by balancing the datasets. In general, increasing the number of the considered studies can produce more sensitive results than the results herein. Moreover, the treatment priority method can also be applied to a real-life dataset. All these methodologies can be adapted to reflect more on the abilities of *fpfs*-matrices. A software program can be derived from this study to use the health system and e-Pulse system, the personal health record system used in Turkiye.

Author Contributions

Zeynep Parla Parmaksız produced the main conceptual ideas, developed the theoretical framework, and carried out the simulations. Burak Arslan and Samet Memiş improved the theoretical framework and simulations. Serdar Enginoğlu encouraged the authors to investigate the applications of the soft decision-making via *fpfs*-matrices to machine learning and supervised the findings of this study. All the authors discussed the results and contributed to the final paper.

Conflict of Interest

The authors declare no conflict of interest.

Acknowledgement

The authors thank Beşiktaş Arts and Sciences Centre and The Scientific and Technological Research Council of Turkiye (TUBİTAK) for their valuable support. This paper was derived from the study presented by Zeynep Parla Parmaksız at Regeneron International Science and Engineering Fair (ISEF) 2022, Atlanta, GA, USA.

References

[1] C. Cortes, V. Vapnik, *Support-vector Networks*, Machine Learning 20 (3) (1995) 273–297.

[2] J. M. Keller, M. R. Gray, J. A. Givens, *A Fuzzy K-nearest Neighbor Algorithm*, IEEE Transactions on Systems, Man, and Cybernetics 15 (1985) 580–585.

[3] Y. Freund, R. E. Schapire, *A Decision-theoretic Generalization of On-line Learning and an Application to Boosting*, Journal of Computer and System Sciences 55 (1) (1997) 119–139.

[4] L. Breiman, J. H. Friedman, R. A. Olshen, C. J. Stone, Classification and Regression Trees. 3rd Edn., CRC Press, Wadsworth, 1998.

[5] B. Handaga, H. Onn, T. Herawan, *FSSC: An Algorithm for Classifying Numerical Data using Fuzzy Soft Set Theory*, International Journal of Fuzzy System Applications 2 (4) (2012) 29–46.

[6] S. A. Lashari, R. Ibrahim, N. Senan, *Medical Data Classification using Similarity Measure of Fuzzy Soft Set-based Distance Measure*, Journal of Telecommunication, Electronic and Computer Engineering 9 (2–9) (2017) 95–99.

[7] I. T. R. Yanto, R. R. Seadudin, S. A. Lashari, Haviluddin *A Numerical Classification Technique Based on Fuzzy Soft Set using Hamming Distance*, in: R. Ghazali, M. M. Deris, N. M. Nawi, J. H. Abawajy (Eds.), Third International Conference on Soft Computing and Data Mining, Johor, Malaysia, 2018, pp. 252–260.

[8] S. Memiş, S. Enginoğlu, U. Erkan, *A Classification Method in Machine Learning Based on Soft Decision-Making via Fuzzy Parameterized Fuzzy Soft Matrices*, Soft Computing 26 (2022) 1165–1180.

[9] S. Memiş, 2021. FPFS-CMC. GitHub Repository. Retrieved from https://github.com/sametmemis/FPFS-CMC.git

[10] D. Dua, C. Graff, 2019. UCI Machine Learning Repository [Database].

[11] A. T. Erol, *Predictive Indicators and Risk Factors in COVID-19 Mortality in Intensive Care: Retrospective Observatory Study*, Master's Thesis in Medicine, University of Health Sciences (2020) İstanbul Turkiye.

[12] F. Çoktaş, *Assessment of Risk Factors Related to COVID-19 Disease in Healthcare Workers*, Master's Thesis in Medicine, University of Health Sciences (2020) İstanbul Turkiye.

[13] M. S. Gold, D. Sehayek, S. Gabrielli, X. Zhang, C. McCusker, M. Ben-Shoshan, *COVID-19 and Comorbidities: A Systematic Review and Meta-Analysis*, Postgraduate Medicine 132(8) (2020) 749–755.

[14] M. Parohan, S. Yaghoubi, A. Seraji, M. H. Javanbakht, P. Sarraf, M. Djalali, *Risk Factors for Mortality in Patients with Coronavirus Disease 2019 (COVID19) Infection: A Systematic Review and Meta-Analysis of Observational Studies*, The Aging Male 23 (5) (2020) 1416–1424.

[15] Turkish Ministry of Health, (2020). COVID-19 Weekly Status Report 12/10/2020 – 18/10/2020 Ankara. Retrieved from https://covid19.saglik.gov.tr/Eklenti/39169/0/covid-19-weekly-situation-report---42-weekpdf.pdf?_tag1=B1A9C0854AC47DADC8FF332CC2CB9A336F580D4B

[16] Turkish Ministry of Health, (2021). Vaccination Group Ranking. Retrieved from https://covid19asi.saglik.gov.tr/EN-80295/list-of-covid-19-vaccination-groups.html

[17] Z. Zheng, F. Peng, B. Xua, J. Zhao, H. Liu, J. Peng, Q. Li, C. Jiang, Y. Zhou, S. Liu, C. Ye, P. Zhang, Y. Xing, H. Guo, W. Tang, *Risk Factors of Critical & Mortal COVID-19 Cases: A Systematic Literature Review and Meta-Analysis*, Journal of Infection 81 (2020) 16–25.

[18] F. Zhou, T. Yu, R. Du, G. Fan, Y. Liu, Z. Liu, J. Xiang, Y. Wang, B. Song, X. Gu, L. Guan, Y. Wei, H. Li, X. Wu, J. Xu, S. Tu, Y. Zhang, H. Chen, B. Cao, *Clinical Course and Risk Factors for Mortality of Adult Inpatients with COVID-19 in Wuhan, China: A Retrospective Cohort Study*, The Lancet 395 (2020) 1054–1062.

[19] H. Harikrishnan, (2020, April). Symptoms and COVID Presence (May 2020 data), Version 1. Retrieved June 21, 2021, from https://www.kaggle.com/datasets/hemanthhari/symptoms-and-covid-presence.

[20] J. Thyadi, (2021, July). Covid-19 Symptoms, Version 1. Retrieved June 21, 2022, from https://www.kaggle.com/datasets/jayasreethyadi/covid19-symptoms.

[21] S. Shahane, (2021, Mar). Brazilian Covid Symptomatic Patients Data, Version 1. Retrieved June 21, 2022, from https://www.kaggle.com/datasets/saurabhshahane/brazilian-covid-symptomatic-patients-data.

[22] M. Mehryar, A. Rostamizadeh, A. Talwalkar, Foundations of Machine Learning. 2nd Edn., The MIT Press, London, 2018.

[23] S. Enginoğlu, N. Çağman, *Fuzzy Parameterized Fuzzy Soft Matrices and Their Application in Decision-making*, TWMS Journal of Applied and Engineering Mathematics 10 (4) (2020) 1105–1115.

[24] N. Çağman, F. Çıtak, S. Enginoğlu, *Fuzzy Parameterized Fuzzy Soft Set Theory and Its Applications*, Turkish Journal of Fuzzy Systems 1 (1) (2010) 21–35.

[25] S. Memiş, S. Enginoğlu, U. Erkan, *Numerical Data Classification via Distance-based Similarity Measures of Fuzzy Parameterized Fuzzy Soft Matrices*, IEEE Access 9 (2021) 88583–88601.

[26] S. Enginoğlu, S. Memiş, F. Karaaslan, *A New Approach to Group Decision-making Method Based on TOPSIS under Fuzzy Soft Environment*, Journal of New Results in Science 8 (2) (2019) 42–52.

[27] S. Memiş, 2021. EMK19. GitHub Repository. Retrieved from https://github.com/sametmemis/EMK19.git

[28] S. Enginoğlu, S. Memiş, *Comment on Fuzzy Soft Sets [The Journal of Fuzzy Mathematics 9(3), 2001, 589–602]*, International Journal of Latest Engineering Research and Applications 3 (9) (2018) 1–9.

[29] T. Aydın, S. Enginoğlu, *A Configuration of Five of The Soft Decision-making Methods via Fuzzy Parameterized Fuzzy Soft Matrices and Their Application to A Performance-based Value Assignment Problem*, in: M. Kılıç, K. Özkan, M. Karaboyacı, K. Taşdelen, H. Kandemir, A. Beram (Eds.), Second International Conferences on Science and Technology: Natural Science and Technology (ICONST-NST) Prizren, Kosovo, 2019, pp. 56–67.

[30] T. Aydın, S. Enginoğlu, *Configurations of SDM Methods Proposed between 1999 and 2012: A Follow-up Study*, in: K. Yıldırım (Ed.) Fourth International Conference on Mathematics: "An İstanbul Meeting for World Mathematicians", İstanbul, Turkiye, 2020, pp. 183–202.

[31] S. Enginoğlu, S. Memiş, *A Configuration of Some Soft Decision-making Algorithms via fpfs-matrices*, Cumhuriyet Science Journal 39 (4) (2018) 871–881.

[32] S. Enginoğlu, T. Öngel, *Configurations of Several Soft Decision-making Methods to Operate in Fuzzy Parameterized Fuzzy Soft Matrices Space*, Eskişehir Technical University Journal of Science and Technology A - Applied Sciences and Engineering 21 (1) (2020) 58–71.

[33] S. Enginoğlu, T. Aydın, S. Memiş, B. Arslan, *Operability-oriented Configurations of The Soft Decision-making Methods Proposed between 2013 and 2016 and Their Comparisons*, Journal of New Theory 2021 (34) (2021) 82–114.

[34] S. Enginoğlu, T. Aydın, S. Memiş, B. Arslan, *SDM Methods' Configurations (2017-2019) and Their Application to A Performance-based Value Assignment Problem: A Follow up Study*, Annals of Optimization Theory and Practice 4 (1) (2021) 41–85.

[35] S. Memiş, B. Arslan, T. Aydın, S. Enginoğlu, Ç. Camcı, *A Classification Method Based on Hamming Pseudo-similarity of Intuitionistic Fuzzy Parameterized Intuitionistic Fuzzy Soft Matrices*, Journal of New Results in Science 10 (2) (2021) 59–76.

[36] M. Stone, *Cross-validatory Choice and Assessment of Statistical Predictions*, Journal of the Royal Statistical Society Series B (Methodological) 36 (1974) 111–147.

[37] D. Üstün, A. Toktaş, A. Akdağlı, *Deep Neural Network–based Soft Computing the Resonant Frequency of E–shaped Patch Antennas*, International Journal of Electronics and Communications 102 (2019) 54–61.

[38] T. Fawcett, *An Introduction to ROC Analysis*, Pattern Recognition Letters 27 (2006) 861–874.

[39] U. Erkan, *A Precise and Stable Machine Learning Algorithm: Eigenvalue Classification (EigenClass)*, Neural Computing and Applications 33 (10) (2021) 5381–5392.

[40] F. Saygılı, Hypertension Diagnosis and Treatment Guide, Turkish Society of Endocrinology and Metabolism, 2019.

[41] Z. Rakipoğlu, (2019, April 4). The Death Rate from Heart Diseases in Turkiye is 42 Percent, Anadolu Agency (2020, July 17). Retrieved from https://www.aa.com.tr/tr/saglik/turkiyede-kalp-hastaliklarinda-olum-orani-yuzde-42/1442301.

[42] TKD, (2020). Cardiovascular Risk Calculator, Turkish Society of Cardiology Web Site. Retrieved on August 18, 2020, from https://tkd.org.tr/cardibil/kalp-damar-sagligi/cardivaskuler-risk-hesaplama.

[43] H. Dülek, Z. Tuzcular Vural, I. Gönenç, *Risk Factors in Cardiovascular Diseases*, The Journal of Turkish Family Physician 9 (2) (2018) 53–58.

[44] M. Özdoğan, (2020, October 6). For Some Common Cancers Lifetime Statistics, Retrieved on June 21, 2021, from https://www.drozdogan.com/kanser-yasam-suresi-istatistikleri/

[45] National Cancer Institute (NCI) (2020) Surveillance, Epidemiology, and End Results (SEER) Program. (2020, October 6). Retrieved from https://seer.cancer.gov/statfacts/html/all.html

[46] F. S. Taş, K. Cengiz, E. Erdem, A. Karataş, C. Kaya, *Causes of Mortality in Acute and Chronic Renal Failure*, Fırat Medical Journal 16 (3) (2011) 120–124.

[47] E. Ahlqvist, P. Storm, A. Käräjämäki, M. Martinell, M. Dorkhan, A. Carlsson, P. Vikman, R. B. Prasad, D. M. Aly, P. Almgren, Y. Wessman, N. Shaat, P. Spégel, H. Mulder, E. Lindholm, O. Melander, O. Hansson, U. Malmqvist, A. Lernmark, K. Lahti, T. Forsén, T. Tuomi, A. H. Rosengren, L. Groop, *Novel Subgroups of Adult-onset Diabetes and Their Association with Outcomes: A Data-driven Cluster Analysis of Six Variables*, Lancet Diabetes Endocrinol 6 (2018) 361–369.

[48] Turkish Diabetes Foundation, Diabetes Diagnosis and Treatment Guide. Armoni Nüans Baskı Sanatları A. Ş., (2017).

[49] T. Chen, D. Wu, H. Chen, W. Yan, D. Yang, G. Chen, K. Ma, D. Xu, H. Yu, H. Wang, T. Wang, W. Guo, J. Chen, C. Ding, X. Zhang, J. Huang, M. Han, S. Li, X. Luo, J. Zhao, Q. Ning, *Clinical Characteristics of 113 Deceased Patients with Coronavirus Disease 2019: Retrospective Study*, British Medical Journal 368 (2020) m1091.

[50] S. Enginoğlu, S. Memiş, A Review on Some Soft Decision-making Methods. Proceedings of The International Conference on Mathematical Studies and Applications 2018 Karamanoğlu Mehmetbey University, Karaman, Turkiye, 4-6 October 2018.

[51] S. Memiş, 2021. YE12. GitHub repository. Retrieved from https://github.com/sametmemis/YE12.git

Journal of
New Theory
ISSN: 2149-1402

39 (2022) 84-93
Journal of New Theory
https://dergipark.org.tr/en/pub/jnt
Open Access

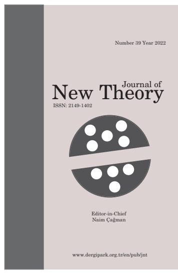

Distribution Formulae of the Solute in Transport of Advection-Dispersion of Air Pollution for Different Wind Velocities and Dispersion Coefficients

Hemant Kumar[1], Mahmood Ahmad Pathan[2], Frédéric Ayant[3]

Article Info
Received: 13 Jun 2022
Accepted: 29 Jun 2022
Published: 30 Jun 2022
doi:10.53570/jnt.1129890
Research Article

Abstract — In this paper, we obtain certain distribution formulae of the solute in transport of the typical advection-dispersion of air pollution through separation in two dimensional space variables by introducing different wind velocities and dispersion coefficients. As a consequence, by introducing different values of the solute velocity and dispersion coefficients, we evaluate the solute distribution formulae of the air pollution in terms of various known and unknown special functions.

Keywords — *Transport of advection-dispersion problems, air pollution, distribution formulae of the solute, wind velocities, dispersion coefficients, special functions*

Mathematics Subject Classification (2020) — 35G61, 33C90

1. Introduction

The solute transport is described by the advection-dispersion equation (in short ADE) (see for example [1])

$$\frac{\partial C}{\partial t}+\mathcal{U}\frac{\partial C}{\partial x}=D\frac{\partial^2 C}{\partial x^2} \tag{1}$$

where, C is solute concentration distribution, the positive constants $\mathcal{U}$ represent the average fluid (wind) velocity; D, the dispersion coefficient; x, the spatial domain and t is time. The ADE is a deterministic equation describing a probability function for the location of particles in a continuum. The fundamental solutions of the ADE over time t have studied in the Gaussian densities with means and variances based on the values of the macroscopic transport coefficients $\mathcal{U}$ and D.

The extension of the Eqn. (1) is presented in the typical advection-dispersion vector equation as

$$\frac{\partial C}{\partial t}+div(C\mathcal{U})=div(D\nabla C)+F \tag{2}$$

Here, the Eqn. (2) consists the scalar quantities C, D, and F, such that $D\neq 0$ and $\mathcal{U}$, a vector quantity.

We refer the principles of air pollution meteorology described in the researches [2–5]. Liu et al. [6,7] presented various computational methods for solute transport in the advection-dispersion problems.

[1]palhemant2007@rediffmail.com; [2]mapathan@gmail.com(Corresponding Author); [3]fredericayant@gmail.com
[1]Department of Mathematics, D. A-V. Postgraduate College, Uttar Pradesh, India
[2]Centre for Mathematical and Statistical Sciences, Peechi Campus, Kerala, India
[3]411, Av. J. Raynaud, Le Parc Fleuri, Bât. B Six-Fours Les Plages, Var, France

The study of wind speed conditions is of interest, partly because the simulation of airborne pollutant dispersion in certain conditions is rather difficult.

In our paper, we determine the distribution formulae of the solute transport by the typical advection-dispersion of air pollution problem (2) through separation in two dimensional space variables. We evaluate the solute distribution formulae of the air pollution in terms of Gauss and confluent hypergeometric functions by introducing different values of the solute velocity and dispersion coefficients.

2. Theory and Methods of Solute Distribution in Advection-dispersion Equation by Separate Variables

In this section, we plug the Eqn. (2) via the theory and methods of separation in two dimensional space variables stated on the basis of the researches done in [8–11].

We suppose that, $\forall x, y \in \mathbb{R}$, the solute concentration distribution $C = C(x, y, t)$, the wind velocity $U = u(x, y, t)i + v(x, y, t)j$; i and j are unit vectors; $u(x, y, t)$ and $v(x, y, t)$ are scalar quantities; the dispersion coefficient $D = D_1(x)D_2(y), D_1(x) \neq 0, D_2(y) \neq 0, \forall x \in \mathbb{R}, y \in \mathbb{R}$, and the scalar quantity

$$F = F(x, y, t), \quad \lim_{t\to 0^+} C(x, y, t) = f(x, y), \quad \lim_{t\to\infty} C(x, y, t) = h(x, y), \quad \nabla \equiv i\frac{\partial}{\partial x} + j\frac{\partial}{\partial y}$$

Also, the concentration distribution $C(x, y, t)$ exists and have non - zero values for $\forall x \in \mathbb{R}, y \in \mathbb{R}, t \geq 0$, and does not exist when $t < 0$.

By above assumptions, we convert the Eqn. (2) in the typical two variables advection-dispersion equation given by

$$\frac{\partial C(x, y, t)}{\partial t} + \frac{\partial}{\partial x}(C(x, y, t)u(x, y, t)) + \frac{\partial}{\partial y}(C(x, y, t)v(x, y, t)) = D_2(y)\frac{\partial}{\partial x}(D_1(x)\frac{\partial}{\partial x}C(x, y, t)) + D_1(x)\frac{\partial}{\partial y}(D_2(y)\frac{\partial}{\partial y}C(x, y, t)) + F(x, y, t) \quad (3)$$

Theorem 2.1. If $u(x, y, t)$ and $v(x, y, t)$ are velocity components along unit vectors i and j $\forall x \in \mathbb{R}, y \in \mathbb{R}, t \geq 0$, and $C(x, y, t) = C_1(x, t)C_2(y, t)$, where, $C_1(x, t) \neq 0, C_2(y, t) \neq 0$ and $F(x, y, t) = f_1(x, t)C_2(y, t) + f_2(y, t)C_1(x, t)$, $\forall x \in \mathbb{R}, y \in \mathbb{R}, t \geq 0$, then by the Eqn. (3), there exists following separate differential equations with variable coefficients

$$D_2(y)\frac{\partial^2}{\partial y^2}C_2(y, t) + \left\{\frac{\partial}{\partial y}D_2(y) - \frac{v(x, y, t)}{D_1(x)}\right\}\frac{\partial}{\partial y}C_2(y, t) + \frac{f_2(y, t)}{D_1(x)} - \frac{1}{D_1(x)}\frac{\partial C_2(y, t)}{\partial t} - \frac{\frac{\partial}{\partial y}v(x, y, t)}{D_1(x)}C_2(y, t) = 0 \quad (4)$$

and

$$D_1(x)\frac{\partial^2}{\partial x^2}C_1(x, t) + \left\{\frac{\partial}{\partial x}D_1(x) - \frac{u(x, y, t)}{D_2(y)}\right\}\frac{\partial}{\partial x}C_1(x, t) + \frac{f_1(x, t)}{D_2(y)} - \frac{1}{D_2(y)}\frac{\partial C_1(x, t)}{\partial t} - \frac{\frac{\partial}{\partial x}u(x, y, t)}{D_2(y)}C_1(x, t) = 0 \quad (5)$$

Proof. Consider the Eqn. (3) and set

$$u(x, y, t) = u_1(x, t)u_2(y, t), v(x, y, t) = u_3(x, t)u_4(y, t) \quad (6)$$

Then, under the conditions given in the Theorem 2.1 and in Eqn. (6), the Eqn. (3) becomes as

$$\begin{aligned} C_1(x,t)\frac{\partial C_2(y,t)}{\partial t} + C_2(y,t)\frac{\partial C_1(x,t)}{\partial t} + u_2(y,t)C_2(y,t)\frac{\partial}{\partial x}(C_1(x,t)u_1(x,t)) \\ + C_1(x,t)u_3(x,t)\frac{\partial}{\partial y}(C_2(y,t)u_4(y,t)) \\ = C_2(y,t)D_2(y)\frac{\partial}{\partial x}(D_1(x)\frac{\partial}{\partial x}C_1(x,t)) + C_1(x,t)D_1(x)\frac{\partial}{\partial y}(D_2(y)\frac{\partial}{\partial y}C_2(y,t)) \\ + f_1(x,t)C_2(y,t) + f_2(y,t)C_1(x,t) \end{aligned} \quad (7)$$

Again, we write the Eqn. (7) in the form

$$\begin{aligned} C_1(x,t)\Big[\frac{\partial C_2(y,t)}{\partial t} + u_3(x,t)\frac{\partial}{\partial y}(C_2(y,t)u_4(y,t)) - D_1(x)\frac{\partial}{\partial y}(D_2(y)\frac{\partial}{\partial y}C_2(y,t)) - f_2(y,t)\Big] + \\ C_2(y,t)\Big[\frac{\partial C_1(x,t)}{\partial t} + u_2(y,t)\frac{\partial}{\partial x}(C_1(x,t)u_1(x,t)) - D_2(y)\frac{\partial}{\partial x}(D_1(x)\frac{\partial}{\partial x}C_1(x,t)) - f_1(x,t)\Big] = 0 \end{aligned} \quad (8)$$

Since in Eqn. (8) $C_1(x,t) \neq 0$ and $C_2(y,t) \neq 0$, then $\forall\ x, y \in \mathbb{R}, t \geq 0$, here the equality holds if following equations satisfy

$$\frac{\partial C_2(y,t)}{\partial t} + u_3(x,t)\frac{\partial}{\partial y}(C_2(y,t)u_4(y,t)) - D_1(x)\frac{\partial}{\partial y}(D_2(y)\frac{\partial}{\partial y}C_2(y,t)) - f_2(y,t) = 0 \quad (9)$$

and

$$\frac{\partial C_1(x,t)}{\partial t} + u_2(y,t)\frac{\partial}{\partial x}(C_1(x,t)u_1(x,t)) - D_2(y)\frac{\partial}{\partial x}(D_1(x)\frac{\partial}{\partial x}C_1(x,t)) - f_1(x,t) = 0 \quad (10)$$

By the Eqn. (9), we obtain

$$\begin{aligned} \frac{\partial C_2(y,t)}{\partial t} + u_3(x,t)\Big\{C_2(y,t)\frac{\partial}{\partial y}u_4(y,t) + u_4(y,t)\frac{\partial}{\partial y}C_2(y,t)\Big\} \\ - D_1(x)\Big\{D_2(y)\frac{\partial^2}{\partial y^2}C_2(y,t) + \frac{\partial}{\partial y}D_2(y)\frac{\partial}{\partial y}C_2(y,t)\Big\} - f_2(y,t) = 0,\ x, y \in \mathbb{R}, t \geq 0 \end{aligned} \quad (11)$$

Then, for $x, y \in \mathbb{R}, t \geq 0$, by Eqn. (11) we find

$$\begin{aligned} \frac{\partial C_2(y,t)}{\partial t} = D_1(x)D_2(y)\frac{\partial^2}{\partial y^2}C_2(y,t) + \Big\{D_1(x)\frac{\partial}{\partial y}D_2(y) - u_3(x,t)u_4(y,t)\Big\}\frac{\partial}{\partial y}C_2(y,t) \\ - u_3(x,t)\frac{\partial}{\partial y}u_4(y,t)C_2(y,t) + f_2(y,t) \end{aligned} \quad (12)$$

Further in a similar manner, $\forall x, y \in \mathbb{R}, t \geq 0$, by Eqn. (10) we find

$$\begin{aligned} \frac{\partial C_1(x,t)}{\partial t} = D_2(y)D_1(x)\frac{\partial^2}{\partial x^2}C_1(x,t) + \Big\{D_2(y)\frac{\partial}{\partial x}D_1(x) - u_1(x,t)u_2(y,t)\Big\}\frac{\partial}{\partial x}C_1(x,t) \\ - u_2(y,t)\frac{\partial}{\partial x}u_1(x,t)C_1(x,t) + f_1(x,t) \end{aligned} \quad (13)$$

Note that $\forall x, y \in \mathbb{R}, t \geq 0$ the Eqns. (12) and (13) may be written as

$$\begin{aligned} \frac{1}{D_1(x)}\frac{\partial C_2(y,t)}{\partial t} = D_2(y)\frac{\partial^2}{\partial y^2}C_2(y,t) + \Big\{\frac{\partial}{\partial y}D_2(y) - \frac{v(x,y,t)}{D_1(x)}\Big\}\frac{\partial}{\partial y}C_2(y,t) \\ - \frac{\frac{\partial}{\partial y}v(x,y,t)}{D_1(x)}C_2(y,t) + \frac{f_2(y,t)}{D_1(x)} \end{aligned} \quad (14)$$

and

$$\frac{1}{D_2(y)}\frac{\partial C_1(x,t)}{\partial t} = D_1(x)\frac{\partial^2}{\partial x^2}C_1(x,t) + \left\{\frac{\partial}{\partial x}D_1(x) - \frac{u(x,y,t)}{D_2(y)}\right\}\frac{\partial}{\partial x}C_1(x,t) - \frac{\frac{\partial}{\partial x}u(x,y,t)}{D_2(y)}C_1(x,t) + \frac{f_1(x,t)}{D_2(y)} \quad (15)$$

Finally, by the Eqns. (14) and (15) we obtain the Eqns. (4) and (5), respectively. □

By the Eqns. (4) and (5), we may obtain various distribution formulae of the solute in the transport of advection-dispersion of air pollution on setting different wind velocities and dispersion coefficients.

3. Distribution Formulae of the Solute in Transport of Advection-dispersion of Air Pollution for Different Wind Velocities and Dispersion Coefficients Involving Special Functions

In this section, we determine the solute distribution formulae in terms of certain special functions whose contiguity and analytic properties are described in the literature of the authors [12, 13]. These special functions are then applied in computation process of the related formulae. We present following theorems for evaluation of our results:

Theorem 3.1. If $\forall x, y \in (0,1), t \geq 0, c_1, c_2 \neq 0, -1, -2, -3, \ldots,$, $D_1(x) = x(1-x)$, $D_2(y) = y(1-y)$, $v(x,y,t) = [1 - c_2 + (a_2 + b_2 - 1)y]\{x(1-x)\}$, and a partial differential equation is satisfied by

$$\frac{1}{C_2(y,t)}\left\{f_2(y,t) - \frac{\partial C_2(y,t)}{\partial t}\right\} = (a_2+b_2-1-a_2b_2)\{x(1-x)\},\ u(x,y,t) = [1-c_1+(a_1+b_1-1)x]\{y(1-y)\}$$

and another partial differential equation is satisfied by

$$\frac{1}{C_1(x,t)}\left\{f_1(x,t) - \frac{\partial C_1(x,t)}{\partial t}\right\} = (a_1 + b_1 - 1 - a_1b_1)\{y(1-y)\}$$

then, by the Eqns. (4) and (5) of the Theorem 2.1, they also satisfy the simultaneous differential equations

$$y(1-y)\frac{\partial^2}{\partial y^2}C_2(y,t) + \{c_2 - (a_2 + b_2 + 1)y\}\frac{\partial}{\partial y}C_2(y,t) - a_2b_2C_2(y,t) = 0 \quad (16)$$

and

$$x(1-x)\frac{\partial^2}{\partial x^2}C_1(x,t) + \{c_1 - (a_1 + b_1 + 1)x\}\frac{\partial}{\partial x}C_1(x,t) - a_1b_1C_1(x,t) = 0 \quad (17)$$

respectively.

PROOF. Consider the Eqn. (4) in which by the statement of this Theorem 3.1, put $D_1(x) = x(1-x)$, $D_2(y) = y(1-y), v(x,y,t) = [1 - c_2 + (a_2 + b_2 - 1)y]\{x(1-x)\}$ and set $\frac{1}{C_2(y,t)}\{f_2(y,t) - \frac{\partial C_2(y,t)}{\partial t}\} = (a_2 + b_2 - 1 - a_2b_2)\{x(1-x)\}$, we get the Eqn. (16).

Similarly, for the particular values $u(x,y,t) = [1 - c_1 + (a_1 + b_1 - 1)x]\{y(1-y)\}$, $\frac{1}{C_1(x,t)}\{f_1(x,t) - \frac{\partial C_1(x,t)}{\partial t}\} = (a_1 + b_1 - 1 - a_1b_1)\{y(1-y)\}$, from the Eqn. (5), we obtain the required Eqn. (17). □

Theorem 3.2. If $\forall x, y \in (0,1), t \geq 0$, in the relation $\frac{1}{C_1(x,t)}\left\{f_1(x,t) - \frac{\partial C_1(x,t)}{\partial t}\right\} = (a_1 + b_1 - 1 - a_1b_1)\{y(1-y)\}$, it is assumed that $\forall x, y$ such that $0 < x < 1, 0 < y < 1$, $C_1(x,t) = e^{-\alpha_1 t}H_1(x,y), \alpha_1 > 0$, then by Eqn. (17) of the Theorem 3.1, there exists a formula

$$C_1(x,t) = \exp[-(a_1 + b_1 - 1 - a_1b_1)\{y(1-y)\}t] \times \int_0^t \exp[(a_1 + b_1 - 1 - a_1b_1)\{y(1-y)\}\tau]f_1(x,\tau)d\tau + \mu_1 \ {}_2F_1\left[\begin{matrix}a_1, b_1;\\ c_1;\end{matrix} x\right] \quad (18)$$

μ_1 is an arbitrary constant and ${}_2F_1$ is Gauss hypergeometric function (see [12,13]). Similarly, for the relation $\frac{1}{C_2(y,t)}\{f_2(y,t)-\frac{\partial C_2(y,t)}{\partial t}\}=(a_2+b_2-1-a_2b_2)\{x(1-x)\}$ and $C_2(y,t)=e^{-\beta_1 t}H_2(x,y),\beta_1>0$, there exists another formula

$$C_2(y,t)=\exp\Bigg[-(a_2+b_2-1-a_2b_2)\{x(1-x)\}t\Bigg] \times\int_0^t \exp\Bigg[(a_2+b_2-1-a_2b_2)\{x(1-x)\}\tau\Bigg]f_2(y,\tau)d\tau+\nu_1\ {}_2F_1\left[\begin{matrix}a_2,b_2;\\ c_2;\end{matrix}y\right] \quad (19)$$

ν_1 is an arbitrary constant.

PROOF. The relation of the Theorem 3.2 is written by the linear differential equation $\frac{\partial C_1(x,t)}{\partial t}+(a_1+b_1-1-a_1b_1)\{y(1-y)\}C_1(x,t)=f_1(x,t)$, so that its solution is found by

$$C_1(x,t)=\exp[-(a_1+b_1-1-a_1b_1)\{y(1-y)\}t] \times\int_0^t \exp[(a_1+b_1-1-a_1b_1)\{y(1-y)\}\tau]f_1(x,\tau)d\tau+\lambda_1(x,y) \quad (20)$$

Now in Eqn. (17) set $C_1(x,t)=e^{-\beta_1 t}H_1(x,y),\beta_1>0$, so that $C_1(x,0)=H_1(x,y)$, and then $\lambda_1(x,y)=H_1(x,y)$ and hence we get

$$C_1(x,t)=\exp[-(a_1+b_1-1-a_1b_1)\{y(1-y)\}t] \times\int_0^t \exp[(a_1+b_1-1-a_1b_1)\{y(1-y)\}\tau]f_1(x,\tau)d\tau+H_1(x,y) \quad (21)$$

Again, by the relation $C_1(x,t)=e^{-\beta_1 t}H_1(x,y),\beta_1>0$ and the Eqn. (17), we get $H_1(x,y)=\mu_1\ {}_2F_1\left[\begin{matrix}a_1,b_1;\\ c_1;\end{matrix}\ x\right]$. Therefore, we obtain

$$C_1(x,t)=\exp[-(a_1+b_1-1-a_1b_1)\{y(1-y)\}t] \times\int_0^t \exp[(a_1+b_1-1-a_1b_1)\{y(1-y)\}\tau]f_1(x,\tau)d\tau+\mu_1\ {}_2F_1\left[\begin{matrix}a_1,b_1;\\ c_1;\end{matrix}x\right] \quad (22)$$

Similarly, we have for $C_2(y,t)=e^{-\alpha_1 t}H_2(x,y),\alpha_1>0$, then by Eqn. (16) we get $H_2(x,y)=\nu_1\ {}_2F_1\left[\begin{matrix}a_2,b_2;\\ c_2;\end{matrix}\ y\right]$ and by the relation $\frac{1}{C_2(y,t)}\left\{f_2(y,t)-\frac{\partial C_2(y,t)}{\partial t}\right\}=(a_2+b_2-1-a_2b_2)\{x(1-x)\}$, we get

$$C_2(y,t)=\exp[-(a_2+b_2-1-a_2b_2)\{x(1-x)\}t] \times\int_0^t \exp[(a_2+b_2-1-a_2b_2)\{x(1-x)\}\tau]f_2(y,\tau)d\tau+\nu_1\ {}_2F_1\left[\begin{matrix}a_2,b_2;\\ c_2;\end{matrix}y\right] \quad (23)$$

□

Theorem 3.3. If $\forall x,y\in(0,1),t\geq 0$, all conditions of the Theorem 3.2 and 3.3 are satisfied, then there exists following distribution formula of the solute as

$$C(x,y,t)=G_1(x,y,t)G_2(x,y,t)+\nu_1 G_1(x,y,t)\ {}_2F_1\left[\begin{matrix}a_2,b_2;\\ c_2;\end{matrix}y\right]+\mu_1 G_2(x,y,t)\ {}_2F_1\left[\begin{matrix}a_1,b_1;\\ c_1;\end{matrix}x\right] +\nu_1\mu_1\ {}_2F_1\left[\begin{matrix}a_1,b_1;\\ c_1;\end{matrix}x\right]\ {}_2F_1\left[\begin{matrix}a_2,b_2;\\ c_2;\end{matrix}y\right] \quad (24)$$

Here in (24), it is given that

$$G_1(x,y,t) = \{\exp[-(a_1+b_1-1-a_1b_1)\{y(1-y)\}t] \times \int_0^t \exp[(a_1+b_1-1-a_1b_1)\{y(1-y)\}\tau] f_1(x,\tau)d\tau \quad (25)$$

and

$$G_2(x,y,t) = \{\exp[-(a_2+b_2-1-a_2b_2)\{x(1-x)\}t] \times \int_0^t \exp[(a_2+b_2-1-a_2b_2)\{x(1-x)\}\tau] f_2(y,\tau)d\tau \quad (26)$$

PROOF. Apply the results of the Theorems 3.1 and 3.2 in the result $C(x,y,t) = C_1(x,t)C_2(y,t)$ of the Theorem 2.1 to find the result (21). □

Theorem 3.4. If $\forall x, y \in (0,1), t \geq 0, c_1, c_2 \neq 0, -1, -2, -3, \ldots,$, $D_1(x) = x$, $D_2(y) = y$

$$v(x,y,t) = [1-(y-c_2)]x, \quad \frac{1}{C_2(y,t)}\left\{\frac{\partial C_2(y,t)}{\partial t} - f_2(y,t)\right\} = (a_2+1)x$$

$$u(x,y,t) = [1-(x-c_1)]y, \quad \frac{1}{C_1(x,t)}\left\{\frac{\partial C_1(x,t)}{\partial t} - f_1(x,t)\right\} = (a_1+1)y$$

then, by the Eqns. (4) and (5) of the Theorem 2.1, they also satisfy following differential equations

$$y\frac{\partial^2}{\partial y^2}C_2(y,t) + (c_2-y)\frac{\partial}{\partial y}C_2(y,t) - a_2C_2(y,t) = 0 \quad (27)$$

and

$$x\frac{\partial^2}{\partial x^2}C_1(x,t) + (c_1-x)\frac{\partial}{\partial x}C_1(x,t) - a_1C_1(x,t) = 0 \quad (28)$$

respectively.

PROOF. Consider the Eqn. (4) in which by the statement of this Theorem, put $D_1(x) = x$, $D_2(y) = y$, $v(x,y,t) = [1-(y-c_2)]x$, then $\frac{\frac{\partial}{\partial y}v(x,y,t)}{x} = -1$, and $\frac{1}{C_2(y,t)}\left\{\frac{\partial C_2(y,t)}{\partial t} - f_2(y,t)\right\} = (a_2+1)x$ to get the Eqn. (27) as

$$y\frac{\partial^2}{\partial y^2}C_2(y,t) + (c_2-y)\frac{\partial}{\partial y}C_2(y,t) - a_2C_2(y,t) = 0$$

Similarly, by the Eqn. (5) in which on putting $u(x,y,t) = [1-(x-c_1)]y$, to get $\frac{\frac{\partial}{\partial x}u(x,y,t)}{y} = -1$, $\frac{1}{C_1(x,t)}\left\{\frac{\partial C_1(x,t)}{\partial t} - f_1(x,t)\right\} = (a_1+1)y$, gives us the Eqn. (28). □

Theorem 3.5. If all the conditions of the Theorem 3.4 are satisfied and $\forall t \geq 0$, let

$$C_1(x,t) = e^{-\alpha_2 t}K_1(x,y) = e^{-\alpha_2 t}K_1(x)K_1(y) = e^{-\alpha_2 t}K_1(x)\,(\text{ for } K_1(y) = 1)\,, \alpha_2 > 0;$$

$$C_2(y,t) = e^{-\beta_2 t}K_2(x,y) = e^{-\beta_2 t}K_2(x)K_2(y) = e^{-\beta_2 t}K_2(y)\,(\textbf{ for } K_2(x) = 1)\,, \beta_2 > 0.$$

Then, there exists the formulae

$$C_1(x,t) = \exp\left[(a_1+1)yt\right]\int_0^t \exp\left[-(a_1+1)y\tau\right]f_1(x,\tau)d\tau + \mu_2\ {}_1F_1\left[\begin{array}{c} a_1; \\ c_1; \end{array} x\right] \quad (29)$$

and

$$C_2(y,t) = \exp\left[(a_2+1)xt\right]\int_0^t \exp\left[-(a_2+1)x\tau\right]f_2(y,\tau)d\tau + v_2\ {}_1F_1\left[\begin{array}{c} a_2; \\ c_2; \end{array} y\right] \quad (30)$$

Proof. Consider the assumptions of the Theorem 3.5 and make an appeal to the Eqns. (27) and (28) to get the confluent differential equations (see [12,13])

$$x\frac{d^2}{dx^2}K_1(x) + (c_1 - x)\frac{d}{dx}K_1(x) - a_1K_1(x) = 0 \text{ and } y\frac{d^2}{dy^2}K_2(y) + (c_2 - y)\frac{d}{dy}K_2(y) - a_2K_2(y) = 0$$

respectively. Then we have their respective solutions

$$K_1(x) = \mu_2\ {}_1F_1\left[\begin{matrix} a_1; \\ c_1; \end{matrix}\ x\right] \text{ and } K_2(y) = \upsilon_2\ {}_1F_1\left[\begin{matrix} a_2; \\ c_2; \end{matrix}\ y\right]$$

Again due to the conditions of the Theorem 3.4, we get the linear partial differential equations

$$\frac{\partial C_1(x,t)}{\partial t} - (a_1 + 1)\, yC_1(x,t) = f_1(x,t) \text{ and } \frac{\partial C_2(y,t)}{\partial t} - (a_2 + 1)\, xC_2(y,t) = f_2(y,t),$$

respectively. We obtain the solutions of these linear partial differential equations

$$C_1(x,t) = \exp\left[(a_1+1)\, yt\right]\int_0^t \exp\left[-(a_1+1)\, y\tau\right] f_1(x,\tau)d\tau + K_1(x,y)$$

$$= \exp\left[(a_1+1)\, yt\right]\int_0^t \exp\left[-(a_1+1)\, y\tau\right] f_1(x,\tau)d\tau + K_1(x)$$

and

$$C_2(y,t) = \exp\left[(a_2+1)\, xt\right]\int_0^t \exp\left[-(a_2+1)\, x\tau\right] f_2(y,\tau)d\tau + K_2(x,y)$$

$$= \exp\left[(a_2+1)\, xt\right]\int_0^t \exp\left[-(a_2+1)\, x\tau\right] f_2(y,\tau)d\tau + K_2(y)$$

respectively.

Finally introduce the values of $K_1(x)$ and $K_2(y)$ in above solutions, we evaluate the required results (29) and (30). □

Theorem 3.6. If $\forall x, y \in (0,1), t \geq 0, c_1, c_2 \neq 0, -1, -2, -3, \ldots,$ all conditions of the Theorems 3.4 and 3.5 are satisfied. Then, by the relation of the Theorem 3.4 there exists then solute distribution in the form

$$C(x,y,t) = G_1'(x,y,t)G_2'(x,y,t) + \nu_2 G_1'(x,y,t)\ {}_1F_1\left[\begin{matrix} a_2; \\ c_2; \end{matrix} y\right] + \mu_2 G_2'(x,y,t)\ {}_1F_1\left[\begin{matrix} a_1; \\ c_1; \end{matrix} x\right] + \nu_2\mu_2\ {}_1F_1\left[\begin{matrix} a_1; \\ c_1; \end{matrix} x\right]\ {}_1F_1\left[\begin{matrix} a_2; \\ c_2; \end{matrix} y\right] \quad (31)$$

where

$$G_1'(x,y,t) = \exp[(a_1+1)yt]\int_0^t \exp[-(a_1+1)y\tau]f_1(x,\tau)d\tau + \mu_2\ {}_1F_1\left[\begin{matrix} a_1; \\ c_1; \end{matrix} x\right]$$

and

$$G_2'(x,y,t) = \exp[(a_2+1)xt]\int_0^t \exp[-(a_2+1)x\tau]f_2(y,\tau)d\tau + \nu_2\ {}_1F_1\left[\begin{matrix} a_2; \\ c_2; \end{matrix} y\right]$$

Proof. Consider the relation of the Theorem 2.1 that $C(x,y,t) = C_1(x,t)C_2(y,t)$, in which by making an appeal to the Theorems 3.4 and 3.5, we find the results of the Theorem 3.6. □

4. Special Cases

Example 4.1. In the Theorem 3.3, $\forall x, y \in (0,1), t \geq 0, c_1, c_2 \neq 0, -1, -2, -3, \ldots$, set $f_1(x,\tau) = e^{\sigma_1 x \tau}$ and $f_2(y,\tau) = e^{\sigma_2 y \tau}$, $\sigma_1 < 0, \sigma_2 < 0$, $a_1 + b_1 > (1 + a_1 b_1)$. Thus we get

$$C(x,y,t) = G_1(x,y,t)G_2(x,y,t) + \nu_1 G_1(x,y,t)\ {}_2F_1\begin{bmatrix} a_2, b_2; \\ c_2; \end{bmatrix} y + \mu_1 G_2(x,y,t)\ {}_2F_1\begin{bmatrix} a_1, b_1; \\ c_1; \end{bmatrix} x + \nu_1\mu_1\ {}_2F_1\begin{bmatrix} a_1, b_1; \\ c_1; \end{bmatrix} x\ {}_2F_1\begin{bmatrix} a_2, b_2; \\ c_2; \end{bmatrix} y. \quad (32)$$

Here in (32), it is given that

$$G_1(x,y,t) = \frac{1}{\{(a_1+b_1-1-a_1b_1)\{y(1-y)\}+\sigma_1 x\}} \times \{\exp[\sigma_1 xt] - \exp[-(a_1+b_1-1-a_1b_1)\{y(1-y)\}t]\} \quad (33)$$

and

$$G_2(x,y,t) = \frac{1}{\{(a_2+b_2-1-a_2b_2)\{x(1-x)\}+\sigma_2 y\}} \times \{\exp[\sigma_2 yt] - \exp[-(a_2+b_2-1-a_2b_2)\{x(1-x)\}t]\} \quad (34)$$

On making an application of the results (32)-(34), and by conditions of Example 4.1, we find that

$$G_1(x,y,0) = 0 = G_2(x,y,0) \text{ and } \lim_{t\to\infty} G_1(x,y,t) = \lim_{t\to\infty} G_2(x,y,t) = 0,$$

hence by Section 2 we get

$$\lim_{t\to 0^+} C(x,y,t) = \lim_{t\to\infty} C(x,y,t) = f(x,y) = h(x,y) = \nu_1\mu_1\ {}_2F_1\begin{bmatrix} a_1, b_1; \\ c_1; \end{bmatrix} x\ {}_2F_1\begin{bmatrix} a_2, b_2; \\ c_2; \end{bmatrix} y \quad (35)$$

Example 4.2. In the Theorem 3.6, $\forall x, y \in (0,1), t \geq 0, c_1, c_2 \neq 0, -1, -2, -3, \ldots$, set $f_1(x,\tau) = e^{-\rho_1 x\tau}$ and $f_2(y,\tau) = e^{-\rho_2 y\tau}$, $\rho_1 > 0, \rho_2 > 0, (a_1+1) < 0$ and get

$$C(x,y,t) = G_1'(x,y,t)G_2'(x,y,t) + \nu_2 G_1'(x,y,t)\ {}_1F_1\begin{bmatrix} a_2; \\ c_2; \end{bmatrix} y + \mu_2 G_2'(x,y,t)\ {}_1F_1\begin{bmatrix} a_1; \\ c_1; \end{bmatrix} x + \nu_2\mu_2\ {}_1F_1\begin{bmatrix} a_1; \\ c_1; \end{bmatrix} x\ {}_1F_1\begin{bmatrix} a_2; \\ c_2; \end{bmatrix} y \quad (36)$$

Here in (36), it is given that

$$G_1'(x,y,t) = \frac{1}{\{(a_1+1)y+\rho_1 x\}}\{\exp[(a_1+1)yt] - \exp[-\rho_1 xt]\} \quad (37)$$

and

$$G_2'(x,y,t) = \frac{1}{\{(a_2+1)x+\rho_2 y\}}\{\exp[(a_2+1)xt] - \exp[-\rho_2 yt]\} \quad (38)$$

On applying the results (36)-(39), and by conditions of the Example 4.2, we find that $G_1'(x,y,0) = 0 = G_2'(x,y,0)$, and $\lim_{t\to\infty} G_1'(x,y,t) = \lim_{t\to\infty} G_2'(x,y,t) = 0$ and hence by Section 2 we get

$$\lim_{t\to 0^+} C(x,y,t) = \lim_{t\to\infty} C(x,y,t) = f(x,y) = h(x,y) = \nu_2\mu_2\ {}_1F_1\begin{bmatrix} a_1; \\ c_1; \end{bmatrix} x\ {}_1F_1\begin{bmatrix} a_2; \\ c_2; \end{bmatrix} y \quad (39)$$

Remark 4.3. Various elementary functions for example $(1-z)^{-a} = {}_2F_1(a,b;b;z), \ln(1+z) = z\,{}_2F_1(1,1;2;-z)$, Legendre functions of the first and second kinds, incomplete Beta function, complete elliptic integrals of the first and second kinds, Jacobi polynomials, Gegenbauer polynomials, Legendre polynomials, Tchebycheff polynomials of the first and second kinds are generally represented in terms of the hypergeometric function ${}_2F_1(.)$. By the Theorem 3.3 and Example 4.1, the solute distribution may be expressed in the form of these known hypergeometric functions,(also see [8, 10, 14]).

Remark 4.4. Various special functions like Bessel functions, Whittaker functions, incomplete Gamma functions, Hermite polynomials and Leguerre functions etc. are represented in terms of the confluent hypergeometric function $_1F_1(.)$. By the Theorem 3.6 and Example 4.2, the solute distribution may be expressed in the form of these known hypergeometric functions,(also see [9, 15, 16]).

5. Conclusion and Discussion

Air pollution meteorology, atmospheric diffusion models for regulatory applications, volume method for transient simulation of time- and scale-dependent transport in heterogeneous aquifer systems are other related topics which can be connected with our present study. A recent work [10,14-16] on obtaining Voigt functions via Quadrature formula for the fractional in time diffusion and wave problem, on a bi-dimensional basis involving Special Functions for partial in space and the time fractional wave mechanical problems and approximation, are such examples. The study of wind speed conditions is of interest, partly because the simulation of airborne pollutant dispersion in certain conditions is rather difficult. We have determined the distribution formulae of the solute transport by the typical advection-dispersion of air pollution problem through separation in two dimensional space variables. Several other methods are available. We have evaluated the solute distribution formulae of the air pollution in terms of Gauss and confluent hypergeometric functions by introducing different values of the solute velocity and dispersion coefficients.

We can determine the solute distribution formulae in terms of certain special functions whose contiguity and analytic properties are described in the literature of the authors [12, 13].The equation (2) via the theory and methods of separation in two dimensional space variables stated on the basis of the researches done in [8-11] may be useful by simply connecting relevant special functions in computation process of the related formulae. By the Theorem 3.6 and Example 4.2, the solute distribution may be expressed in the form of known special functions,(also see [9, 15, 16]). As a consequence, by introducing different values of the solute velocity and dispersion coefficients, we can evaluate the solute distribution formulae of the air pollution in terms of various known and unknown special functions.

Author Contributions

All authors contributed equally to this work. They all read and approved the last version of the paper.

Conflicts of Interest

The authors declare no conflict of interest.

References

[1] S. Salsa, Partial Differential Equations in Action. From Modelling to Theory, Springer, Switzerland, 2016.

[2] S. R. Hanna, *Review of Atmospheric Diffusion Models for Regulatory Applications*, World Meteorological Organization (WMO), Technical Note No. 177, WMO No. 581, Geneva, Switzerland, 1982.

[3] S. R. Hanna, G. A. Briggs, R. P. Hosker, *Handbook on Atmospheric Diffusion*, Technical Information Center U. S. Department of Energy, Technical Report No. DOE/TIC-11223, United States, 1982.

[4] R. M. Harrison, R. Perry, Handbook of Air Pollution Analysis, Chapman and Hall and Methuen, New York, 1986.

[5] T. J. Lyons, W. D. Scott, Principles of Air Pollution Meteorology, CBS Publishers and Distributers, New Delhi, 1992.

[6] F. Liu, I. Turner, V. Anh, *An Unstructured Mesh Finite Volume Method for Modelling Saltwater Intrusion into Coatal Aquifer*, Korean Journal of Computational & Applied Mathematics 9 (2002) 391–407.

[7] F. Liu, I. Turner, V. Anh, N. Su, *A Two-dimensional Finite Volume Method for Transient Simulation of Time- and Scale-dependent Transport in Heterogeneous Aquifer Systems*, Journal of Applied Mathematics and Computing 11 (2003) 215–241.

[8] H. Kumar, *On Three Dimensional Legendre Sturm Liouville Diffusion and Wave Problem Generated due to Fractional Derivative*, Jñānābha 48 (1) (2018) 129–141.

[9] H. Kumar, S. K. Rai, *On a Fractional Time Derivative and Multi-dimensional Space Evolution Bessel Sturm Liouville Diffusion and Wave Problem*, Jñānābha Special Issue (2018) 61–71.

[10] H. Kumar, M. A. Pathan, S. K. Rai, *On Certain Solutions of a Generalized Perl's Vector Equation Involving Fractional Time Derivative*, Montes Taurus Journal of Pure and Applied Mathematics 1 (2) (2019) 42–57.

[11] H. Kumar, S. K. Rai, *Multiple Fractional Diffusions via Multivariable H-function*, Jñānābha 50 (1) (2020) 253–264.

[12] H. Hochstadt, The Functions of Mathematical Physics, Dover Publications, New York, 1986.

[13] H. M. Srivastava, H. L. Manocha, A Treatise on Generating Functions, John Wiley and Sons, New York, 1984.

[14] H. Kumar, S. P. S. Yadav, *Application of Generalized Polynomials of Several Variables and Multivariable H-function in One Dimensional Advective Diffusion Problem*, Bulletin of Pure and Applied Mathematics 4 (2) (2010) 353–362.

[15] H. Kumar, M. A. Pathan, S. K. Rai, *Obtaining Voigt Functions via Quadrature Formula for the Fractional in Time Diffusion and Wave Problem*, Kragujevac Journal of Mathematics 46 (5) (2022) 759–772.

[16] H. Kumar, H. Srivastava, S. K. Rai, *On a Bi Dimensional Basis Involving Special Functions for Partial in Space and the Time Fractional Wave Mechanical Problems and Approximation*, Jñānābha 47 (2) (2017) 291–300.

Journal of
New Theory
ISSN: 2149-1402

39 (2022) 94-103
Journal of New Theory
https://dergipark.org.tr/en/pub/jnt
Open Access

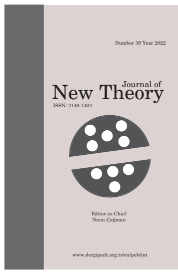

A Generalization of p-Adic Factorial

Rafik Beldahef[1]

Article Info
Received: 17 Mar 2022
Accepted: 30 Jun 2022
Published: 30 Jun 2022
doi:10.53570/jnt.1089241
Research Article

Abstract — In this paper, we establish a new approach of the p-adic analogue of Roman factorial, called p-adic Roman factorial. We define this new concept and demonstrate its properties and some properties of p-adic factorial.

Keywords — *Roman factorial, p-adic number, p-adic factorial, p-adic gamma function*

Mathematics Subject Classification (2020) — 05A10, 11D88

1. Introduction

In the literature, the Roman factorial in the real case is one of the generalizations of the classical factorial for negative integers. This concept has been used by Steve Roman [1] to study the formal series and the harmonic logarithm. It has also been studied by Loeb and Rota in [2], and [3]. The above authors have used the notation $\lfloor m \rceil!$ to define the Roman factorial of an integer $m \in \mathbb{Z}$.
The p-adic domain has an important applications in a cryptography, number theory, algebraic geometry, and arithmetic dynamics. However, the definition of the p-adic factorial of a positive integer was considered by Alain Robert in [4] as restricted factorial, and denoted by

$$n!^* = \prod_{1 \le j \le n, p \nmid j} j$$

Another notation for the p-adic factorial $(n!)_p$ was adopted by Menken and Çolakoğlu [5]. Both of Robert and Menken have used the p-adic factorial only to define the p-adic gamma function, without giving its properties. Furthermore, Aidagulov and Alekseyev in [6] have also used the so-called modified (p-adic) factorial, with the notation $n!_p$, to study the modified (p-adic) binomial coefficients. It can be remarked that the previous authors have given the definition of p-adic factorial without giving the properties.
Taken into previous considerations, in the present paper, we firstly demonstrate some properties of p-adic factorial (see Lemma 2.3, Theorem 2.4, Proposition 2.7, Proposition 2.8, Corollary 2.9, and Corollary 2.10). Secondly, we propose a definition of p-adic analogue of Roman factorial named *p-adic Roman factorial* (see Definition 3.1). Next, we demonstrate some combinatorial properties of this factorial, using the concept of p-adic gamma function (see Lemma 3.2, Theorems 3.4-3.6, Corollaries 3.7-3.8, Theorems 3.9-3.11). Finally, some numerical examples are given (Examples 2.5 and 3.12).

[1] `belhadef_rafik@univ-jijel.dz` (Corresponding Author)
[1] Department of Mathematics, University Mohamed Seddik Benyahia, BP 98, Ouled Aissa, Jijel, Algeria

2. Preliminary

Throughout this paper, p is a prime number, $\mathbb{Z}$ is the set of all the real integers, $\mathbb{Z}_-$ (resp. $\mathbb{Z}_+$) is the set of all the negative real integers (resp. all the positive real integers), $\mathbb{N}$ is the set of all the non-negative integers, $\mathbb{Q}$ is the field of rational numbers, and $\mathbb{R}$ is the field of real numbers. We use $|.|$ to denote the ordinary absolute value, $[.]$ the real integer part, ν_p the p-adic valuation, and $|.|_p$ the p-adic absolute value. The field of p-adic numbers $\mathbb{Q}_p$ is the completion of $\mathbb{Q}$ with respect to the p-adic absolute value. The ring of p-adic integers $\mathbb{Z}_p$ is such that $|x|_p \leq 1$.

2.1. Roman Factorial in Real Domain

Roman in [1] proposed the factorial of negative integer $n \in \mathbb{Z}_-$ as $\lfloor n \rceil ! = \dfrac{(-1)^{-n-1}}{(-n-1)!}$. So, for $n \in \mathbb{Z}_+$ we have $\lfloor n \rceil ! = n!$. Also, the Roman factorial satisfies a characteristic functional equation $\lfloor n \rceil ! = \lfloor n \rceil \cdot \lfloor (n-1) \rceil !$, where $\lfloor n \rceil = n$ if $n \neq 0$, and $\lfloor 0 \rceil = 1$ is called Roman n.

For example, we give the Roman factorial of some integers in table1:

Table 1. oman factorial of some integers

n	**0**	**1**	**2**	**3**	**4**	**5**	**6**	**7**
$\lfloor n \rceil !$	1	1	2	6	24	120	720	5040
$-n$	0	-1	-2	-3	-4	-5	-6	-7
$\lfloor -n \rceil !$	1	1	-1	$\frac{1}{2}$	$-\frac{1}{6}$	$\frac{1}{24}$	$-\frac{1}{120}$	$\frac{1}{720}$

The complement formula of the factorial function, known as Knuth's theorem [7], is as follows:

$$\lfloor n \rceil ! \, \lfloor -n \rceil ! = (-1)^n \, |n|$$

and the Roman factorial can be rewritten using the gamma function Γ as follows:

$$\lfloor n \rceil ! = \begin{cases} \Gamma(n+1), & \text{for} \quad n \geq 0 \\ \dfrac{(-1)^{-n-1}}{\Gamma(-n)}, & \text{for} \quad n < 0 \end{cases} \tag{1}$$

2.2. p-adic Factorial and p-adic Gamma Function

In this subsection, we provide definitions of p-adic analogue of factorial function and gamma function and some of their basic properties, to be needed in the next section.

Definition 2.1. [4] The p-adic factorial of $n \in \mathbb{N}$ is defined by $0!_p = 1$ and for $n > 0$

$$n!_p = \prod_{\substack{j=1 \\ (p,j)=1}}^{n} j \tag{2}$$

Remark 2.2. If $1 \leq n \leq p-1$, then $(p,j) = 1$, for all $1 \leq j \leq n$. Then, $n!_p = n!$.

Lemma 2.3. For $p = 2$, then we have $(2k)!_2 = (2k-1)!_2$.

PROOF. The result comes from the fact that if $p = 2$, we have $n!_2 = \prod\limits_{\substack{j=1 \\ j \text{ is odd}}}^{n} j$. □

As in the real case, we define the p-adic Roman of a positive integer n as

$$\lfloor n \rceil_p = \begin{cases} n, & \text{if} \quad |n|_p = 1 \\ 1, & \text{if} \quad |n|_p < 1 \end{cases} \tag{3}$$

Therefore, the first property similar to that of the real factorial is given by the following

Theorem 2.4. Let $n \in \mathbb{N}$, with $n \geq 1$. Then $n!_p = \lfloor n \rceil_p (n-1)!_p$.

PROOF. Two cases are considered.

1) We suppose $|n|_p = 1$, so $(p, n) = 1$. Thus

$$n!_p = \prod_{\substack{j=1 \\ (p,j)=1}}^{n} j = n \prod_{\substack{j=1 \\ (p,j)=1}}^{n-1} j = \lfloor n \rceil_p (n-1)!_p$$

2) We suppose $|n|_p < 1$, so $(p, n) \neq 1$. Thus

$$n!_p = \prod_{\substack{j=1 \\ (p,j)=1}}^{n} j = 1 \cdot \prod_{\substack{j=1 \\ (p,j)=1}}^{n-1} j = \lfloor n \rceil_p (n-1)!_p$$

□

Example 2.5. In Tables 2-5, we calculate some p-adic factorials of some positive integers. For $p = 2, 3, 5, 7$.

Table 2. The 2-adic factorial

n	**0**	**1**	**2**	**3**	**4**	**5**	**6**	**7**	**8**	**9**	**10**	**11**
$n!_2$	1	1	1	3	3	15	15	105	105	945	945	10395

Table 3. The 3-adic factorial

n	**0**	**1**	**2**	**3**	**4**	**5**	**6**	**7**	**8**	**9**	**10**	**11**
$n!_3$	1	1	2	2	8	40	40	280	2240	2240	22400	246400

Table 4. The 5-adic factorial

n	**0**	**1**	**2**	**3**	**4**	**5**	**6**	**7**	**8**	**9**	**10**	**11**
$n!_5$	1	1	2	6	24	24	144	1008	8064	72576	72576	798336

Table 5. The 7-adic factorial

n	**0**	**1**	**2**	**3**	**4**	**5**	**6**	**7**	**8**	**9**	**10**	**11**
$n!_7$	1	1	2	6	24	120	720	720	5760	51840	518400	5702400

The next theorem represents a generalization of the Wilson congruence; it's the key of some results in this section.

Theorem 2.6. [4] Let $a \in \mathbb{Z}$ and $s \in \mathbb{Z}_+$. Then

1) For $p \geq 3$ and $s \geq 1$, we have $\prod\limits_{\substack{j=a \\ (p,j)=1}}^{a+p^s-1} j \equiv -1 \, (mod \; p^s)$.

2) For $p = 2$ and $s \geq 3$, we have $\prod_{\substack{j=a \\ j odd}}^{a+2^s-1} j \equiv 1\,(mod\ 2^s)$.

From this generalization of the classical Wilson theorem, we obtain the following congruences:

Proposition 2.7. Let $n \in \mathbb{N}$ and $s \in \mathbb{Z}_+$.

1) If $p \geq 3$ and $s \geq 1$, then $\dfrac{(n+p^s)!_p}{n!_p} \equiv -1\,(mod\ p^s)$.

2) If $p = 2$ and $s \geq 3$, then $\dfrac{(n+2^s)!_2}{n!_2} \equiv 1\,(mod\ 2^s)$.

Proof. We have

$$\frac{(n+p^s)!_p}{n!_p} = \prod_{\substack{j=n+1 \\ (p,j)=1}}^{n+p^s} j$$

From the case 1 of Theorem 2.6 with $a = n+1$, we obtain the congruence for $p \geq 3$ and $s \geq 1$. From the case 2 of the same Theorem with $a = n+1$, we obtain the congruence for $p = 2$ and $s \geq 3$. □

More generally, we have the following theorem:

Proposition 2.8. Let $n \in \mathbb{N}$, and $m, s \in \mathbb{Z}_+$.

1) If $p \geq 3$ and $s \geq 1$, then $\dfrac{(n+mp^s)!_p}{n!_p} \equiv (-1)^m\,(mod\ p^s)$.

2) If $p = 2$ and $s \geq 3$, then $\dfrac{(n+m2^s)!_2}{n!_2} \equiv 1\,(mod\ 2^s)$.

Proof. The proof is done by induction on m. □

Corollary 2.9. For $p \geq 3$, $n \in \mathbb{N}$ and $s \in \mathbb{Z}_+$, we have $|n!_p|_p = 1$ and

$$|(n+p^s)!_p + n!_p|_p \leq \frac{1}{p^s}$$

Corollary 2.10. For $p = 2$, $n \in \mathbb{N}$ and $s \in \mathbb{Z}_+$ with $s \geq 3$, we have $|n!_2|_2 = 1$ and

$$|(n+2^s)!_2 - n!_2|_2 \leq \frac{1}{2^s}$$

In dynamic system and string theory, the p-adic gamma function has been well used. This function studied by [8], [9] and [10], to give some properties of polynomials.
The function $n!$ cannot be extended by continuity on $\mathbb{Z}_p$, because $\lim_{n \to +\infty} n! = 0$ in $\mathbb{Z}_p$. So, we have the definition of p-adic gamma function as follows:

Definition 2.11. [11] The p-adic gamma function is defined by Morita as the continuous function

$$\Gamma_p : \mathbb{Z}_p \longrightarrow \mathbb{Z}_p$$

as an extension of the following sequence, with $n \in \mathbb{Z}_+$

$$\Gamma_p(n) = (-1)^n \prod_{j=1,(p,j)=1}^{n-1} j \tag{4}$$

Furthermore,

$$\Gamma_p(z) = \lim_{\substack{n \to z \\ \text{in } \mathbb{Z}_p}} \Gamma_p(n) = \lim_{\substack{n \to z \\ \text{in } \mathbb{Z}_p}} (-1)^n \prod_{\substack{j=1 \\ (p,j)=1}}^{n-1} j$$

Here, we cite some properties of Γ_p that we need to prove the theorems in the next section.

Proposition 2.12. [4] The function Γ_p satisfies the following properties:

1) $\Gamma_p(0) = 1$, $\Gamma_p(1) = -1$, $\Gamma_p(2) = 1$

2) $\Gamma_p(n+1) = (-1)^{n+1} n!_p$, $\forall n \in \mathbb{N}$

Other some important arithmetic formulas are given in the following proposition:

Proposition 2.13. [4] Let $n \geq 1$, its p-adic expansion be $\sum_{i=0}^{\ell} n_i p^i$, and the sum of digits be $S_n = \sum_{i=0}^{\ell} n_i$. Then,

1) $\Gamma_p(n+1) = \dfrac{(-1)^{n+1}\, n!}{\left[\frac{n}{p}\right]! \times p^{\left[\frac{n}{p}\right]}}$. In particular, $\Gamma_p(p^n) = \dfrac{(-1)^p\, p^n!}{p^{n-1}! \times p^{p^{n-1}}}$.

2) $\Gamma_p(np+k+1) = \dfrac{(-1)^{np+k+1}\,(np+k)!}{n! \times p^n}$, for $0 \leq k < p$.

3) $n! = (-1)^{n+1-\ell}\,(-p)^{\frac{n-S_n}{p-1}} \prod_{i=0}^{\ell} \Gamma_p\left(\left[\frac{n}{p^i}\right]+1\right)$.

3. Main Results and Proofs

Inspired by the works of Roman [1], Loeb and Rota [2], we will establish a p-adic analogue of the Roman factorial, so-called *the p-adic generalized factorial*, or *the p-adic Roman factorial*. We define of this new concept and demonstrate some of its properties.

Definition 3.1. For $n \in \mathbb{Z}$, we define the p-adic Roman factorial of n as

$$\lfloor n \rceil !_p = \begin{cases} n!_p, & \text{for} \quad n \geq 0 \\ \dfrac{(-1)^{-n-1}}{(-n-1)!_p}, & \text{for} \quad n < 0 \end{cases} \tag{5}$$

Remark 3.2. It can be remarked that

1) If $0 \leq n \leq p-1$, the we have $n!_p = n!$. Then, $\lfloor n \rceil !_p = \lfloor n \rceil ! = n!$.

2) If $-p \leq n \leq -1$, the we have $(-n-1)!_p = (-n-1)!$. Then, $\lfloor n \rceil !_p = \lfloor n \rceil !$.

Lemma 3.3. For $p = 2$, then

$$\lfloor n \rceil !_p = \begin{cases} \lfloor n-1 \rceil !_p, & \text{for} \quad n = 2k \geq 0 \\ -\lfloor n-1 \rceil !_p, & \text{for} \quad n = -2k < 0 \end{cases}$$

PROOF. From Lemma 2.3, we have $(2k)!_2 = (2k-1)!_2$, thus $\lfloor 2k \rceil !_p = \lfloor 2k-1 \rceil !_p$. For the second case, we have $(-2k-1)!_2 = (-2k)!_2$, thus $\lfloor -2k-1 \rceil !_p = \lfloor -2k \rceil !_p$ □

We keep the notation of the p-adic Roman for a negative integer $n \in \mathbb{Z}_-$ and define it as

$$\lfloor n \rceil_p = \begin{cases} n, & \text{if } \ |n|_p = 1 \\ -1, & \text{if } \ |n|_p < 1 \end{cases} \tag{6}$$

So, it can easily verified that $\lfloor -n \rceil_p = -\lfloor n \rceil_p$.

Therefore, the first property similar to that of the real Roman factorial is as follows:

Theorem 3.4. For all $n \in \mathbb{Z}$, we have $\lfloor n+1 \rceil !_p = \lfloor n+1 \rceil_p \lfloor n \rceil !_p$.

Proof. We consider the following three cases:
1) If $n \geq 0$, then $n+1 \geq 1$. Then, from Proposition 2.4 we have

$$\lfloor n+1 \rceil !_p = (n+1)!_p = \lfloor n+1 \rceil_p n!_p = \lfloor n+1 \rceil_p \lfloor n \rceil !_p$$

2) If $n < -1$, then $n+1 < 0$. Then, from Proposition 2.4 we have

$$\lfloor n+1 \rceil !_p = \frac{(-1)^{-n} \lfloor -n-1 \rceil_p}{\lfloor -n-1 \rceil_p (-n-2)!_p} = \frac{(-1)^{-n-1} \lfloor n+1 \rceil_p}{(-n-1)!_p} = \lfloor n+1 \rceil_p \lfloor n \rceil !_p$$

3) If $n = -1$, then, we have in the left side $\lfloor n+1 \rceil !_p = 0!_p = 1$, and in the right side $\lfloor n+1 \rceil_p \lfloor n \rceil !_p = 1 \cdot \lfloor -1 \rceil !_p = 1$. □

The following congruences hold from the properties of p-adic factorial.

Theorem 3.5. Let $n \in \mathbb{Z}$ and $s \in \mathbb{Z}_+$. Then

1) If $p \geq 3$ and $s \geq 1$, then we have

$$\begin{cases} \dfrac{\lfloor n+p^s \rceil !_p}{\lfloor n \rceil !_p} \equiv -1 \,(mod\ p^s)\,, & \text{if } \ n \geq 0 \\ \dfrac{\lfloor n \rceil !_p}{\lfloor n-p^s \rceil !_p} \equiv -1 \,(mod\ p^s)\,, & \text{if } \ n < 0 \end{cases}$$

2) If $p = 2$ and $s \geq 3$, then we have

$$\begin{cases} \dfrac{\lfloor n+2^s \rceil !_2}{\lfloor n \rceil !_2} \equiv 1 \,(mod\ 2^s)\,, & \text{if } \ n \geq 0 \\ \dfrac{\lfloor n \rceil !_2}{\lfloor n-2^s \rceil !_2} \equiv 1 \,(mod\ 2^s)\,, & \text{if } \ n < 0 \end{cases}$$

Proof. The case $n \geq 0$ comes from the Proposition 2.8. It only remains to explain the case $n < 0$. Indeed, we have

$$\frac{\lfloor n \rceil !_p}{\lfloor n-p^s \rceil !_p} = (-1)^{p^s} \frac{(-n-1+p^s)!_p}{(-n-1)!_p}$$

The result comes from Proposition 2.8, for two cases $p \geq 3$ and $p = 2$. □

More generally, we have the following Theorem

Theorem 3.6. Let $n \in \mathbb{Z}$ and $s, m \in \mathbb{Z}_+$. Then,

1) If $p \geq 3$ and $s \geq 1$, then we have

$$\begin{cases} \dfrac{\lfloor n+mp^s\rceil!_p}{\lfloor n\rceil!_p} \equiv (-1)^m \,(mod\ p^s)\,, & \text{if} \quad n \geq 0 \\[2ex] \dfrac{\lfloor n\rceil!_p}{\lfloor n-mp^s\rceil!_p} \equiv (-1)^m \,(mod\ p^s)\,, & \text{if} \quad n < 0 \end{cases}$$

2) If $p = 2$ and $s \geq 3$, then we have

$$\begin{cases} \dfrac{\lfloor n+m2^s\rceil!_2}{\lfloor n\rceil!_2} \equiv 1 \,(mod\ 2^s)\,, & \text{if} \quad n \geq 0 \\[2ex] \dfrac{\lfloor n\rceil!_2}{\lfloor n-m2^s\rceil!_2} \equiv 1 \,(mod\ 2^s)\,, & \text{if} \quad n < 0 \end{cases}$$

Proof. Easy recursion on m. □

The following corollaries follow from the two previous theorems.

Corollary 3.7. Let $p \geq 3$, $n \in \mathbb{Z}$ and $s, m \in \mathbb{Z}_+$. Then, $|\lfloor n\rceil!_p|_p = 1$ and

$$\begin{cases} |\lfloor n+mp^s\rceil!_p + \lfloor n\rceil!_p|_p \leq \dfrac{1}{p^s}, & \text{if} \quad n \geq 0 \\[2ex] |\lfloor n-mp^s\rceil!_p + \lfloor n\rceil!_p|_p \leq \dfrac{1}{p^s}, & \text{if} \quad n < 0 \end{cases}$$

Corollary 3.8. Let $p = 2$, $n \in \mathbb{Z}$, and $s, m \in \mathbb{Z}_+$ with $s \geq 3$. Then, $|\lfloor n\rceil!_2|_2 = 1$ and

$$\begin{cases} |\lfloor n+m2^s\rceil!_2 - \lfloor n\rceil!_2|_2 \leq \dfrac{1}{2^s}, & \text{if} \quad n \geq 0 \\[2ex] |\lfloor n-m2^s\rceil!_2 - \lfloor n\rceil!_2|_2 \leq \dfrac{1}{2^s}, & \text{if} \quad n < 0 \end{cases}$$

Next, we give the p-adic complement formula for p-adic Roman factorial function, in other words, the p-adic version of Knuth's theorem

Theorem 3.9. (p-adic Knuth's theorem)
For all $n \in \mathbb{Z}$, we have

$$\lfloor n\rceil!_p \lfloor -n-1\rceil!_p = \begin{cases} (-1)^n\,, & \text{for} \quad n \geq 0 \\[2ex] (-1)^{n+1}\,, & \text{for} \quad n < 0 \end{cases}$$

Proof. If $n \geq 0$, then $-n-1 < 0$. From Definition 3.1, we have $\lfloor n\rceil!_p = n!_p$ and the result comes from

$$\lfloor -n-1\rceil!_p = \frac{(-1)^n}{n!_p}$$

For the case $n < 0$, we use the same reasoning. □

As we have seen before for p-adic factorial, we can rewrite the p-adic Roman factorial using the p-adic gamma function, as follows:

Theorem 3.10. Let $n \in \mathbb{Z}$. Then, the relationship between p-adic Roman factorial and p-adic gamma function is given by

$$\lfloor n \rceil !_p = (-1)^{\delta(n)} \Gamma_p(n+1)$$

where

$$\delta(n) = \begin{cases} n+1, & \text{for} \quad n \geq 0 \\ n+1+\left[-\frac{n+1}{p}\right], & \text{for} \quad n < 0 \end{cases}$$

Proof. For the case of $n \geq 0$, the result comes from Proposition 2.12 (2). We show the theorem only for negative integers. Indeed, we proof $n < 0$, so $-n-1 > 1$. From Proposition 2.12, we have $(-n-1)!_p = (-1)^{-n}\Gamma_p(-n)$. On the other hand, from the complement formula of the p-adic gamma function (see [4]), we have

$$\Gamma_p(n+1)\Gamma_p(-n) = (-1)^{-n-[-\frac{n+1}{p}]}$$

Hence, we obtain

$$\begin{aligned} \lfloor n \rceil !_p &= \frac{-1}{\Gamma_p(-n)} \\ &= \frac{-\Gamma_p(n+1)}{(-1)^{-n-[-\frac{n+1}{p}]}} \\ &= (-1)^{n+1+\left[-\frac{n+1}{p}\right]}\Gamma_p(n+1) \end{aligned}$$

□

In the following theorem, we give some properties related to the p-adic gamma function.

Theorem 3.11. Let $n \in \mathbb{Z}$, and $m \in \mathbb{N}$. Then

1) We have

$$\lfloor n \rceil !_p = \begin{cases} \dfrac{\lfloor n \rceil !}{\left[\frac{n}{p}\right]! \times p^{\left[\frac{n}{p}\right]}}, & \text{for} \quad n \geq 0 \\ (-1)^n \lfloor n \rceil ! \left[-\frac{n+1}{p}\right]! \times p^{\left[-\frac{n+1}{p}\right]}, & \text{for} \quad n < 0 \end{cases}$$

2) In particular, $p^{m+1}!_p = \dfrac{p^{m+1}!}{p^m! \times p^{p^m}}$.

3) $(mp+k)!_p = \dfrac{(mp+k)!}{m!\ p^m}$, for $0 \leq k < p$.

4) $n! = (-1)^n (-p)^{\frac{n-S_n}{p-1}} \prod_{i=0}^{\ell} \left((-1)^{\left[\frac{n}{p^i}\right]} \left\lfloor \left[\frac{n}{p^i}\right] \right\rceil !_p\right)$, for $n \in \mathbb{N}$ given by its p-adic expansion $\sum_{i=0}^{\ell} n_i p^i$ and with the sum of digits $S_n = \sum_{i=0}^{\ell} n_i$.

Proof. The proof is clear from Proposition 2.13 and Theorem 3.10. □

Example 3.12. We give p-adic Roman factorial of the first ten negative integers in Tables 6-9. For positive numbers are the same that given in example 2.5.

Table 6. The 2-adic Roman factorial

n	**-1**	**-2**	**-3**	**-4**	**-5**	**-6**	**-7**	**-8**	**-9**	**-10**
$-n-1$	0	1	2	3	4	5	6	7	8	9
$(-n-1)!_2$	1	1	1	3	3	15	15	105	105	945
$\lfloor n \rceil !_2$	1	-1	1	$-\frac{1}{3}$	$\frac{1}{3}$	$-\frac{1}{15}$	$\frac{1}{15}$	$-\frac{1}{105}$	$\frac{1}{105}$	$-\frac{1}{945}$

Table 7. The 3-adic Roman factorial

n	**-1**	**-2**	**-3**	**-4**	**-5**	**-6**	**-7**	**-8**	**-9**	**-10**
$-n-1$	0	1	2	3	4	5	6	7	8	9
$(-n-1)!_3$	1	1	2	2	8	40	40	280	2240	2240
$\lfloor n \rceil !_3$	1	-1	$\frac{1}{2}$	$-\frac{1}{2}$	$\frac{1}{8}$	$-\frac{1}{40}$	$\frac{1}{40}$	$-\frac{1}{280}$	$\frac{1}{2240}$	$-\frac{1}{2240}$

Table 8. The 5-adic Roman factorial

n	**-1**	**-2**	**-3**	**-4**	**-5**	**-6**	**-7**	**-8**	**-9**	**-10**
$-n-1$	0	1	2	3	4	5	6	7	8	9
$(-n-1)!_5$	1	1	2	6	24	24	144	1008	8064	72576
$\lfloor n \rceil !_5$	1	-1	$\frac{1}{2}$	$-\frac{1}{6}$	$\frac{1}{24}$	$-\frac{1}{24}$	$\frac{1}{144}$	$-\frac{1}{1008}$	$\frac{1}{8064}$	$-\frac{1}{72576}$

Table 9. The 7-adic Roman factorial

n	**-1**	**-2**	**-3**	**-4**	**-5**	**-6**	**-7**	**-8**	**-9**	**-10**
$-n-1$	0	1	2	3	4	5	6	7	8	9
$(-n-1)!_7$	1	1	2	6	24	120	720	720	5760	51840
$\lfloor n \rceil !_7$	1	-1	$\frac{1}{2}$	$-\frac{1}{6}$	$\frac{1}{24}$	$-\frac{1}{120}$	$\frac{1}{720}$	$-\frac{1}{720}$	$\frac{1}{5760}$	$-\frac{1}{51840}$

4. Conclusion

In this article, we have given some properties of the p-adic factorial. Then, we have defined a generalization of this factorial, so-called p-adic Roman factorial, with the proof of some properties and a congruances modulo a power of a prime number. Also, a numerical examples have been given. This concept will be used to define the p-adic binomial coefficients and its generalzation, in a future paper.

Author Contributions

The author read and approved the last version of the paper.

Conflicts of Interest

The author declares no conflict of interest.

Acknowledgements

This paper is supported by the Scientific Research Project N° C00L03UN180120180006, in University Mohamed Seddik Benyahia of Jijel.

References

[1] S. Roman, *The Logarithmic Binomial Formula*. The American Mathematical Monthly 99 (7) (1992) 641–648.

[2] D. E. Loeb, G. C. Rota, *Formal Power Series of Logarithmic Type*. Advances in Mathematics 75 (1) (1989) 1–118.

[3] D. E. Loeb, *A Generalization of the Binomial Coefficients*. Discrete Mathematics 105 (1-3) (1992) 143–156.

[4] A. M. Robert, A Course in p-Adic Analysis, Springer-Verlag, Graduate Texts in Mathematics 198, 2000.

[5] H. Menken, Ö. Çolakoğlu, *Some Properties of the p-Adic Beta Function. European Journal of Pure and Applied Mathematics* 8 (2) (2015) 214–231.

[6] R. R. Aidagulov, M. A. Alekseyev, *On p-Adic Approximation of Sums of Binomial Coefficients. Journal of Mathematical Sciences* 233 (5) (2018) 626–634.

[7] D. Knuth, *Subspaces, Subsets, and Partitions. Journal of Combinatorial Theory* 10 (2) (1971) 178–180.

[8] U. Duran, M. Açıkgöz, *A Study on Novel Extensions for the p-Adic Gamma and p-Adic Beta Functions. Mathematical and Computational Applications* 24 (2) (2019) 1–20.

[9] U. Duran, M. Açıkgöz, *On p-Ddic Gamma Function Related to q-Daehee Polynomials and Numbers*. Proyecciones (Antofagasta) 38 (4) (2019) 799–810.

[10] Ö. H. Çolakoğlu, H. Menken, *On the p-Adic Gamma Function and Changhee Polynomials. Turkish Journal of Analysis and Number Theory* 6 (4) (2018) 120–123.

[11] Y. A. Morita, *A p-Adic Analogue of the Gamma Function. Journal of the Faculty of Science, the University of Tokyo, Section 1A* 22 (2) (1975) 255–266.